

# Automated Input Variable Selection for Analog Methods Using Genetic Algorithms

Pascal Horton<sup>1</sup>, Olivia Martius<sup>1</sup>, and Simon Lukas Grimm<sup>1</sup>

<sup>1</sup>University of Bern

July 31, 2023

## Abstract

Analog methods (AMs) have long been used for precipitation prediction and climate studies. However, they rely on manual selections of parameters, such as the predictor variables and analogy criterion. Previous work showed the potential of genetic algorithms (GAs) to optimize most parameters of AMs. This research goes one step further and investigates the potential of GAs for automating the selection of the input variables and the analogy criteria (distance metric between two data fields) in AMs. Our study focuses on daily precipitation prediction in central Europe, specifically Switzerland, as a representative case. Comparative analysis against established reference methods demonstrates the superiority of the GA-optimized AM in terms of predictive accuracy. The selected input variables exhibit strong associations with key meteorological processes that influence precipitation generation. Further, we identify a new analogy criterion inspired by the Teweles-Wobus criterion, but applied directly to grid values, which consistently performs better than other Euclidean distances. It shows potential for further exploration regarding its unique characteristics. In contrast to conventional stepwise selection approaches, the GA-optimized AM displays a preference for a flatter structure, characterized by a single level of analogy and an increased number of variables. Although the GA optimization process is computationally intensive, we highlight the use of GPU-based computations to significantly reduce computation time. Overall, our study demonstrates the successful application of GAs in automating input variable selection for AMs, with potential implications for application in diverse locations and data exploration for predicting alternative predictands.

# Automated Input Variable Selection for Analog Methods Using Genetic Algorithms

P. Horton<sup>1</sup>, O. Martius<sup>1</sup>, and S. L. Grimm<sup>2</sup>

<sup>1</sup>Institute of Geography, Oeschger Centre for Climate Change Research, University of Bern, Bern,  
Switzerland

<sup>2</sup>Physikalisches Institut, University of Bern, Gesellschaftsstrasse 6, 3012 Bern, Switzerland

## Key Points:

- Genetic algorithms were successful in selecting relevant input variables for the prediction of precipitation by analog methods
- The analogy criteria were automatically selected, resulting in the discovery of a new promising criterion
- The optimization resulted in a structure combining different predictors into a single level of analogy, while outperforming stepwise methods

---

Corresponding author: Pascal Horton, [pascal.horton@giub.unibe.ch](mailto:pascal.horton@giub.unibe.ch)

**Abstract**

Analog methods (AMs) have long been used for precipitation prediction and climate studies. However, they rely on manual selections of parameters, such as the predictor variables and analogy criterion. Previous work showed the potential of genetic algorithms (GAs) to optimize most parameters of AMs. This research goes one step further and investigates the potential of GAs for automating the selection of the input variables and the analogy criteria (distance metric between two data fields) in AMs. Our study focuses on daily precipitation prediction in central Europe, specifically Switzerland, as a representative case. Comparative analysis against established reference methods demonstrates the superiority of the GA-optimized AM in terms of predictive accuracy. The selected input variables exhibit strong associations with key meteorological processes that influence precipitation generation. Further, we identify a new analogy criterion inspired by the Teweles-Wobus criterion, but applied directly to grid values, which consistently performs better than other Euclidean distances. It shows potential for further exploration regarding its unique characteristics. In contrast to conventional stepwise selection approaches, the GA-optimized AM displays a preference for a flatter structure, characterized by a single level of analogy and an increased number of variables. Although the GA optimization process is computationally intensive, we highlight the use of GPU-based computations to significantly reduce computation time. Overall, our study demonstrates the successful application of GAs in automating input variable selection for AMs, with potential implications for application in diverse locations and data exploration for predicting alternative predictands.

**1 Introduction**

Analog methods (AMs) are statistical downscaling techniques (Maraun et al., 2010) that rely on inherent relationships between meteorological predictors, usually at a synoptic scale, and local weather (Lorenz, 1956, 1969). AMs look for similar meteorological situations in the past to that of a target date of interest. They provide a conditional prediction based on the observed predictand values at these analog dates. Daily precipitation has been the predictand of interest, either in the context of operational forecasting (e.g. T. Hamill & Whitaker, 2006; Bliefernicht, 2010; Marty et al., 2012; Horton et al., 2012; T. M. Hamill et al., 2015; Ben Daoud et al., 2016), climate change studies (e.g. Dayon et al., 2015; Raynaud et al., 2016), or past climate reconstruction (Caillouet et al., 2016). AMs are also used for other predictands, such as precipitation radar images (Panziera et al., 2011; Foresti et al., 2015), temperature (Delle Monache et al., 2013; Caillouet et al., 2016; Raynaud et al., 2016; Jézéquel et al., 2017), wind (Delle Monache et al., 2013, 2011; Vanvyve et al., 2015; Alessandrini, Delle Monache, Sperati, & Nissen, 2015; Junk, Delle Monache, Alessandrini, Cervone, & von Bremen, 2015; Junk, Delle Monache, & Alessandrini, 2015), and solar radiation or power production (Alessandrini, Delle Monache, Sperati, & Cervone, 2015; Bessa et al., 2015; Raynaud et al., 2016).

AMs may consist of a stepwise selection of similar meteorological situations based on multiple predictors organized in different consecutive levels of analogy, each of which

55 conditions the subsequent selection. Each predictor consists of a specific meteorologi-  
56 cal variable at a specific time and vertical level (if relevant). The similarity between two  
57 situations is computed using an analogy criterion (distance metric) over a relevant spa-  
58 tial domain. For each level of analogy, a certain number of analogs are selected (Obled  
59 et al., 2002; Bontron, 2004).

60 AMs for predicting precipitation commonly have a first level of analogy based on  
61 the atmospheric circulation. The variable of interest is the geopotential height ( $Z$ ) at var-  
62 ious pressure levels and specific times throughout the day (Table 2; Obled et al., 2002;  
63 Horton et al., 2018). Bontron (2004) introduced a second level of analogy based on a mois-  
64 ture index that is the product of the relative humidity at 850 hPa and the total precip-  
65 itable water (method RM3 in Table 2). Other consecutive studies selected different pres-  
66 sure levels (method RM4 in Table 2) or added a wind component to the moisture index  
67 (Marty, 2010; Horton et al., 2018). Ben Daoud et al. (2016) inserted an additional level  
68 of analogy between the circulation and the moisture analogy based on the vertical ve-  
69 locity at 850 hPa (methods RM6 in Table 2) and named it "SANDHY" for Stepwise Ana-  
70 log Downscaling method for Hydrology (Ben Daoud et al., 2016; Caillouet et al., 2016).

71 To calibrate the method, a semi-automatic sequential procedure (Bontron, 2004;  
72 Radanovics et al., 2013; Ben Daoud et al., 2016) has often been used to optimize the size  
73 of the domain and the number of analogs. However, the predictor variables, vertical lev-  
74 els, temporal windows (time of the day), and analogy criteria were selected manually.  
75 This manual selection requires the comparison of numerous combinations and a compre-  
76 hensive assessment of some parameter ranges. Moreover, the sequential calibration pro-  
77 cedure successively calibrates the different levels of analogy, and thus it does not han-  
78 dle parameters inter-dependencies. Considering these limitations, Horton et al. (2017)  
79 introduced a global optimization of the AM using genetic algorithms (GAs). Using this  
80 approach, an automatic and objective selection of the temporal windows, the vertical lev-  
81 els, the domains, and the number of analogs became possible, improving the method's  
82 prediction skills (Horton et al., 2018). A weighting of the predictor variables has also been  
83 introduced. The only parameters left for a manual selection were the meteorological vari-  
84 ables and the analogy criteria.

85 Selecting predictors for precipitation prediction with AMs in Europe has been the  
86 focus of multiple studies aiming to improve prediction skills (Obled et al., 2002; Bon-  
87 tron, 2004; Gibergans-Báguena & Llasat, 2007; Radanovics et al., 2013; Ben Daoud et  
88 al., 2016). Thus, the relevant predictors are likely to be known nowadays and supported  
89 by expert knowledge. However, transferring AMs to a region with different climatic con-  
90 ditions or to another predictand would involve reconsidering the selected meteorologi-  
91 cal variables. This work aims to test a fully automatic optimization of all AM param-  
92 eters, including the selection of the meteorological variables and even the analogy cri-  
93 teria, using GAs. GAs have already been used for input variable selection (IVS) in other  
94 contexts (D'heygere et al., 2003; Huang et al., 2007; Cateni et al., 2010; Gobeyn et al.,  
95 2017).

96 We here seek to assess the potential of GAs for input variable selection in the con-  
97 text of the analog method. Moreover, we want to test the GAs' ability to jointly select  
98 the distance metric in addition, i.e., the analogy criteria. To compare with well-established  
99 AMs, daily precipitation in central Europe, specifically in Switzerland, has been chosen  
100 as predictand. Also, as is often the case, the AMs were optimized in the perfect prog-  
101 nosis framework, using predictors from reanalyses. This work focuses mainly on the proof  
102 of concept of automatic input variable selection for AMs rather than the details of the  
103 obtained results for the case study.

104 The paper is organized as follows. Section 2 describes the datasets, the fundamen-  
105 tals of AMs, the characteristics of the GAs implementation, the software used, and the  
106 experiment setup details. Section 3 presents the results of different analyses, such as the  
107 selection of the best predictor variable, the relevance of various AM structures, and the  
108 skill of the optimized methods. Section 4 discusses some findings of the work. Finally,  
109 section 5 summarizes the main contributions of the work and open perspectives for ap-  
110 plications of the developed approach.

## 111 2 Material and Methods

### 112 2.1 Data

113 The target variable (predictand) is daily precipitation derived from the RhiresD  
114 gridded dataset from MeteoSwiss. It is a daily aggregation (from 06 UTC of day D to  
115 06 UTC of day D+1) at a 2 km resolution with data from 1961 onward. It is produced  
116 using an interpolation scheme between gauging stations (Frei & Schär, 1998). The grid-  
117 ded data was here spatially aggregated across 25 catchments of about 200 km<sup>2</sup> (Table  
118 1). These catchments were chosen to cover the different climatic regions of Switzerland  
119 (Schüepp & Gensler, 1980), as illustrated in Fig. 1.

120 As often done in the context of the perfect prognosis framework, we used variables  
121 provided by global reanalyses. Even though most reanalyses provide good quality data  
122 over Europe, differences still exist, and the choice of the reanalysis dataset can impact  
123 the skill score of the AM even more significantly than the choice of the predictor vari-  
124 ables (Horton & Brönnimann, 2019). Thus, it was considered advisable to test some of  
125 the following analyses with another reanalysis to assess the robustness of the selected  
126 variables.

127 The main reanalysis used in this work is ERA-Interim (ERA-I, Dee et al., 2011),  
128 which was produced by the European Centre for Medium-Range Weather Forecasts (ECMWF)  
129 and covers the period from 1979 to 2019. The forecast model uses a hybrid sigma-pressure  
130 vertical coordinate on 60 layers and has a T255 horizontal resolution (about 79 km) and  
131 a 30 min time step. The output variables have a grid resolution of 0.75°. The present  
132 work started before the release of ERA5, the successor of ERA-I.

133 The Climate Forecast System Reanalysis (CFSR, Saha et al., 2010), provided by  
134 NCEP, was used for the first experiment to compare the results obtained with ERA-I.  
135 The model used to produce CFSR has a horizontal resolution of T382 (about 38 km) and

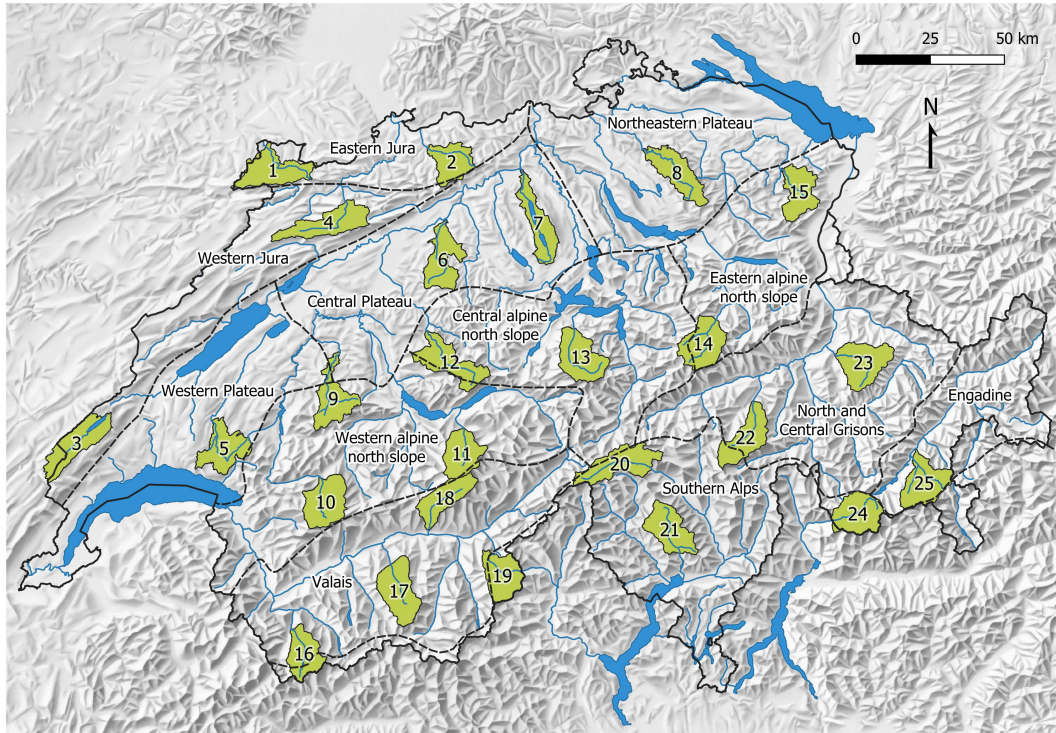


**Figure 1.** Location of the 25 selected catchments in Switzerland along with the climatic regions (dashed lines) and the river network (source: SwissTopo, HADES).

136 64 levels on sigma-pressure hybrid vertical coordinates. The period covered is from 1979  
 137 to August 2019, and the output variables have a spatial resolution of  $0.5^\circ$ .

138 Finally, ERA5 (Hersbach et al., 2019) was used for the last analysis. ERA5 pro-  
 139 vides more variables and a higher spatial grid ( $0.25^\circ$ , but used here at  $0.5^\circ$ ) and tem-  
 140 poral resolution (hourly, but used here at a 3-hourly time step). ERA5 assimilates sig-  
 141 nificantly more data than ERA-I and provides, among others, more consistent sea sur-  
 142 face temperature and sea ice, an improved representation of tropical cyclones, a better  
 143 balance of evaporation and precipitation, and improved soil moisture. ERA5 also relies  
 144 on more appropriate radiative forcing and boundary conditions (e.g., changes in green-  
 145 house gases, aerosols, SST, and sea ice) (Hersbach et al., 2019).

## 146 2.2 Analog Methods

147 AMs are based on the rationale that two similar synoptic situations may produce  
 148 similar local weather (Lorenz, 1956, 1969). It thus consists of extracting past atmospheric  
 149 situations similar to a target date. Selected predictor fields define this similarity. The  
 150 conditional distribution of the predictand of interest (here, daily precipitation) is extracted  
 151 from these analog dates. The analogy is defined by:

- 152 1. The selected meteorological variables (predictors).
- 153 2. The vertical levels at which the predictors are selected.

**Table 1.** Characteristics of the 25 selected catchments in Switzerland

| Id | Name of the river  | Climatic region            | Area<br>(km <sup>2</sup> ) | Mean elevation<br>(m a.s.l.) |
|----|--------------------|----------------------------|----------------------------|------------------------------|
| 1  | L'Allaine          | Eastern Jura               | 209.1                      | 571                          |
| 2  | Ergolz             | Eastern Jura               | 150.3                      | 589                          |
| 3  | L'Orbe             | Western Jura               | 209.3                      | 1229                         |
| 4  | La Birse           | Western Jura               | 203.3                      | 920                          |
| 5  | La Broye           | Western Plateau            | 184.5                      | 791                          |
| 6  | Murg               | Central Plateau            | 184.8                      | 658                          |
| 7  | Aabach             | Central Plateau            | 180.0                      | 562                          |
| 8  | Töss               | Northeastern Plateau       | 189.3                      | 745                          |
| 9  | Sense              | Western alpine north slope | 179.6                      | 1238                         |
| 10 | La Sarine          | Western alpine north slope | 200.8                      | 1779                         |
| 11 | Weisse Lütschine   | Western alpine north slope | 165.0                      | 2149                         |
| 12 | Emme               | Central alpine north slope | 206.9                      | 1151                         |
| 13 | Engelberger Aa     | Central alpine north slope | 204.3                      | 1654                         |
| 14 | Linth              | Eastern alpine north slope | 195.7                      | 1959                         |
| 15 | Sitter             | Eastern alpine north slope | 162.2                      | 1069                         |
| 16 | Dranse d'Entremont | Valais                     | 154.2                      | 2340                         |
| 17 | La Navisence       | Valais                     | 210.5                      | 2541                         |
| 18 | Lonza              | Valais                     | 161.7                      | 2370                         |
| 19 | Doveria            | Southern Alps              | 170.5                      | 2241                         |
| 20 | Ticino             | Southern Alps              | 208.5                      | 2019                         |
| 21 | Verzasca           | Southern Alps              | 187.4                      | 1656                         |
| 22 | Valser Rhein       | North and Central Grisons  | 185.8                      | 2215                         |
| 23 | Plessur            | North and Central Grisons  | 207.7                      | 1928                         |
| 24 | Mera               | Southern Alps              | 190.6                      | 2142                         |
| 25 | Flaz               | Engadine                   | 193.1                      | 2599                         |

- 154 3. The spatial windows (domains) over which the predictors are compared.  
155 4. The hours of the day at which the predictors are considered.  
156 5. The analogy criteria (distance metric to rank candidate situations).  
157 6. Possible weights between the predictors.  
158 7. The number of analog situations  $N_i$  to select for the level of analogy  $i$ .

159 AMs usually start with a seasonal preselection to cope with seasonal effects (Lorenz,  
160 1969). The seasonal preselection is often implemented as a moving window of 120 days  
161 centered around the target date (Bontron, 2004; Marty et al., 2012; Horton et al., 2012;  
162 Ben Daoud et al., 2016). Alternatively, the candidate dates can be preselected based on  
163 similar air temperature at the nearest grid point (Ben Daoud et al., 2016, methods RM5  
164 and RM6 in Table 2). In this work, we used the temporal moving window to reduce the  
165 number of potential candidate dates and, thus, the computing time.

166 The first level of analogy in AMs for precipitation is often based on the atmospheric  
167 circulation using the geopotential height ( $Z$ ) at different pressure levels and hours of the  
168 day (Table 2). The distance (analogy criterion) between two  $Z$  fields is computed on the  
169 vector components of the gradient, i.e., using the difference between adjacent grid cells,  
170 rather than comparing absolute values. The Teweles–Wobus criterion ( $S_1$ , Eq. 1, Tewe-  
171 les & Wobus, 1954; Drosowsky & Zhang, 2003) was identified as the most suited by dif-

**Table 2.** Some analog methods listed by increasing complexity. The analogy criterion is  $S_1$  for Z and RMSE for the other variables.

| Method     | Preselection         | First level                                    | Second level                 | Third level                  | Reference               |
|------------|----------------------|--|------------------------------|------------------------------|-------------------------|
| <b>RM1</b> | $\pm 60$ days        | Z1000@12h<br>Z500@24h                          |                              |                              | Bontron (2004)          |
| <b>RM2</b> | $\pm 60$ days        | Z1000@06h<br>Z1000@30h<br>Z700@24h<br>Z500@12h |                              |                              | Horton et al. (2018)    |
| <b>RM3</b> | $\pm 60$ days        | Z1000@12h<br>Z500@24h                          | MI850@12+24h                 |                              | Bontron (2004)          |
| <b>RM4</b> | $\pm 60$ days        | Z1000@30h<br>Z850@12h<br>Z700@24h<br>Z400@12h  | MI700@24h<br>MI600@12h       |                              | Horton et al. (2018)    |
| <b>RM5</b> | T925@36h<br>T600@12h | Z1000@12h<br>Z500@24h                          | MI925@12+24h<br>MI700@12+24h |                              | Ben Daoud et al. (2016) |
| <b>RM6</b> | T925@36h<br>T600@12h | Z1000@12h<br>Z500@24h                          | W850@06-24h                  | MI925@12+24h<br>MI700@12+24h | Ben Daoud et al. (2016) |

Z, geopotential height; T, air temperature; W, vertical velocity; MI, moisture index.

172 ferent studies (Wilson & Yacowar, 1980; Woodcock, 1980; Guilbaud & Obled, 1998; Bon-  
173 tron, 2004). It is defined as:

$$S_1 = 100 \frac{\sum_i |\Delta \hat{z}_i - \Delta z_i|}{\sum_i \max\{|\Delta \hat{z}_i|, |\Delta z_i|\}} \quad (1)$$

174 where  $\Delta \hat{z}_i$  is the gradient component between the  $i$ th pair of adjacent points from the  
175 geopotential field of the target situation, and  $\Delta z_i$  is the corresponding observed gradi-  
176 ent component in the candidate situation. The gradient components are computed in  
177 both latitude and longitude directions.  $S_1$  ranges from 0 to 200. The smaller the  $S_1$  val-  
178 ues, the more similar the pressure fields. The  $S_1$  criterion characterizes the wind's di-  
179 rection and strength, allowing a comparison of the atmospheric circulation.

180 For other predictors than the geopotential height (e.g., for moisture variables), clas-  
181 sic criteria representing Euclidean distances between grid point values are used: Mean  
182 Absolute Error (MAE) and Root Mean Squared Error (RMSE), the latter being used  
183 most often.

184 The output of the AM is a probabilistic prediction for the target day. It is provided  
185 by the empirical conditional distribution of the  $N_i$  predictand values corresponding to  
186 the  $N_i$  dates selected at the last level of analogy.

187

### 2.3 Genetic Algorithms

188

189

190

191

192

193

194

195

196

GA is a global optimization technique inspired by genetics and natural selection (Holland, 1992). It belongs to the family of evolutionary algorithms and comprises different operators such as natural selection, selection of couples, chromosome crossover, mutation, and elitism. These operators act on parameter sets of the problem to optimize by mixing, combinations, and random modifications. GA aims at combining, over time, the strength of different parameter sets and at exploring the parameters space while converging toward the global optimum. The optimization starts with 2000 random parameter sets (as defined in Sect. 2.2) and is stopped when the best parameter set cannot be improved after 30 iterations.

197

198

199

200

201

202

203

A variant of genetic algorithms (GAs) has been tailored to optimize AMs by Horton et al. (2017). All the method's parameters except the meteorological predictor variables and the analogy criteria have already been successfully optimized using GAs (Horton et al., 2018). The use of GAs provided for the first time an objective and global optimization of AMs, which resulted in gains in prediction skills. To bring the optimization further, the selection of the predictor variables and the analogy criteria were performed here by GAs.

204

205

206

207

208

209

210

211

212

213

214

The reason why the predictor variables and analogy criteria were left out in the previous GA-AM set-up Horton et al. (2017) is the different nature of these variables. The parameters optimized so far by Horton et al. (2017) were quantitative variables, i.e., numerical values (e.g., location and size of the spatial windows or the number of analogs), which have a notion of continuity. The meteorological predictors or analogy criteria, however, are categorical variables that have no relationship among options. They are treated as arrays of independent values by the algorithm. Therefore the mutation operator relying on a search radius in the parameters space (Horton et al., 2017) cannot be applied. Instead, a simple random sampling was used for these parameters when selected for mutation. In addition to the increased difficulty due to the higher number of parameters to optimize, this aspect will likely slow down the optimization.

215

216

217

218

219

220

221

222

223

224

225

226

227

228

In GAs, the mutation operator changes a parameter value (gene) if this parameter was selected to mutate (all parameters have a certain mutation probability). The new value assigned depends on the rules of the mutation operator applied. This operator enables the optimization to explore new areas of the parameters space and was shown to have the most significant impact on the success of the optimization (Horton et al., 2017). Thus, as suggested in Horton et al. (2017), five variants of this operator were used in parallel optimizations (see details in Appendix B): three variants of the non-uniform mutation (Michalewicz, 1996), the multiscale mutation (Horton et al., 2017), and the chromosome of adaptive search radius (Horton et al., 2017). The non-uniform mutation aims to reduce the magnitude of the search in the parameters space with the evolution of the population to transition from the exploration of the whole parameter space to the exploitation of local solutions. This operator has three controlling variables, which makes it difficult to adjust, and thus is used with three different configurations. The multiscale mutation considers both exploration and exploitation in parallel. It has no controlling

229 parameters and no evolution during the optimization. The chromosome of adaptive search  
230 radius was introduced by Horton et al. (2017) and is inspired by the non-uniform mu-  
231 tation. It takes an auto-adaptive approach by adding two chromosomes, one for the mu-  
232 tation rate and one for controlling the search magnitude (see details in Horton et al., 2017).  
233 Therefore, it has no controlling parameters, is thus easier to use, and automatically trans-  
234 sitions from the exploration phase to exploitation.

## 235 2.4 Software

236 The optimization of AMs with GAs is implemented in the open-source AtmoSwing  
237 software<sup>1</sup> (Horton, 2019a) that has been used for this work. AtmoSwing is written in object-  
238 oriented C++ and has been optimized for computational performance. It scales well on  
239 HPC infrastructures as the different members of the GAs populations, i.e., the various  
240 parameter sets, can be assessed in parallel using multiple independent threads. However,  
241 due to the increasingly large number of assessments needed by GAs with the increasing  
242 complexity of the problem, a further reduction in computing time became necessary. In-  
243 deed, while applying AMs to perform a prediction for a single target date is a very fast  
244 and light process, GAs require a substantial amount of parameter assessment over long  
245 calibration periods.

246 A first attempt was based on storing the whole history of the optimization in mem-  
247 ory and looking up for equal – or similar – already-assessed parameters to a newly gen-  
248 erated parameters set. However, this approach turned out to be even more time-consuming  
249 after several generations and led to memory issues for long optimizations.

250 Despite being simple methods, AMs require many comparisons of gridded fields dur-  
251 ing the calibration phase. For example, this work used a 24-year calibration period. For  
252 each target day, a gridded predictor needs to be compared to about 2820 candidate sit-  
253 uations (24\*120-60, using a 120-day temporal window minus 60 days in the target year  
254 that are excluded). Over the entire calibration period, this amounts to about  $24.7 \cdot 10^6$   
255 field comparisons per predictor of the first level of analogy. Here, one optimization re-  
256 quired, on average, about 200 generations made of 2000 individuals, which brings the  
257 average number of grid comparisons to about  $1 \cdot 10^{13}$  per predictor of the first level of  
258 analogy. The comparison of the gridded predictors – i.e., the calculation of the analogy  
259 criteria – was identified by profilers as the most time-consuming task, despite using the  
260 efficient linear algebra library Eigen 3 (Guennebaud et al., 2010).

261 To reduce the processing time, computation using graphics processing units (GPUs)  
262 was implemented for this study in a new release of AtmoSwing, v.2.1.2 (Horton, 2019b).  
263 The calculation of the analogy criteria has been written using NVIDIA’s CUDA. The  
264 implementation details and the results of a benchmark experiment can be found in Ap-  
265 pendix A. When optimizing the methods using ERA5 at a 3-hourly time step and  $0.5^\circ$   
266 resolution, the difference is substantial. One generation (2000 evaluations) took 8 to more

---

<sup>1</sup> <https://atmoswing.org/>

267 than 10 hours using 20 CPU threads, while 50 to 80 minutes were needed using 3 CPU  
 268 threads and 3 GPU devices (NVIDIA GeForce703 RTX 2080).

## 269 2.5 Experiments Setup

270 The experiments were conducted over a 30-year period, from 1981 to 2010, divided  
 271 into a calibration period (CP) and an independent validation period (VP – note that the  
 272 years 2011-2018 were reserved for an additional test period, which was in the end not  
 273 used). To reduce the impact of potential inhomogeneities in the time series, the selec-  
 274 tion of the validation period (VP) was evenly distributed over the entire series (as in Ben  
 275 Daoud, 2010). A total of 6 years was used for the VP by selecting one year out of ev-  
 276 ery five (explicitly: 1985, 1990, 1995, 2000, 2005, 2010). The archive period (AP), where  
 277 the analog dates are being retrieved, is the same as the CP. The VP is also excluded from  
 278 the AP (days from the VP were never used as candidate situations for the selection of  
 279 analogs), as well as a period of  $\pm 30$  days around the target date to exclude potential de-  
 280 pendent meteorological situations. Unless stated otherwise, all results are presented for  
 281 the VP.

282 The GAs optimized all parameters of the method. Only the AM structure (num-  
 283 ber of analogy levels and predictors) was not optimized. Different structures were tested  
 284 in section 3.2. For each level of analogy and each predictor, the following parameters were  
 285 optimized within the corresponding ranges:

- 286 1. Meteorological variable: see section 2.5.1.
- 287 2. Vertical level: see section 2.5.1.
- 288 3. Temporal windows (time of the day): from day D 00 UTC to D+1 06 UTC (c.f.  
 289 precipitation accumulation period, sect 2.1)
- 290 4. Spatial window (domain): latitudes=[35, 55], longitudes=[-10, 20]. The spatial win-  
 291 dows differ between predictors, even in the same level of analogy.
- 292 5. Analogy criterion: see section 2.5.2.
- 293 6. Weight: [0, 1] with a precision of 0.01 (0.05 for experiment 2). The optimizer can  
 294 turn off a variable by setting its weight to zero.
- 295 7. Number of analogs: varies according to the structure, but with an overall range  
 296 of [5, 300] and a step of 5. The optimizer can turn off a level of analogy by set-  
 297 ting its number of analogs to the same value as the previous level of analogy.

298 The CRPS (Continuous Ranked Probability Score; Brown, 1974; Matheson & Win-  
 299 kler, 1976; Hersbach, 2000) was used to assess the skill of the predictions. It evaluates  
 300 the predicted cumulative distribution functions  $F(y)$ , here of the precipitation values  $y$   
 301 associated with the analog situations, compared to the single observed value  $y^0$  for a day  
 302  $i$ :

$$CRPS_i = \int_0^{+\infty} [F_i(y) - H_i(y - y_i^0)]^2 dy, \quad (2)$$

303 where  $H(y - y_i^0)$  is the Heaviside function that is null when  $y - y_i^0 < 0$ , and 1 other-  
 304 wise; the better the prediction, the lower the score.

### 305 **2.5.1 Meteorological Variables**

306 The meteorological variables were considered for different types of vertical levels:  
 307 surface or entire atmosphere (to capture e.g., the moisture content of an entire air col-  
 308 umn), pressure levels (1000, 950, 900, 850, 800, 700, 600, 500, 400, 300, 200 hPa, to cap-  
 309 ture the vertical structure), potential temperature levels (290, 300, 310, 320, 330, 350,  
 310 400 K, necessary to include potential vorticity), and potential vorticity levels. The se-  
 311 lected variables are listed in Table 3. The optimization can pick any variable on any level  
 312 type and value, as long as it is available. Precipitation variables from reanalyses were  
 313 not considered potential predictors. Precipitation is usually not considered as a predic-  
 314 tor in AMs, as a method developed in the perfect prognosis context would then be dif-  
 315 ficult to use in other conditions due to the high uncertainties and the biases associated  
 316 with precipitation predicted by an NWP or a climate model.

317 The variables were standardized (using the overall climatology) on-the-fly by At-  
 318 moSwing when loaded from files. The standardization has no impact on the selection of  
 319 analog situations for a single predictor, but it makes the combination of predictors within  
 320 one level of analogy more balanced, as they might have very different orders of magni-  
 321 tude and units. It allows a more effective optimization of the weights between predic-  
 322 tors.

### 323 **2.5.2 Analogy Criteria**

324 The most common analogy criteria in AMs are the Root Mean Squared Error (RMSE)  
 325 and the Teweles–Wobus criterion ( $S_1$ , see section 2.2). Other criteria were made avail-  
 326 able to the GAs in order to explore potential new characterizations of the analogy met-  
 327 rics. Two of these criteria are new and derived from  $S_1$ . The potential criteria made avail-  
 328 able to the GAs are the following:

- 329 1. RMSE: the Root Mean Squared Error.
- 330 2. MD: the Mean Absolute Difference, or Mean Absolute Error. It differs from the  
 331 RMSE in that the differences are not squared.
- 332 3.  $S_1$ : the Teweles–Wobus index as defined in Eq. 1 from section 2.2. It consists of  
 333 a comparison of the gradients, primarily used for the geopotential height.
- 334 4.  $S_2$ : inspired by the Teweles–Wobus index, we introduced a new criterion based  
 335 on the second derivative of the fields instead of the gradients:

$$S_2 = 100 \frac{\sum_i |\nabla^2 \hat{x}_i - \nabla^2 x_i|}{\sum_i \max\{|\nabla^2 \hat{x}_i|, |\nabla^2 x_i|\}} \quad (3)$$

336 where  $\nabla^2 \hat{x}_i$  is the second derivative between the  $i$ th triplet of adjacent points from  
 337 the predictor field of the target situation, and  $\nabla^2 x_i$  is the corresponding observed

**Table 3.** Selected variables for ERA-I, CFSR, and ERA5 for different types of vertical levels.

| Variable                      | Id    | Unit  | ERA-I |    |    |                | CFSR |    |    |                 | ERA5 |    |                |
|-------------------------------|-------|---|-------|----|----|----------------|------|----|----|-----------------|------|----|----------------|
|                               |       |   | PL    | PT | PV | SC             | PL   | PT | PV | SC              | PL   | SC |                |
| <b>CIRCULATION VARIABLES</b>  |       |   |       |    |    |                |      |    |    |                 |      |    |                |
| Geopotential height           | Z     | gpm   | •     |    | •  |                | •    |    | •  | •               |      | •  |                |
| Geopotential height anomaly   | ZA    | gpm   |       |    |    |                | •    |    |    |                 |      |    |                |
| Zonal wind                    | U     | $\text{m s}^{-1}$                           | •     | •  | •  | • <sup>a</sup> | •    | •  | •  |                 |      | •  | • <sup>a</sup> |
| Meridional wind               | V     | $\text{m s}^{-1}$                           | •     | •  | •  | • <sup>a</sup> | •    | •  | •  |                 |      | •  | • <sup>a</sup> |
| Pressure                      | PRES  | Pa  |       | •  | •  | • <sup>c</sup> |      |    | •  | •• <sup>c</sup> |      |    | • <sup>c</sup> |
| Vertical velocity             | W     | $\text{Pa s}^{-1}$                          | •     | •  |    |                | •    | •  |    |                 |      | •  |                |
| Divergence                    | D     | $\text{s}^{-1}$                             | •     | •  |    |                |      |    |    |                 |      | •  |                |
| Vorticity                     | VO    | $\text{s}^{-1}$                             | •     |    |    |                | •    |    |    |                 |      |    |                |
| Potential vorticity           | PV    | $\text{m}^2 \text{s}^{-1} \text{K kg}^{-1}$ | •     | •  |    |                |      | •  |    |                 |      | •  |                |
| Stream function               | STRM  | $\text{m}^2 \text{s}^{-1}$                  |       |    |    |                | •    |    |    |                 |      |    |                |
| Velocity potential            | VPOT  | $\text{m}^2 \text{s}^{-1}$                  |       |    |    |                | •    |    |    |                 |      |    |                |
| Montgomery potential          | MONT  | $\text{m}^2 \text{s}^{-2}$                  |       | •  |    |                |      |    |    |                 |      |    |                |
| Montgomery stream function    | MNTSF | $\text{m}^2 \text{s}^{-1}$                  |       |    |    |                |      | •  |    |                 |      |    |                |
| <b>MOISTURE VARIABLES</b>     |       |   |       |    |    |                |      |    |    |                 |      |    |                |
| Relative humidity             | RH    | %   | •     |    |    |                | •    | •  |    |                 | •    | •  |                |
| Specific humidity             | SH    | $\text{kg kg}^{-1}$                         | •     | •  |    |                | •    |    |    |                 |      |    |                |
| Total column water            | TCW   | $\text{kg m}^{-2}$                          |       |    |    | •              |      |    |    |                 |      |    | •              |
| Total column water vapour     | TCWV  | $\text{kg m}^{-2}$                          |       |    |    | •              |      |    |    |                 | •    |    |                |
| Cloud water                   | CWAT  | $\text{kg m}^{-2}$                          |       |    |    |                |      |    |    |                 | •    |    |                |
| Surface moisture flux         | IE    | $\text{kg m}^{-2} \text{s}^{-1}$            |       |    |    | •              |      |    |    |                 |      |    |                |
| <b>TEMPERATURE VARIABLES</b>  |       |   |       |    |    |                |      |    |    |                 |      |    |                |
| Temperature                   | T     | K   | •     |    |    | • <sup>b</sup> | •    | •  | •  |                 |      | •  | • <sup>b</sup> |
| Potential temperature         | PT    | K   |       |    | •  |                |      |    |    |                 |      |    |                |
| Dewpoint temperature*         | DT    | K   |       |    |    | • <sup>a</sup> |      |    |    |                 |      |    |                |
| Sea surface temperature       | SST   | K   |       |    |    | •              |      |    |    |                 |      |    |                |
| 0° C isothermal level         | DEG0L | m   |       |    |    | •              |      |    |    |                 |      |    | •              |
| <b>RADIATION VARIABLES</b>    |       |   |       |    |    |                |      |    |    |                 |      |    |                |
| Surf. net solar radiation     | SSR   | $\text{J m}^{-2}$                           |       |    |    | •              |      |    |    |                 |      |    | •              |
| Surf. solar rad. downwards    | SSRD  | $\text{J m}^{-2}$                           |       |    |    | •              |      |    |    |                 |      |    | •              |
| Surf. net thermal radiation   | STR   | $\text{J m}^{-2}$                           |       |    |    | •              |      |    |    |                 |      |    | •              |
| Surf. thermal rad. downwards  | STRD  | $\text{J m}^{-2}$                           |       |    |    | •              |      |    |    |                 |      |    | •              |
| Surf. latent heat flux        | SLHF  | $\text{J m}^{-2}$                           |       |    |    |                |      |    |    |                 |      |    | •              |
| Surf. sensible heat flux      | SSHF  | $\text{J m}^{-2}$                           |       |    |    |                |      |    |    |                 |      |    | •              |
| Top net solar radiation       | TSR   | $\text{J m}^{-2}$                           |       |    |    |                |      |    |    |                 |      |    | •              |
| Top net thermal radiation     | TTR   | $\text{J m}^{-2}$                           |       |    |    |                |      |    |    |                 |      |    | •              |
| <b>STABILITY INDICES</b>      |       |   |       |    |    |                |      |    |    |                 |      |    |                |
| Convective avail. pot. energy | CAPE  | $\text{J kg}^{-1}$                          |       |    |    | •              |      |    |    |                 | •    |    | •              |
| Convective inhibition         | CIN   | $\text{J kg}^{-1}$                          |       |    |    |                |      |    |    |                 | •    |    | •              |
| Best (4 layer) lifted index   | 4LFTX | K   |       |    |    |                |      |    |    |                 | •    |    |                |
| Surface lifted index          | LFTX  | K   |       |    |    |                |      |    |    |                 | •    |    |                |
| Lapse rate                    | LAPR  | $\text{K m}^{-1}$                           |       |    |    |                |      | •  |    |                 |      |    |                |
| <b>OTHERS</b>                 |       |   |       |    |    |                |      |    |    |                 |      |    |                |
| Cloud cover                   | CC    | (0 - 1)                                     |       |    |    |                |      |    |    |                 |      | •  |                |
| Low cloud cover               | LCC   | (0 - 1)                                     |       |    |    |                |      |    |    |                 |      |    | •              |
| Total cloud cover             | TCC   | (0 - 1)                                     |       |    |    |                |      |    |    |                 |      |    | •              |
| Snow depth                    | SD    | m of w.e.                                   |       |    |    | •              |      |    |    |                 |      |    |                |

PL = pressure levels, PT = pot. temp. levels, PV = pot. vorticity levels, SC = single level, surface or total column  
 \*moisture and temperature variable, <sup>a</sup>at 10 m, <sup>b</sup>at 2 m, <sup>c</sup>at mean sea level.

338 second derivative in the candidate situation. Please note that it differs from the  
 339  $S_2$  index from Teweles and Wobus (1954).

340 5.  $S_0$ : as with  $S_2$ , this new criterion derives from  $S_1$  and is processed on the raw grid  
 341 values. It differs from the MD mainly in that it is normalized by the sum of the  
 342 maximum values instead of the number of points:

$$S_0 = 100 \frac{\sum_i |\hat{x}_i - x_i|}{\sum_i \max\{|\hat{x}_i|, |x_i|\}} \quad (4)$$

343 where  $\hat{x}_i$  is the  $i$ th point from the predictor field of the target situation, and  $x_i$   
 344 is the corresponding observed point in the candidate situation. The reason for adding  
 345 such a criterion was accidental, as it was an erroneous implementation of  $S_2$ . How-  
 346 ever, it turned out to be relevant (see sections 3 and 4.2).

347 6. DSD: difference in standard deviation over the spatial window. It is a non-spatial  
 348 criterion, as the location of the features does not matter.

349 7. DMV: absolute difference in mean value. It is also non-spatial, as the means are  
 350 computed over the spatial window before comparison.

### 351 *2.5.3 Design of Experiments*

352 The input variables selection with GAs has been assessed in sequential steps. First,  
 353 GAs were used to identify the single best predictor variables and their associated anal-  
 354 ogy criteria for each catchment (Sect. 3.1). The objective was to assess the consistency  
 355 of the selected variables in the most straightforward configuration. Then, as AMs can  
 356 be made of different levels of analogy with multiple predictors, the second experiment  
 357 assessed the skill associated with different structures and the ability of GAs to deal with  
 358 these, using a limited number of catchments (Sect. 3.2). Based on these results, the third  
 359 experiment performs the input variables selection for each catchment (Sect 3.3).

## 360 **3 Results**

### 361 **3.1 Best Single Variables**

362 The first experiment assesses the use of GAs to select a single predictor variable  
 363 and analogy criterion for each catchment. The selection has been performed on ERA-  
 364 I (Fig. 2) but also on CFSR for comparison (Fig. 3), with six optimizations per catch-  
 365 ment and dataset. The six optimizations were based on different mutation operators (the  
 366 five variants but twice the chromosome of adaptive search radius). The purpose of us-  
 367 ing two reanalyses is to assess the consistency and possible differences in the variables  
 368 selection between two datasets.

369 One of the first elements that can be seen for both datasets is the dominance of  
 370 the  $S_0$  criterion, selected 60% of the time for ERA-I and more than 55% of the time for  
 371 CFSR, along with the other Teweles–Wobus-based criteria (Fig. 4). The other analogy  
 372 criteria were rarely selected, if at all. The same applies to the RMSE, commonly used

373 in analog methods. The GAs could better predict using  $S_0$  as a metric for the Euclid-  
 374 ian distance between the predictor fields. This result is further discussed in Sect. 4.2.

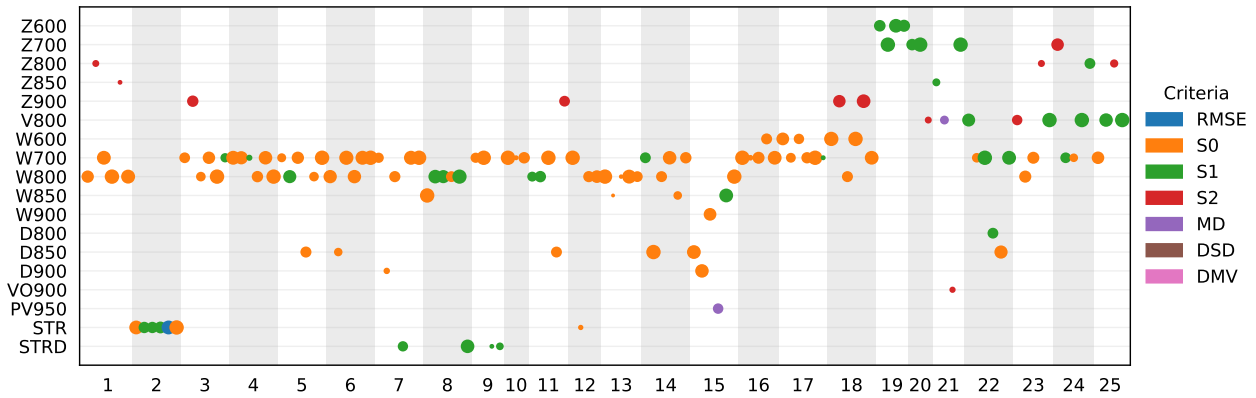


**Figure 2.** Best single variable selected (ordinate; see Table 3 for the variables abbreviations) from ERA-I for the 25 catchments (abscissa). The colors represent the analogy criteria, and the size of the dots is proportional to the skill score of the resulting method (the larger the dots, the better), within a range of 5% of the best result (those with lower skill are hidden).

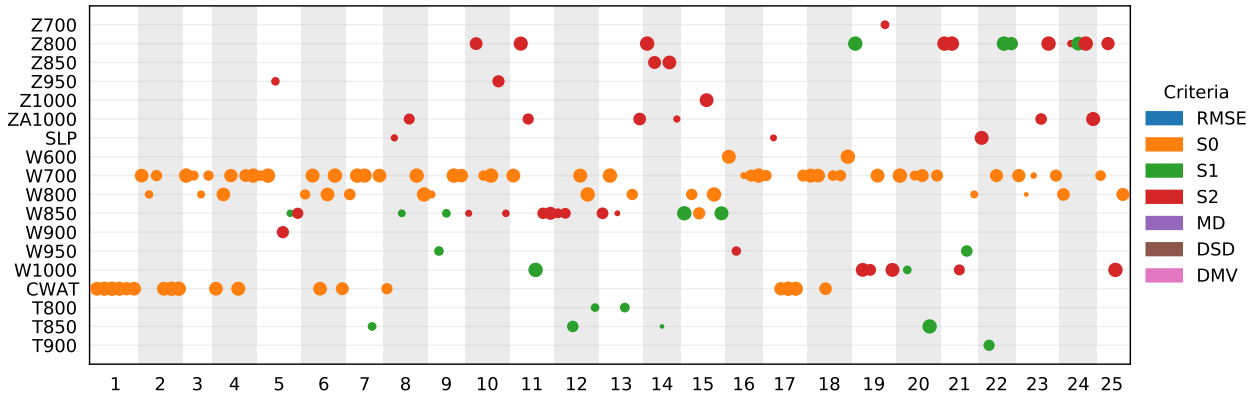


**Figure 3.** Same as Fig. 2 but for CFSR.

375 The variable selection results show some variability per catchment but similar skill  
 376 scores. Although GAs can, in theory, identify the global optimum, this search is highly  
 377 time-consuming for such complex problems, and we have to stop the optimizations at  
 378 a good-enough solution. These factors explain the variability that can be observed in the  
 379 results. Nevertheless, this variability provides information about alternative variables  
 380 with almost the same predictive skills.

381 Figures 2 and 3 demonstrate that optimal variables can vary across different re-  
 382 gions. Figure 5 illustrates this information spatially for ERA-I variables. In terms of sim-  
 383 ilarities, the vertical velocity ( $W$ ) at 700 and 800 hPa is the most frequently selected vari-

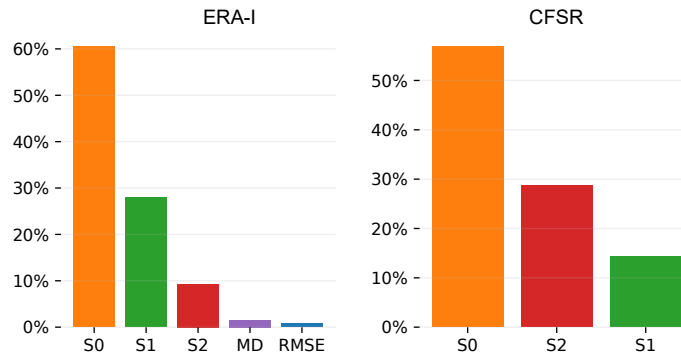


**Figure 4.** Frequency of the criteria selection for both reanalysis datasets.

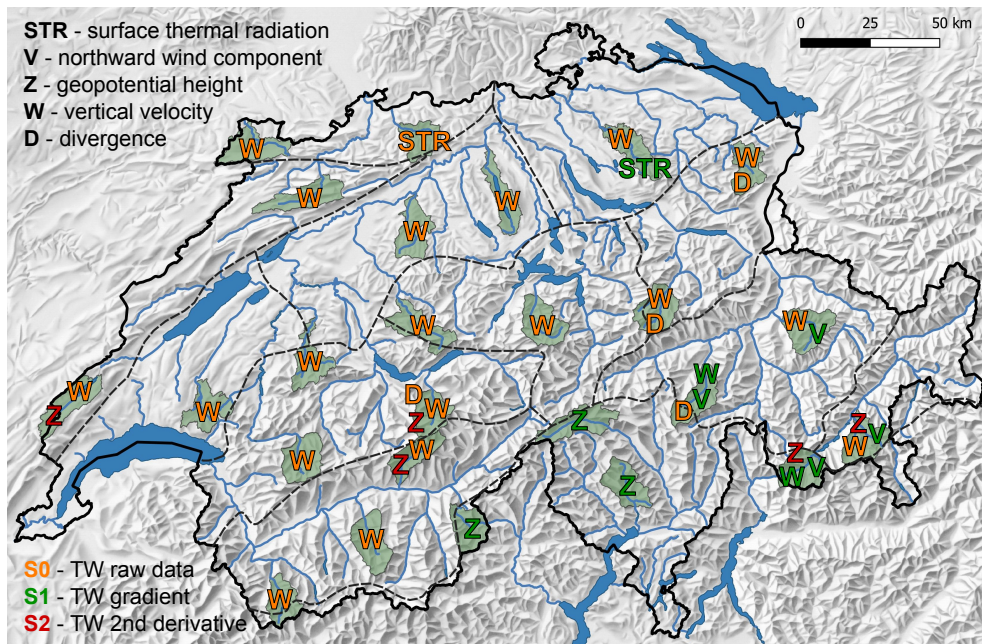


**Figure 5.** Map of the best variables for ERA-I for each catchment.

384 able for both datasets and is quantified using the  $S_0$  criteria. Upward vertical winds at  
 385 these levels are typically associated with precipitation generation. Within the Southern  
 386 Alpine climatic region (catchments 19, 20, 21), Z (based on the  $S_1$  criterion) emerges as  
 387 the best single predictor for ERA-I, which is not so clear with CFSR. Heavy precipita-  
 388 tion events in this region predominantly result from orographic effects related to sustained  
 389 southerly advection of moisture-laden air masses (Massacand et al., 1998). Other regional  
 390 clusters can be observed using ERA-I, such as the meridional wind V (with  $S_1$ ) in the  
 391 eastern part of Switzerland, also likely related to the southerly advection, STR(D) (sur-  
 392 face net thermal radiation and surface thermal radiation downwards) in northern Switzer-  
 393 land, maybe related to cloud cover, and the second derivative of Z (with  $S_2$ ) for several  
 394 catchments at similar latitudes. The second derivative of Z is also frequently selected for  
 395 CFSR. While the variable of cloud water (CWAT) from CFSR is often chosen, it is not  
 396 directly available in ERA-I.

### 3.2 Assessment of AM Structures

The analysis of different AM structures (Sect. 2.5.3) aims to identify the best-performing structures, i.e., the optimal number of analogy levels and predictors. We first considered one to four levels of analogy, with one to four predictors per level. Five optimizations were performed for each of these 16 structures with the different mutation operators. As this assessment requires 80 optimizations, it was performed on only four catchments (L'Allaine (1), Sitter (15), Doveria (19), Flaz (25)). These were selected to maximize the diversity of climatic conditions represented. A complementary analysis was performed on two catchments (L'Allaine (1) and Doveria (19)) to explore the use of up to eight predictors on one and two levels of analogy. These experiments also allowed comparing the performance of the mutation operators for different problem complexities.

Even though the structure is provided to the GAs, it can still evolve to a simpler version by assigning a zero weight to some predictors or by setting the same number of analogs for two successive levels of analogy. This simplification often happened, such as that no solution ended up with the structure 4 x 4 (four levels of analogy with four predictors each). The best-performing methods on the validation period were always made of one or two levels of analogy (Fig. 6 and 7). While some reference methods have up to four levels of analogy (Sect. 2.2), the use of normalized variables and weights might here favor their combination in the same level of analogy. The methods with fewer levels of analogy present less of a hierarchy among the predictors. However, not having a systematic constraint by the atmospheric circulation, as in the reference methods, results in more influence from other variables. Although atmospheric circulation is often of primary importance for heavy precipitation events, there can be situations where it is preferable to relax these constraints. However, we cannot conclude that two levels of analogy are the maximum to be considered, as the optimizer might have failed to optimize complex structures satisfactorily.

The results also depict significant performance differences between the mutation operators (Sect. 2.3). The chromosome of adaptive search radius (option #1) provides the best-performing parameter sets 76.3% of the time for the calibration period and 62.5% of the time for the validation period (Fig. B1). The second best is the non-uniform mutation with a mutation probability ( $p_{mut}$ ) of 0.1 (option #4), being the best option for 11.3% of the optimizations for the calibration period and 21.3% for the validation period. However, the same operator with a mutation probability ( $p_{mut}$ ) of 0.2 (option #5;  $G_{m,r}=100$ ) is the worst-performing option, with a success rate of 1.3% for the calibration period and 2.5% for the validation period. It quite well illustrates the difficulty of tuning such operators and the risk of a badly-configured mutation operator, and thus the benefit of an auto-adaptive option such as the chromosome of adaptive search radius with no controlling parameters. Moreover, it usually performed better for more complex AM structures.

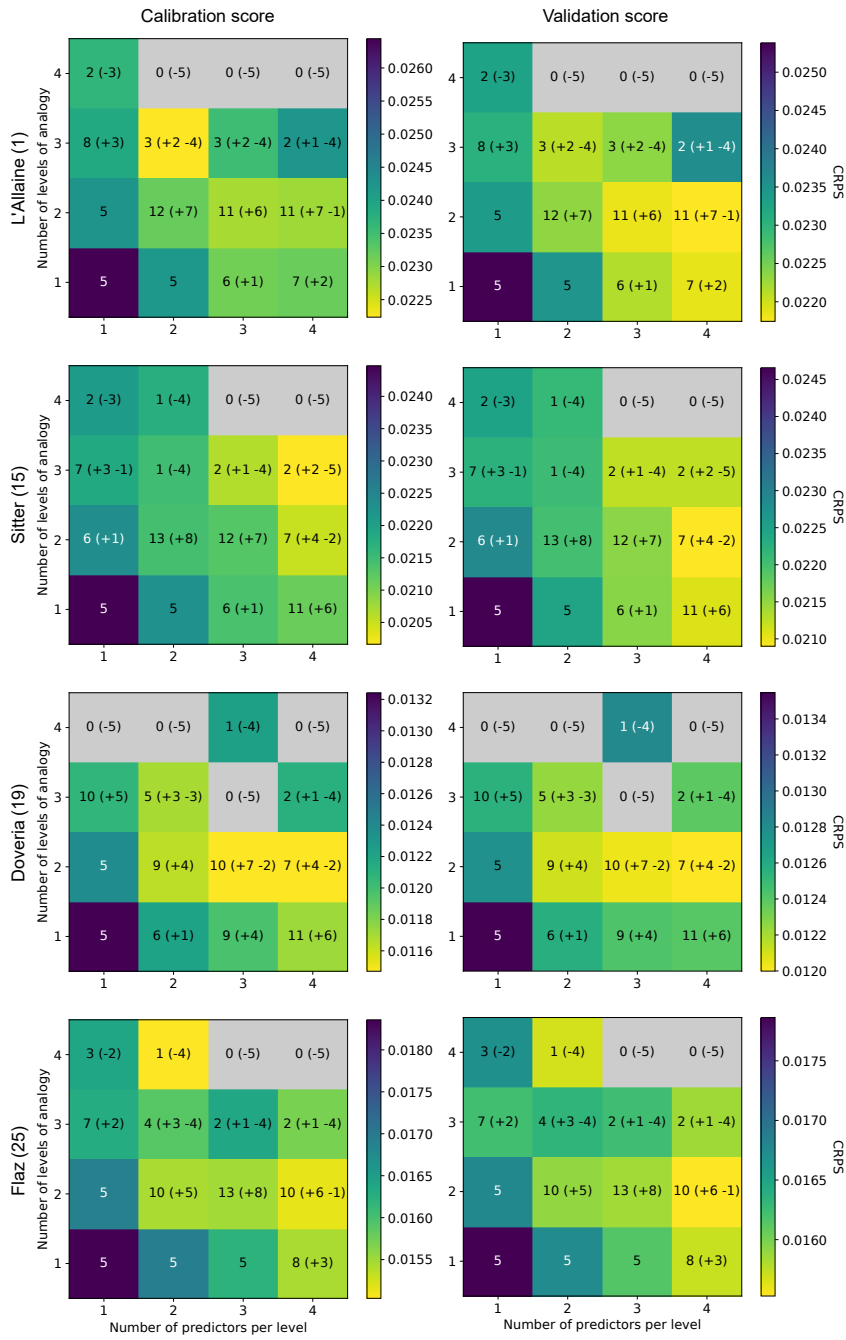


**Figure 6.** CRPS scores obtained for different AM structures with up to four levels of analogy and four variables per level for four catchments in Switzerland. Lower CRPS (yellow) represents a better skill.

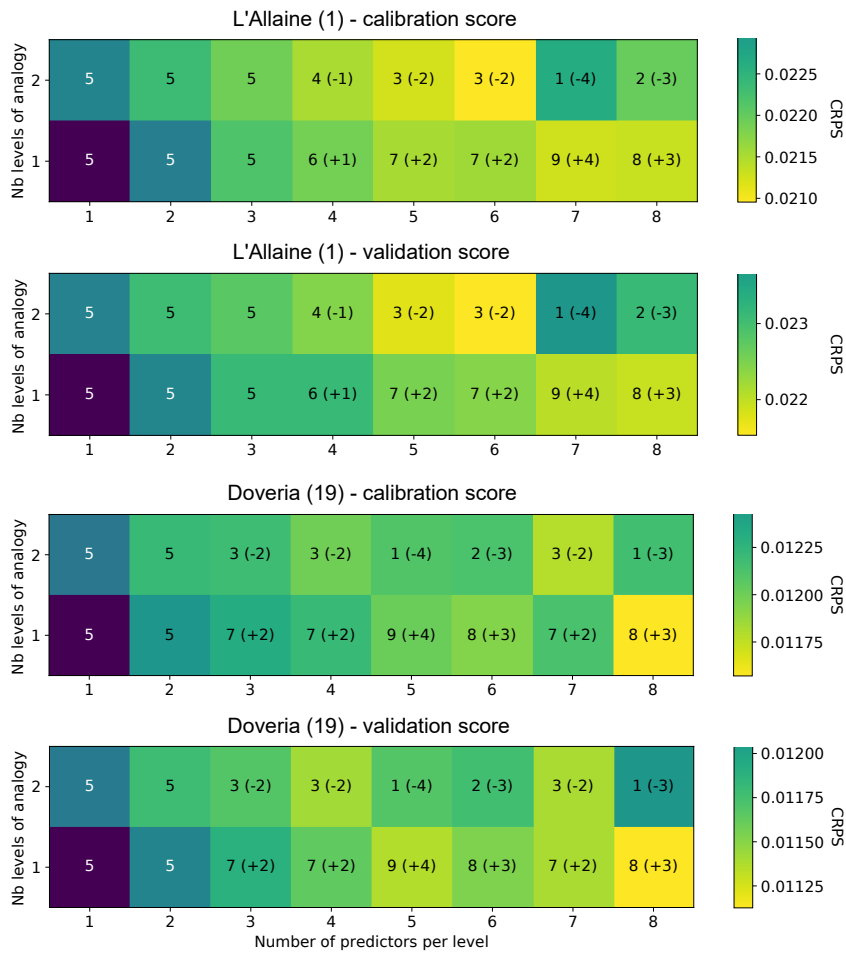


**Figure 7.** CRPS scores obtained for different AM structures with up to two levels of analogy and eight variables per level for two catchments in Switzerland. Lower CRPS (yellow) represents a better skill.

### 436 **3.3 Full Optimization**

437 The third experiment used different AM structures to perform the full input vari-  
438 able selection for each catchment. Only the chromosome of adaptive search radius has  
439 been used because of its higher performance.

#### 440 **3.3.1 Using Variables from ERA-I**

441 Based on the previous results, three AM structures were selected: 1 level of anal-  
442 ogy with 8 (1 x 8) or 12 predictors (1 x 12), and 2 levels with 6 predictors (2 x 6) (Sect.  
443 2.5.3). Two optimizations were performed by structure and catchment. The structure  
444 with two levels of analogy (2 x 6) turned out to be simplified by the GAs to a single level  
445 of analogy (1 x 6) for several catchments. Consequently, this structure resulted in lower  
446 skill scores (Figure 12) as fewer predictors were used. Thus, only structures with a sin-  
447 gle level of analogy (1 x 8 and 1 x 12) are further analyzed here.

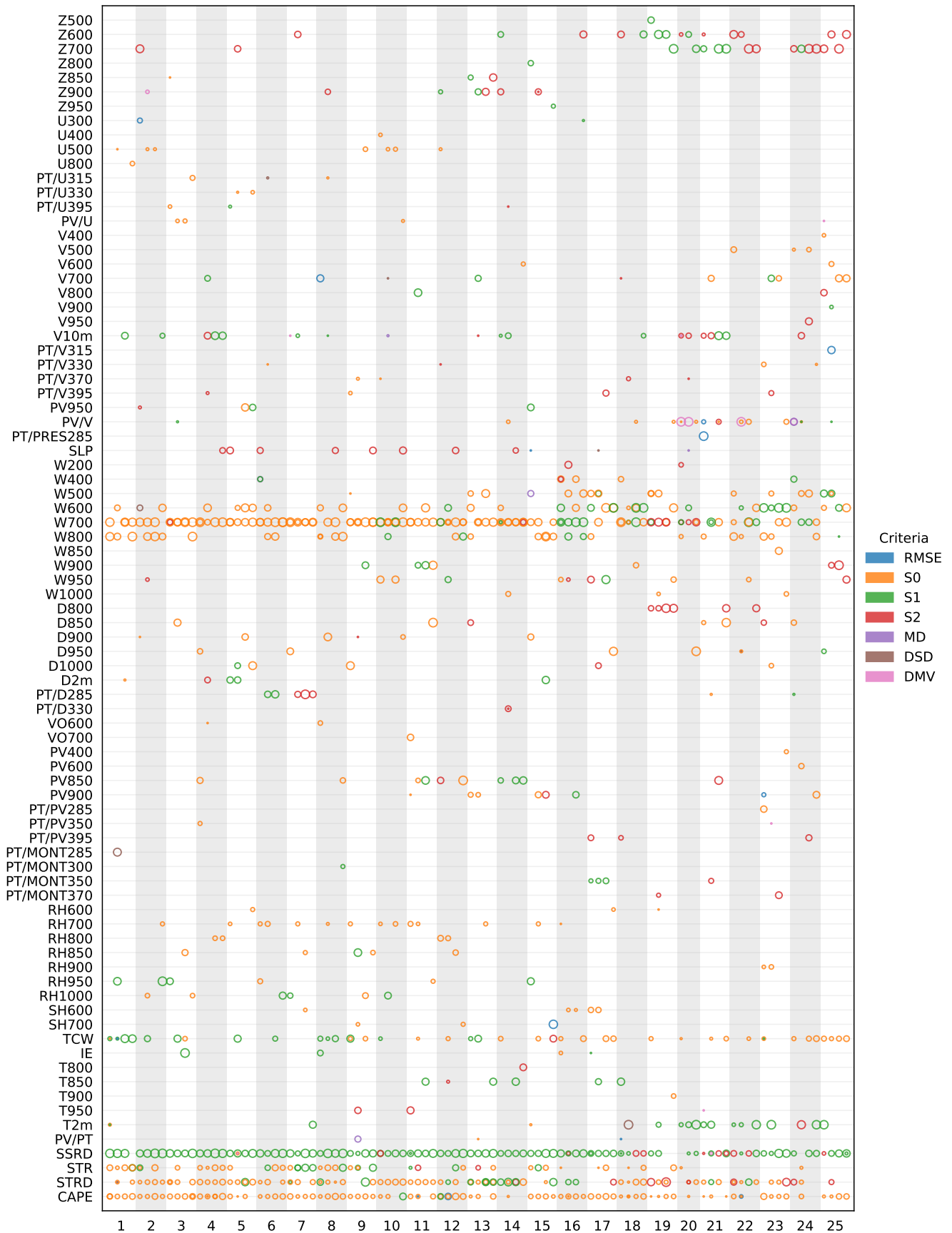


**Figure 8.** Selected variables (see Table 3 for the variables abbreviations) from ERA-I for the 1 x 8 and 1 x 12 structures for the different catchments. The colors represent the analogy criteria, and the size of the dots is proportional to the weight given to the predictor within the range [0.02, 0.2]. Variables that were never selected with a weight equal to or larger than 0.05 are not represented.

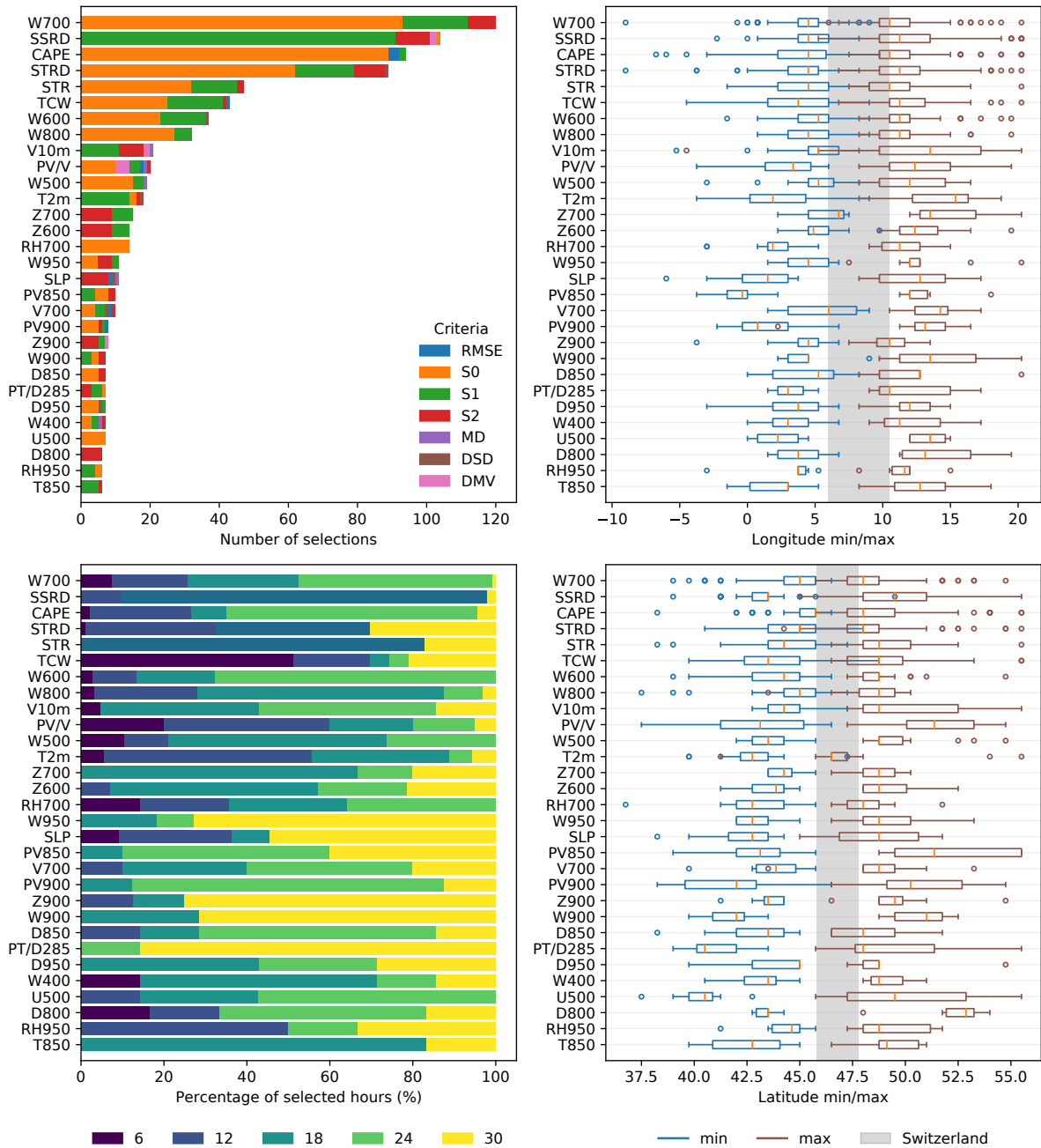


**Figure 9.** Statistics of the 30 most selected variables from ERA-I for the 1 x 8 and 1 x 12 structures for the different catchments (100 optimizations) along with the analogy criteria, the temporal window (30 = next day at 06 UTC; some radiation variables were considered at 15 UTC), and the spatial windows (longitudes and latitudes). The extent of Switzerland is shown in gray on the plots of the spatial windows.

448

449

Figure 8 shows the different variables selected for each catchment along with the analogy criteria (color) and the weights (size). Figure 9 synthesizes the 30 most often

450 selected variables and the associated analogy criteria, temporal windows, and spatial win-  
 451 dows across catchments. These results show again a strong dominance of the  $S_0$ ,  $S_1$ , and  
 452  $S_2$  analogy criteria, with the others being only rarely selected, including RMSE.  $S_0$  is  
 453 most often selected. The properties of  $S_0$  are further investigated in Sect. 4.2.

454 Vertical velocity (W) at 700 hPa (and sometimes at 600 or 800 hPa) is the most  
 455 frequently selected variable, also for catchments that were previously selecting another  
 456 best single variable (Sect. 3.1). Those with higher elevations and located in the south-  
 457 ern part of the country additionally selected W at 500 hPa or even higher.

458 The surface solar radiation downwards (SSRD) is the second most selected vari-  
 459 able and is mainly relevant when compared in terms of gradients ( $S_1$ ) rather than ab-  
 460 solute values. It might thus be used as a proxy for clouds. Other radiation variables oc-  
 461 cupy the fourth and fifth ranks, such as surface thermal radiation downwards (STRD)  
 462 and surface net thermal radiation (STR). These are mainly relevant when compared in  
 463 terms of absolute values ( $S_0$ ), although there is a non-negligible representation of the  $S_1$   
 464 criteria. These can also be used as proxies for cloud cover information.

465 CAPE is the third most selected variable, and the total column water (TCW) is  
 466 the sixth variable. At the ninth position comes the meridional wind at 10 m, but using  
 467  $S_1$  or even  $S_2$ . The derivative of the wind can be informative on the location of frontal  
 468 systems and convergence or divergence zones. Then comes the meridional wind on the  
 469 PV level. The 2 m temperature has the 12th position and is compared in terms of gra-  
 470 dients ( $S_1$ ), which can reflect the position of fronts. Follows the geopotential height (Z)  
 471 at 700 and 600 hPa compared primarily using the second derivatives of the fields ( $S_2$ ).  
 472 The curvature of the geopotential height helps identify and characterize synoptic-scale  
 473 features such as ridges and troughs in the atmosphere. A bit further down on the list,  
 474 SLP is also compared in terms of its second derivative. Other variables such as RH, PV,  
 475 D, and U also populate the 30 best variables.

476 The optimal spatial windows (Figure 9) cover Switzerland most of the time, with  
 477 different extents depending on the variables. For example, while the medians of the op-  
 478 timal domains for W and CAPE are slightly larger than Switzerland, PV is here con-  
 479 sidered on a larger domain. The 2m temperature (T2m) is characterized by unusual, lon-  
 480 gitudinally extended domains, with the main body in southern Switzerland extending  
 481 to the northern Mediterranean. Thus, it likely represents information at a synoptic scale,  
 482 such as the location of fronts, rather than local conditions. Note that SST was also in  
 483 the pool of potential variables but has never been selected as relevant.

484 The optimal temporal windows (time of the day) show substantial variability be-  
 485 tween the predictor variables. At the lower end of the range is TCW, which is consid-  
 486 ered better at the beginning of the precipitation accumulation period (06 UTC). The top  
 487 of the range (06 UTC the next day, corresponding to the end of the accumulation pe-  
 488 riod) was favored by the divergence (D at 285°K) and some low-level W (W900 and W950)  
 489 or Z (Z900). It should be noted here that the radiation variables used were cumulative  
 490 variables that were not decomposed prior to the analysis. Thus, most of the selected tem-  
 491 poral windows correspond to the beginning of the accumulation period, i.e., 15 UTC.

492

### 3.3.2 Using Variables from ERA5

493

494

495

496

497

498

499

500

501

A similar experiment has been conducted using ERA5 and a single method structure (1 x 12). ERA5 has been used at a 3-hourly time step, which might be more relevant than 6-hourly when considering radiation variables, and at a 0.5° spatial resolution. The potential analogy criteria were limited to  $S_0$ ,  $S_1$  and  $S_2$  and the spatial domains were slightly reduced (latitudes=[39, 55], longitudes=[-4, 20]). If previously the weights could be null for a predictor, a minimum of 0.01 was enforced here to force the GAs to select a relevant predictor. Finally, some predictors, often selected in the previous experiment, were fixed: W700 (with  $S_0$  criterion), CAPE (with  $S_0$  criterion), TCW (with  $S_0$  or  $S_1$  criteria); leaving nine predictors unconstrained.

502

503

504

505

506

507

In addition, only the variables found relevant when using ERA-I were selected as potential predictors, thus decreasing the pool of variables. Also, potential temperature levels and PV levels were not considered further. However, cloud cover variables were added to the potential predictors to assess whether SSRD served as a proxy for cloud cover. Thus, this experiment should not be considered a full exploration of ERA5 as it builds on the results obtained for ERA-I.

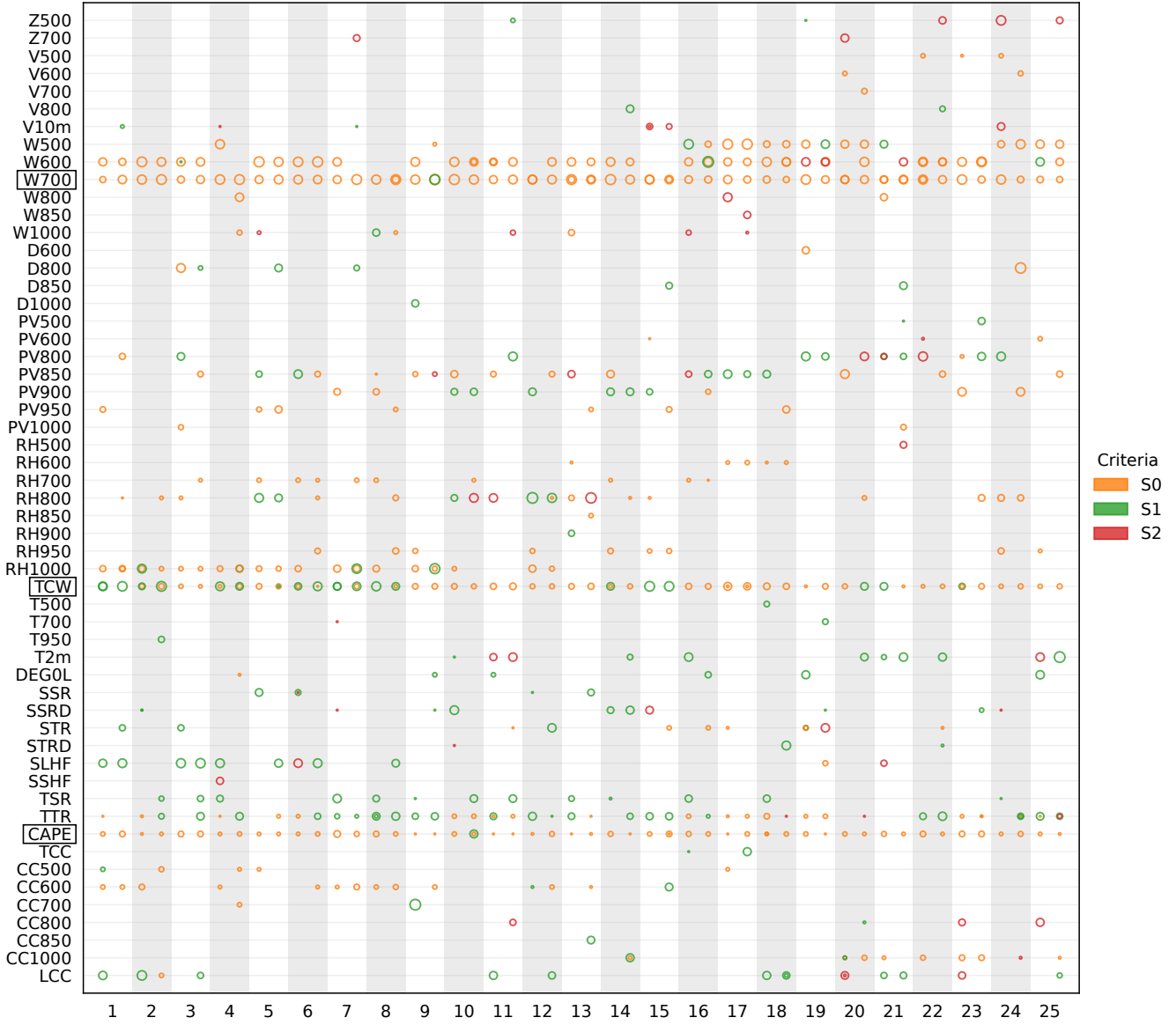


**Figure 10.** Selected variables (see Table 3 for the variables abbreviations) from ERA5 for the 1 x 12 structure for the different catchments. The variables that were forced into the AM are marked with a rectangle. The colors represent the analogy criteria, and the size of the dots is proportional to the weight given to the predictor within the range [0.02, 0.2]. Variables that were never selected with a weight equal to or larger than 0.05 are not represented.

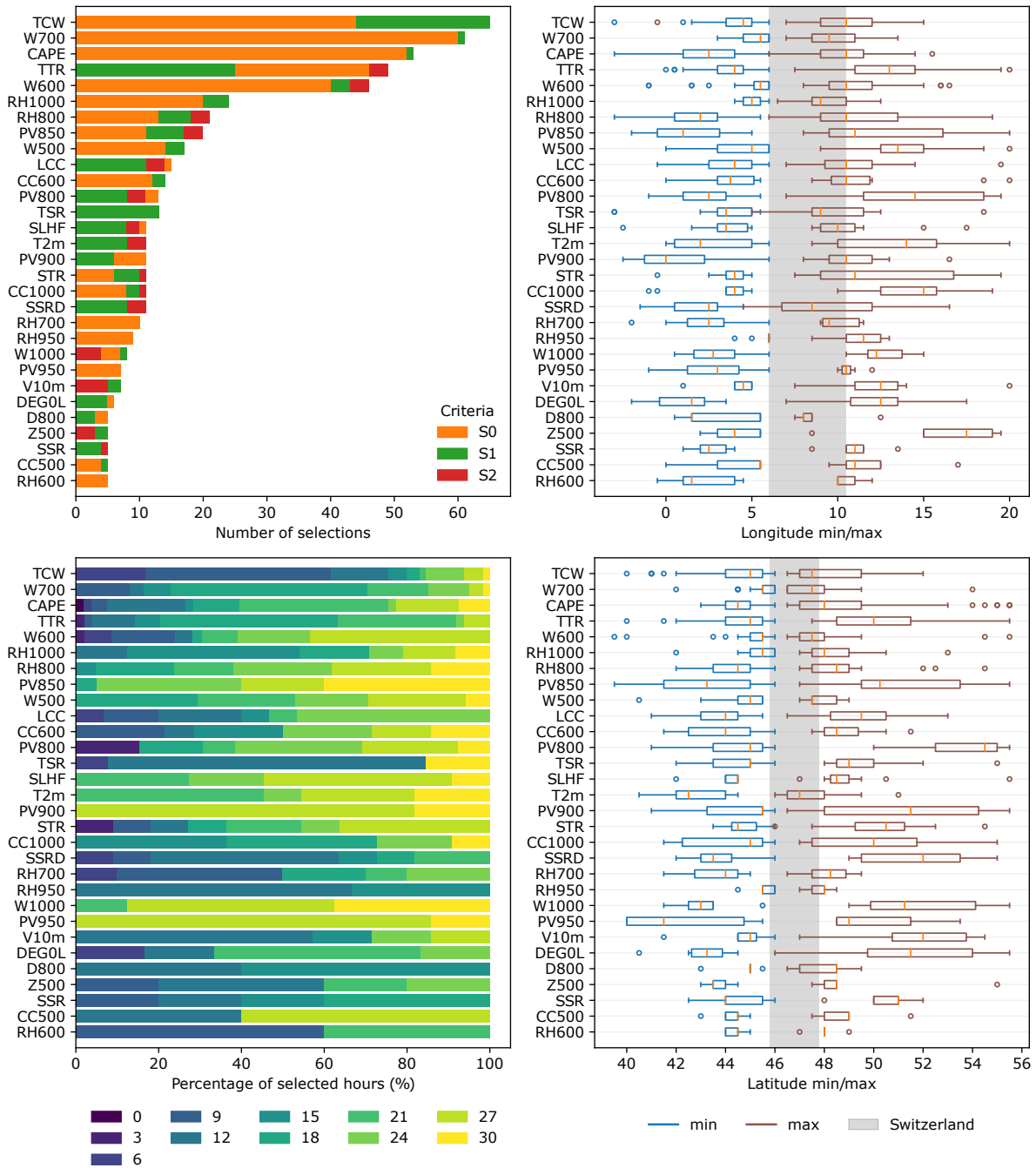


**Figure 11.** Statistics of the 30 most selected variables from ERA5 for the 1 x 12 structure for the different catchments (50 optimizations) along with the analogy criteria, the temporal window (30 = next day at 06 UTC), and the spatial windows (longitudes and latitudes). The extent of Switzerland is shown in gray on the plots of the spatial windows.

508 The selected variables from ERA5 are shown in Figure 10 and 11. When compar-  
 509 ing with ERA-I results, TCW gained importance as it was the most selected variable here.  
 510 Similarly, the relative humidity at 1000 and 850 hPa increased in importance as if its rel-

511 evance improved in ERA5. There were also changes in the radiation variables, with the  
 512 added top (top-of-atmosphere) net thermal radiation (TTR) taking the fourth slot and  
 513 being completed by other ones in the top 30 variables: top net solar radiation (TSR),  
 514 surface latent heat flux (SLHF), surface net thermal radiation (STR), surface solar ra-  
 515 diation downwards (SSRD), and surface net solar radiation (SSR). These variables are  
 516 likely highly correlated, and the selection could be reduced. It can also be noted that  
 517 these variables are still often considered in terms of gradient (using  $S_1$ ), even though cloud  
 518 cover variables were made available. As for cloud cover variables, different ones were se-  
 519 lected in the top 30: the low cloud cover (LCC) and the cloud cover (CC) at 600, 1000,  
 520 and 500 hPa. While LCC was most often considered in terms of gradients, the absolute  
 521 values of the other cloud cover variables were mostly selected. The importance of low  
 522 level PV also increased compared to ERA-I. Conversely, the geopotential height was only  
 523 selected at 500 hPa in the top 30 predictors, SLP is not among the best ones anymore,  
 524 and the presence of the divergence variables also decreased.

525 The optimal spatial domains are comparable with those selected for ERA-I, includ-  
 526 ing the 2-meter temperature extension to the south. As for the temporal windows, TCW  
 527 is again mainly selected between 6 and 12 UTC, and RH at different times of the day.  
 528 PV is often selected at the end of the day, along with W at 1000 hPa, the surface latent  
 529 heat flux (SLHF), and the 2-meter temperature (T2m). The other variables are mainly  
 530 selected during the daytime.

### 531 3.4 Skill Scores

532 To assess the relevance of the methods optimized in this work, they have been com-  
 533 pared to the reference methods (Sect. 2.2). Figure 12 shows the CRPS score improve-  
 534 ment for the different reference and resulting methods compared to the simplest RM1  
 535 method. The CRPS values being heavily influenced by the climatology and thus signif-  
 536 icantly different from one catchment to another, they are best compared relatively to a  
 537 reference catchment-wise.

538 The improvement of the CRPS is shown for the first single variable selection from  
 539 ERA-I (ERA-I GAS 1x1), the full optimizations using ERA-I (ERA-I GAS 1x8, 1x12,  
 540 1/2x6) or ERA5 (ERA5 GAS 1x12). An additional experiment has been attempted by  
 541 pre-selecting the predictor variables (along with their vertical level and their time) and  
 542 the analogy criteria and letting the GAs optimize the weights between these variables,  
 543 along with the spatial domains. To this end, 26 of the most commonly selected ERA5  
 544 variables were provided to the optimizer, organized in a single level of analogy (1x26).  
 545 The results are shown in Appendix C. As shown in Figure 12, this approach does not  
 546 provide the best skill scores. It can be due to non-optimal choices made to homogenize  
 547 the vertical levels or times of the day, for example. In addition, this approach is not com-  
 548 putationally efficient as it requires loading variables that barely play a role in the selec-  
 549 tion of analog situations. Therefore, we do not recommend using such a strategy.

550 One can see in Fig. 12 that the selection of a single best variable (GAS 1x1) al-  
 551 ready achieves better skill than the RM1 method. Obviously, the skill provided by a sin-

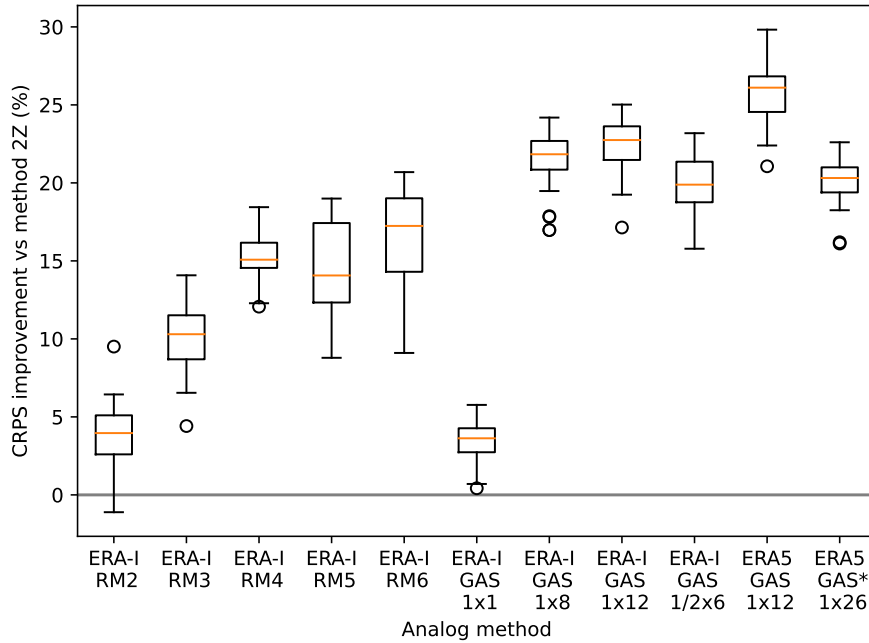


**Figure 12.** Performance scores of the different reference and optimized methods on the validation period for the 25 catchments. The skill score is expressed as a percentage improvement (lower values) in terms of the CRPS when considering RM1 as a benchmark. An LxP code represents the structures, with L being the number of levels of analogy and P being the number of predictors per level.

552 gle variable remains lower than more complex AMs. All other optimized methods per-  
 553 form substantially better than the reference methods. Thus, despite having a single level  
 554 of analogy, they outperform complex stepwise AMs. The gain obtained using ERA5 in-  
 555 stead of ERA-I can be due to higher spatial and temporal resolutions or better variables  
 556 (Horton, 2021). The selection of the predictor variables and the analogy criteria by GAs,  
 557 along with all other parameters, provides AMs that prove relevant, also on the valida-  
 558 tion period.

## 559 4 Discussion

### 560 4.1 Transferability of the Results

561 The main aim of this work was to test the ability of GAs to select input variables  
 562 for analog methods. It was found that GAs could select relevant predictors with the anal-  
 563 ogy criteria to quantify their similarity. However, it may not be optimal to use the se-  
 564 lected predictors in another context blindly. Indeed, the list of potential variables must  
 565 be adapted to the application of the AM.

566 Depending on the application, some specific constraints should be considered for  
 567 optimizing AMs. For example, for use in forecasting, only meteorological variables that  
 568 are considered sufficiently well-predicted should be selected. As for climate impact stud-

ies, the availability of meteorological variables is significantly more limited than what a reanalysis and standard climate model output can offer. In addition, care should be taken to select variables that have a causal effect on the predictand of interest and avoid undesirable co-variability.

#### 4.2 What About this $S_0$ Criteria?

The success of the  $S_0$  criteria over RMSE was unexpected. Overall, the triplet  $S_0$ ,  $S_1$  and  $S_2$  dominate the selection of analogy criteria.  $S_1$  was developed to verify prognostic charts (Teweles & Wobus, 1954). It was computed using pressure differences between stations arranged in north-south and east-west lines. The "difficulty coefficient" (the denominator) reduces the influence of the seasons and weather systems' strength on the score. About forty other scores were developed and assessed by Teweles and Wobus (1954), but  $S_1$  was the most stable. It was also selected to penalize forecasters who tended to be overly conservative by forecasting weak systems too often. Indeed, the denominator being the sum of the maximum gradients of the forecast or the observation, the forecast of a weaker system is more penalized than that of a stronger system. However, this could result in the opposite effect as it is safer for the forecaster to predict a stronger system with larger gradients and thus make the denominator larger (Thompson & Carter, 1972).

The  $S_0$  and  $S_2$  criteria have the same characteristic as  $S_1$ , i.e., they penalize more heavily weaker fields. Let us consider a field F1 with values 50% lower than the target field (F), and another one, F2, with values 50% higher. Then,  $S_0(F, F1) = 50$  and  $S_0(F, F2) = 33.3$  while the absolute differences between the target (F) and F1 or F2 are equal. F2 will then be selected as a better analog. To get the same  $S_0$  value, F2 would need to double the target field values. The consequence is that the selection of analogs based on  $S_0$ ,  $S_1$  and  $S_2$  is not symmetrical, and these criteria tend to select fields that are close to the reference but preferably stronger than weaker.

To investigate further the characteristics of  $S_0$ , we considered a variation named here  $S_{0obs}$  that uses the observation (here, target situation) values only for the denominator and not the maximum between observation and forecast (here, candidate analog). It is then similar to the MAPE (Mean Absolute Percent Error) and is symmetrical. We performed a classic calibration of a simple AM using only W700 with (1) the  $S_0$  criteria, (2) the RMSE criteria, and (3) the  $S_{0obs}$  criteria. The calibration was performed for each setup separately. Using RMSE deteriorates the skill score by 8.7% on average, and  $S_{0obs}$  also deteriorates the skill score by 9.8%. Thus, the asymmetrical property of  $S_0$  is beneficial for the prediction.

We then considered the reference method RM3 and performed a classic calibration for the 25 catchments by replacing one or the other criterion. When using  $S_{1obs}$  ( $S_1$  normalized by the gradients of the observations only) instead of  $S_1$  for Z, the skill score deteriorates by 4.8% on average. However, when replacing the RMSE of the second level of analogy (MI) with  $S_0$ , there is a slight loss in performance of 0.5%. As there is strong conditioning by the first level of analogy that provides the sample of candidate analog

610 dates to be subsampled on moisture variables, the criterion of the second level of anal-  
 611 ogy has a lower impact.

612 It seems therefore that the asymmetrical properties of  $S_0$ ,  $S_1$ , and  $S_2$  are benefi-  
 613 cial for the prediction. Analog situations are best considered a bit stronger than weaker  
 614 while being close to the target situation. The CRPS is mainly sensitive to high precip-  
 615 itation values, even more when the precipitation is not transformed (see Bontron, 2004,  
 616 for precipitation transformation). Thus, one hypothesis is that large precipitation events  
 617 being underrepresented in the archive, AMs are better off selecting stronger predictor  
 618 fields, often associated with higher precipitation. It might then play a role of bias com-  
 619 pensation for underrepresented high precipitation events. The reason for such behavior  
 620 should be investigated further.

## 621 5 Conclusions

622 The objective of the work was to assess the ability of GAs to select the input vari-  
 623 ables of the analog method along with the analogy criteria. The experiment was success-  
 624 ful as the selected predictors provided better skills than the reference methods. More-  
 625 over, most of the selected variables can be related to meteorological processes involved  
 626 in precipitation generation. For example, among the most selected variables are: the ver-  
 627 tical velocity (W) at 700 hPa (along with other levels), the total column water (TCW),  
 628 the convective available potential energy (CAPE), radiation variables, the potential vor-  
 629 ticity (PV), the relative humidity (RH), cloud cover variables, wind components, the geopo-  
 630 tential height, air temperature, and the divergence.

631 The selection of analogy criteria also proved fruitful, as there were clear trends to-  
 632 ward a dominant criterion for a given variable. The unexpected result was the success  
 633 of the criterion  $S_0$ , inspired by the Teweles-Wobus criterion. This new  $S_0$  turned out to  
 634 be the most often selected analogy criterion, replacing the RMSE for the characteriza-  
 635 tion of Euclidean distances. Three analogy criteria were most often selected, and all are  
 636 derived from the Teweles-Wobus criterion; one is based on the raw point values, another  
 637 on the gradients, and the third on the second derivative of the fields. All of them are nor-  
 638 malized by the sum of the largest point(pair)-wise values from the target and the can-  
 639 didate fields. This normalization makes the criteria asymmetrical, so that higher values  
 640 are preferred to lower ones. Heavy precipitation, which substantially influences the CRPS,  
 641 is often associated with more dynamic situations, characterized by higher values. The  
 642 GAs may try to compensate for the under-representation of heavy precipitation events  
 643 by favoring situations associated with higher precipitation values. These assumptions  
 644 would need to be further investigated.

645 Another unexpected result is the preferred structure for the analog methods. While  
 646 most reference methods build on a stepwise selection of predictors with successive lev-  
 647 els of analogy subsampling from the previous one by using different predictors, here, the  
 648 GAs preferred a flatter structure, mainly with a single level of analogy, but more vari-  
 649 ables. The reference methods most often start with selecting candidate analogs using the  
 650 geopotential height and then narrowing down the selection using vertical velocity or mois-

651 ture variables. A primary difference with the reference methods is that the variables are  
652 standardized here, and weights are used (and optimized) to combine them in a given level  
653 of analogy. These two elements make the combination of variables with different value  
654 ranges easier. However, it cannot be excluded that deeper structures can provide bet-  
655 ter results, but that GAs did not find these solutions.

656 Such optimization is computationally intensive. The new GPU-based computations  
657 brought significant time improvement, particularly for high-resolution data. Other ap-  
658 proaches could be considered to decrease the computation time, such as a faster explo-  
659 ration of the dataset using a smaller period for data pre-screening, or the division of the  
660 whole period into smaller batches. An alternative could be to reduce the number of days  
661 with small precipitation amounts, as they have a small impact on the CRPS, while weight-  
662 ing their contributions by using a weighted CRPS approach.

663 This work opens new perspectives for input variables selection in the context of the  
664 analog method. While the variables selected in these experiments might not be trans-  
665 ferable to other contexts, the approach was proven successful and can be applied to other  
666 datasets. The potential variables must be chosen wisely regarding the application intended.  
667 Such an approach can, for example, be used to select the relevant variables to predict  
668 precipitation for a new location, or as a data mining technique to explore a dataset to  
669 predict a new predictand of interest.

## 670 **Appendix A GPU Implementation and Benchmark**

671 Several GPU implementations were tested, with the most successful aiming to re-  
672 duce the data copy to the device while increasing the load of parallel processing. It con-  
673 sisted in copying the predictor data to the device and calling the kernel<sup>2</sup> for every tar-  
674 get date, thus assessing all candidates for that target date in one call. The main ben-  
675 efit of this variant is that it allows overlapping – using streams – the calculation of the  
676 analogy criteria on the GPU and other calculations on the CPU, such as the extraction  
677 of the indices corresponding to the candidate dates (using a temporal moving window  
678 of 120 days) and the sorting of the resulting analogy criteria.

679 Threads on the GPU are organized in dynamically defined blocks, with a size from  
680 32 to 1024 threads. Here, every candidate date is assigned to a different block, with in-  
681 ternal loops for cases where the number of grid points is higher than the number of threads  
682 in the block. All analogy criteria need a reduction step to synthesize a two-dimensional  
683 array into a single value. The reduction is part of the analogy criteria calculation and  
684 is thus also done on the GPU. The threads are organized in groups of 32, called warps,  
685 that are synchronous and can access each other’s registers. The reduction on the device  
686 was performed with an efficient warp-based reduction using the CUDA shuffle instruc-  
687 tion. Different block sizes were assessed, and the size of 64 threads was identified as op-  
688 timal as it leaves fewer threads inactive during the reduction. Access to the GPU’s global  
689 memory has also been kept to a minimum due to its higher latency.

---

<sup>2</sup> A kernel is a numerical function executed in parallel on the GPU.

690 The Google benchmark library was used to assess the computing time of different  
 691 AM structures – single or two levels of analogy and up to four predictors per level – along  
 692 with various grid sizes. Figure A1 shows the results for the analogy criterion  $S_1$ , with  
 693 gradients being pre-processed using CPUs only (counted in the total time). The other  
 694 analogy criteria showed similar results. The task consisted of extracting analogs for 32  
 695 years using the other 31 years as archives for candidate situations within a 120-days tem-  
 696 poral window. It makes a total of  $43.5 \cdot 10^6$  field comparisons per predictor of the first  
 697 level of analogy.

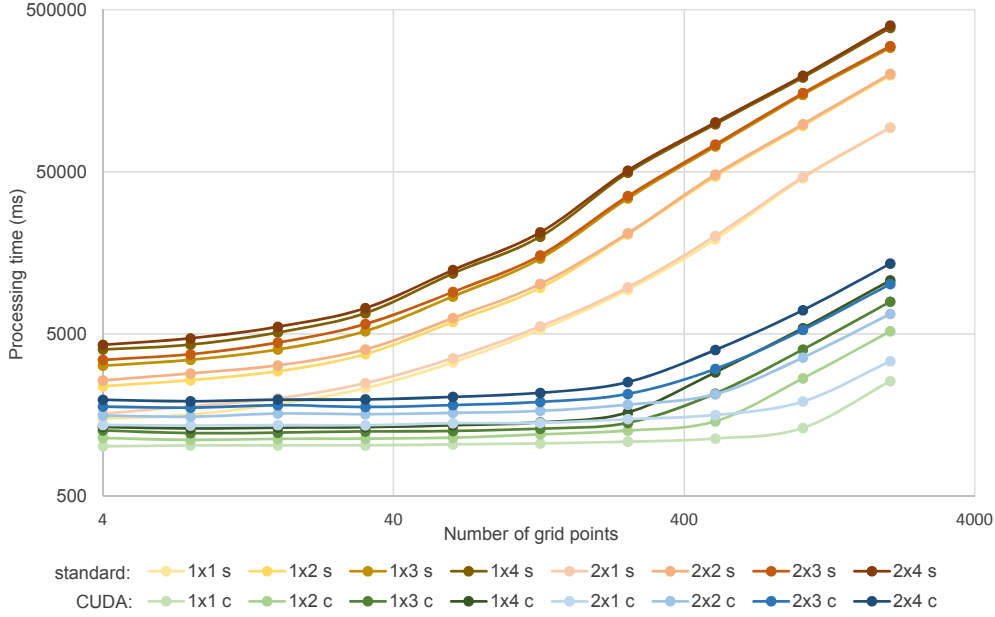


**Figure A1.** Computing time for the extraction of analogs over 32 years using the  $S_1$  criteria for different grid sizes and various structures of AMs. An LxP code represents the structures, with L being the number of levels of analogy and P being the number of predictors per level. Time is given for using (s) standard CPUs and (c) CUDA on GPUs (NVIDIA GeForce RTX 2080). Note the logarithmic axes.

698 The experiment was conducted on the UBELIX cluster of the University of Bern,  
 699 using the same node for the whole benchmark and processing on a single NVIDIA GeForce  
 700 RTX 2080 graphics card. The CPU processing – using the linear algebra library Eigen  
 701 3 (Guennebaud et al., 2010) – was done on a single thread. Although AtmoSwing can  
 702 parallelize the calculation of the analogy criteria on multiple CPU threads, it uses a sin-  
 703 gular thread for this task when optimizing with GAs because it parallelizes the evaluation  
 704 of the different individuals on multiple threads. With GPUs, it still assesses the individ-  
 705 uals on multiple CPU threads, each of them being able to use a different GPU device  
 706 to calculate the analogy criteria. It is thus parallelizing both on CPUs and GPUs.

707 The benchmark (Fig. A1) shows that the GPU computations are systematically  
 708 faster than those on the CPU, and this difference increases with the number of grid points.  
 709 The GPU computations were 13 times faster on average and up to 38 times faster (5.2 sec

710 instead of 3.3 min) when using 2048 points. Model outputs and reanalyses show an in-  
 711 crease in spatial resolution; thus, the impact on the computation time will become in-  
 712 creasingly important. When using CPU only, adding a predictor in the first level of anal-  
 713 ogy has a much higher impact on time than adding a second level of analogy. It is ex-  
 714 plained by the fact that it needs to process the analogy criteria for the whole archive for  
 715 each predictor of the first level of analogy, while the second level has only a few candi-  
 716 date situations to assess.

## 717 **Appendix B Performance of the Mutation Operators**

718 As suggested in Horton et al. (2017), five variants of the mutation operator were  
 719 used in parallel optimizations:

- 720 1. Chromosome of adaptive search radius (Horton et al., 2017)
- 721 2. Multiscale mutation (Horton et al., 2017)
- 722 3. Non-uniform mutation ( $p_{mut}=0.1$ ,  $G_{m,r}=50$ ,  $w=0.1$ )
- 723 4. Non-uniform mutation ( $p_{mut}=0.1$ ,  $G_{m,r}=100$ ,  $w=0.1$ )
- 724 5. Non-uniform mutation ( $p_{mut}=0.2$ ,  $G_{m,r}=100$ ,  $w=0.1$ )

725 where  $p_{mut}$  is the mutation probability,  $G_{m,r}$  is the maximum number of gener-  
 726 ations (G) during which the magnitude of the research varies, and  $w$  is a chosen thresh-  
 727 old to maintain a minimum search magnitude when  $G > G_{m,r}$ .

728 Figure B1 shows the performance of these five mutation operators for different AM  
 729 structures and the different catchments considered in Sect. 3.2. Overall, the chromosome  
 730 of adaptive search radius has a success rate of 76.25% in calibration and 62.5% in val-  
 731 idation, the multiscale mutation 7.5%, and 8.75% respectively, and the non-uniform mu-  
 732 tation with its different options: (3) 11.25% and 10%, (4) 11.25% and 21.25%, and (5)  
 733 1.25% and 2.5% respectively.

734 Thus, it is quite clear that the chromosome of adaptive search radius obtains the  
 735 best results, all the more so with more complex structures, i.e., more predictor variables.  
 736 Although its success rate decreases slightly in validation, it remains much larger than  
 737 the other options. The non-uniform mutation shows significant variability of performance  
 738 depending on its options.

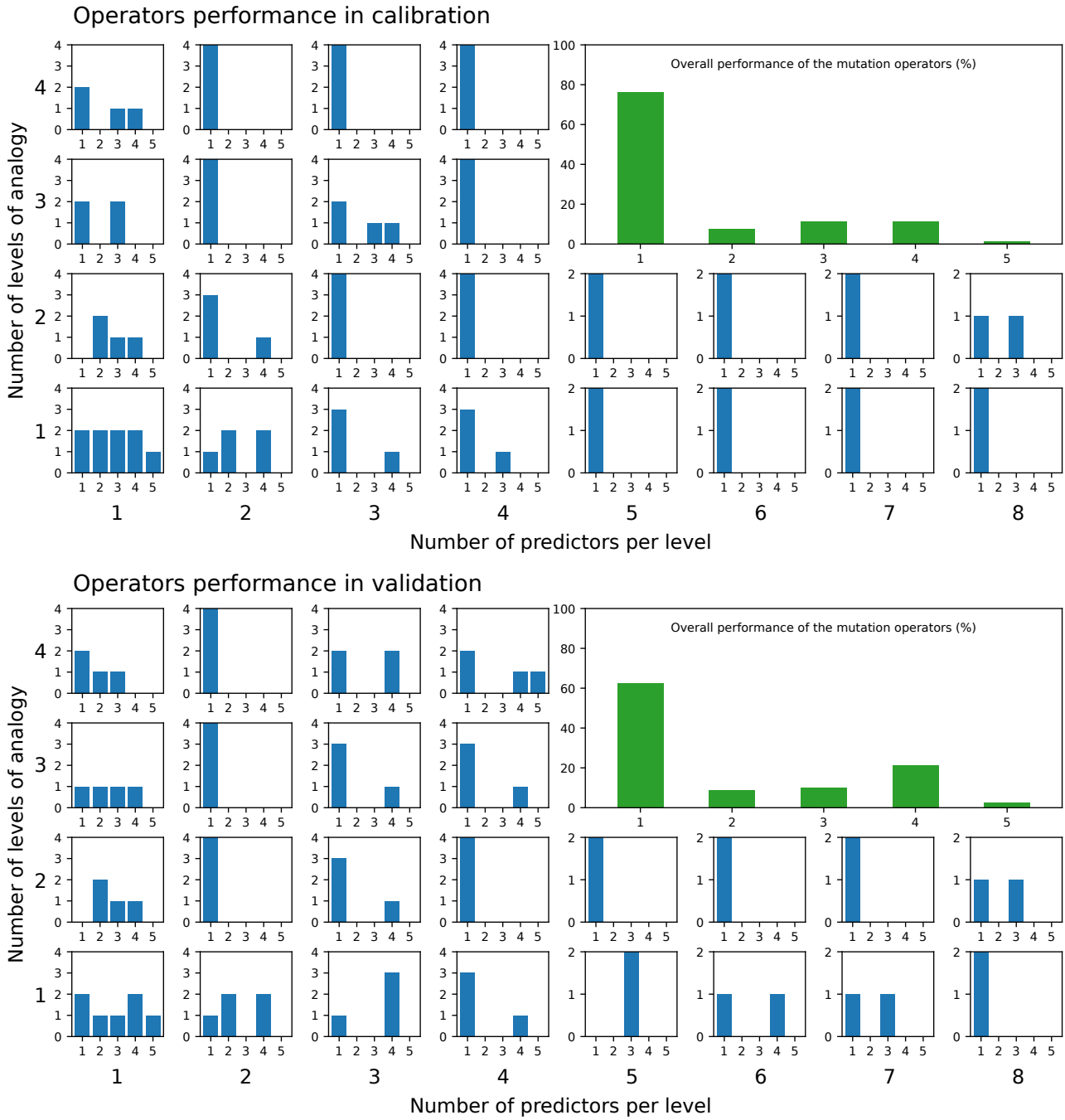


**Figure B1.** Performance of the five mutation operators (Sect. 2.3) for different AM structures and the different catchments considered in Sect. 3.2. The values represent the number of optimizations for one mutation operator that resulted in the best performing AM. Results are shown for both calibration and validation. When multiple operators obtain the same skill score, they all get a point.

**739 Appendix C An Attempt to Constrain the Algorithms**

740 An additional experiment has been attempted by pre-selecting the predictor vari-  
741 ables (along with their vertical level and their time) and the analogy criteria and letting  
742 the GAs optimize the weights between these variables, along with the spatial domains.  
743 To this end, 26 of the most commonly selected ERA5 variables were provided to the op-  
744 timizer, organized in a single level of analogy. The results are shown in Figure C1 and  
745 depict high weight values for  $W$  at 600 and 700 hPa. Surprisingly,  $Z_{700}$  based on  $S_2$  also  
746 gets relatively high weight values.

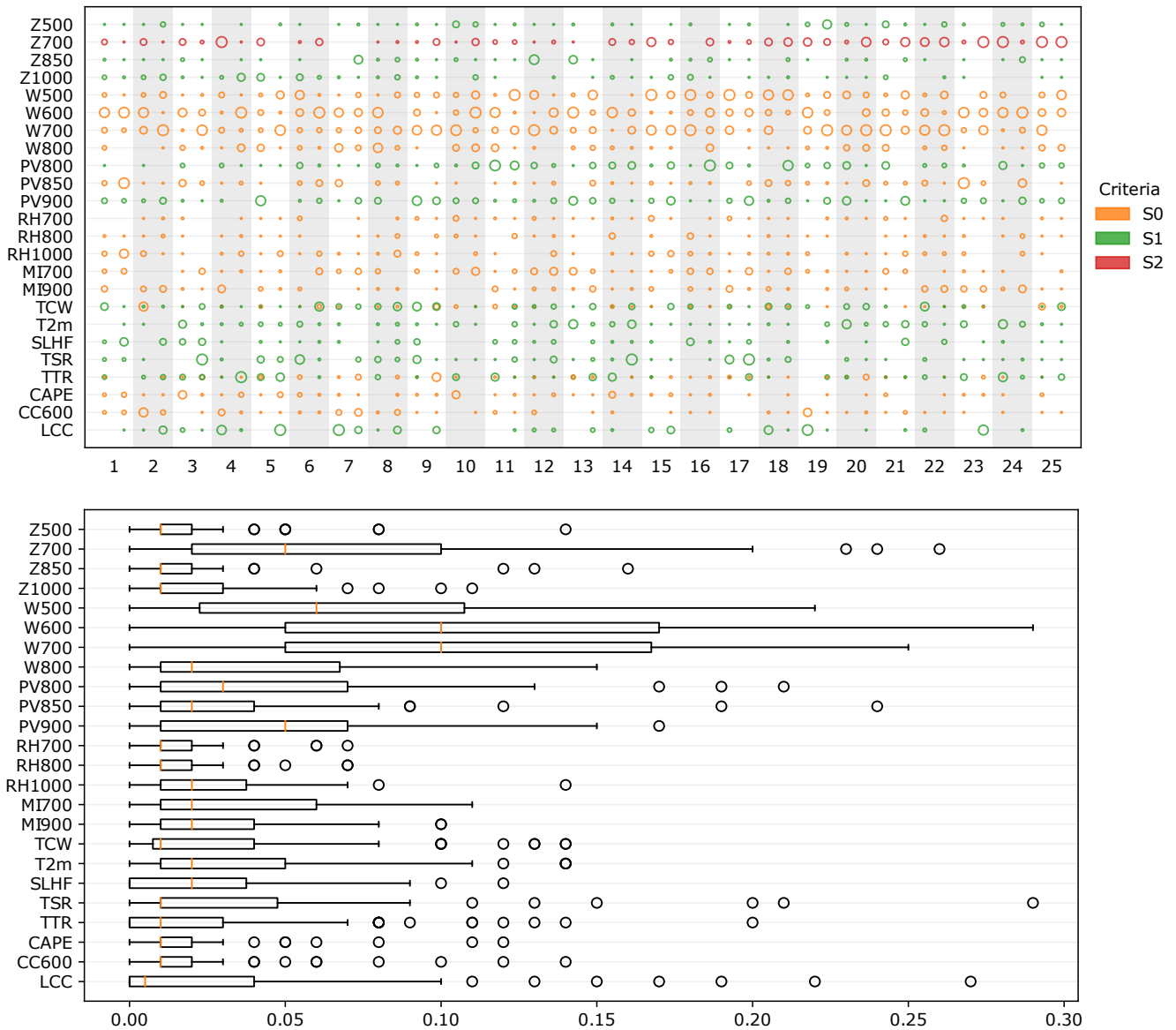


**Figure C1.** Results of the optimization with preselected 26 variables for the different catchments. (top) The colors represent the analogy criteria, and the size of the dots is proportional to the weight given to the predictor within the range [0.01, 0.2]. (bottom) Boxplot of the weight values for the different variables.

## Open Research

Reanalysis datasets can be obtained from the respective providers (see Acknowledgements). Precipitation data can be obtained from MeteoSwiss (for research purpose only). The software used, AtmoSwing (<https://atmoswing.org>, Horton, 2019a), is open-source and can be used without restrictions.

## Acknowledgments

Precipitation time series were provided by MeteoSwiss. The catchment extents were provided by the Hydrological Atlas of Switzerland (hydrologicalatlas.ch). The ERA-Interim reanalysis was obtained from the ECMWF Data Server at <http://apps.ecmwf.int/datasets>. The Climate Forecast System Reanalysis (CFSR) was obtained from the Computational & Information Systems Lab (CISL) Research Data Archive (<http://rda.ucar.edu/>). The CFSR project is carried out by the Environmental Modeling Center (EMC), National Centers for Environmental Prediction (NCEP). ERA5 (Complete ERA5 global atmospheric reanalysis) was obtained from the C3S climate data store (CDS) at <https://cds.climate.copernicus.eu>. Calculations were performed on UBELIX (<http://www.id.unibe.ch/hpc>), the HPC cluster at the University of Bern.

## References

- Alessandrini, S., Delle Monache, L., Sperati, S., & Cervone, G. (2015). An analog ensemble for short-term probabilistic solar power forecast. *Applied Energy*, *157*, 95–110. doi: 10.1016/j.apenergy.2015.08.011
- Alessandrini, S., Delle Monache, L., Sperati, S., & Nissen, J. N. (2015). A novel application of an analog ensemble for short-term wind power forecasting. *Renewable Energy*, *76*, 768–781. doi: 10.1016/j.renene.2014.11.061
- Ben Daoud, A. (2010). *Améliorations et développements d’une méthode de prévision probabiliste des pluies par analogie*. (Unpublished doctoral dissertation). Université de Grenoble.
- Ben Daoud, A., Sauquet, E., Bontron, G., Obled, C., & Lang, M. (2016). Daily quantitative precipitation forecasts based on the analogue method: improvements and application to a French large river basin. *Atmos. Res.*, *169*, 147–159. doi: 10.1016/j.atmosres.2015.09.015
- Bessa, R., Trindade, A., Silva, C. S., & Miranda, V. (2015). Probabilistic solar power forecasting in smart grids using distributed information. *International Journal of Electrical Power & Energy Systems*, *72*, 16–23. doi: 10.1016/j.ijepes.2015.02.006
- Bliefernicht, J. (2010). *Probability forecasts of daily areal precipitation for small river basins* (Unpublished doctoral dissertation). Universität Stuttgart.
- Bontron, G. (2004). *Prévision quantitative des précipitations: Adaptation probabiliste par recherche d’analogues. Utilisation des Réanalyses NCEP/NCAR et application aux précipitations du Sud-Est de la France*. (Unpublished doctoral dissertation). Institut National Polytechnique de Grenoble.
- Brown, T. (1974). *Admissible Scoring Systems for Continuous Distributions*. (Tech. Rep.). Retrieved from <http://eric.ed.gov/?id=ED135799>
- Caillouet, L., Vidal, J.-P., Sauquet, E., & Graff, B. (2016). Probabilistic precipitation and temperature downscaling of the Twentieth Century Reanalysis over France. *Clim. Past*, *12*(3), 635–662. doi: 10.5194/cp-12-635-2016
- Cateni, S., Colla, V., & Vannucci, M. (2010). Variable selection through genetic algorithms for classification purposes. *Proceedings of the 10th IASTED International Conference on Artificial Intelligence and Applications, AIA 2010*,

- 795 6–11. doi: 10.2316/p.2010.674-080
- 796 Dayon, G., Boé, J., & Martin, E. (2015, feb). Transferability in the future climate of  
797 a statistical downscaling method for precipitation in France. *J. Geophys. Res.*  
798 *Atmos.*, *120*(3), 1023–1043. doi: 10.1002/2014JD022236
- 799 Dee, D. P., Uppala, S. M., Simmons, A. J., Berrisford, P., Poli, P., Kobayashi, S.,  
800 ... Vitart, F. (2011). The ERA-Interim reanalysis: Configuration and perfor-  
801 mance of the data assimilation system. *Quart. J. Roy. Meteor. Soc.*, *137*(656),  
802 553–597. doi: 10.1002/qj.828
- 803 Delle Monache, L., Eckel, F. A., Rife, D. L., Nagarajan, B., & Searight, K. (2013).  
804 Probabilistic Weather Prediction with an Analog Ensemble. *Mon. Weather*  
805 *Rev.*, *141*, 3498–3516. doi: 10.1175/MWR-D-12-00281.1
- 806 Delle Monache, L., Nipen, T., Liu, Y., Roux, G., & Stull, R. (2011). Kalman Fil-  
807 ter and Analog Schemes to Postprocess Numerical Weather Predictions. *Mon.*  
808 *Weather Rev.*, *139*(11), 3554–3570. doi: 10.1175/2011MWR3653.1
- 809 D’heygere, T., Goethals, P. L., & De Pauw, N. (2003). Use of genetic algo-  
810 rithms to select input variables in decision tree models for the prediction of  
811 benthic macroinvertebrates. *Ecological Modelling*, *160*(3), 291–300. doi:  
812 10.1016/S0304-3800(02)00260-0
- 813 Drosowsky, W., & Zhang, H. (2003). Verification of Spatial Fields. In I. T. Jol-  
814 liffe & D. B. Stephenson (Eds.), *Forecast verif. a pract. guid. atmos. sci.* (pp.  
815 121–136). Wiley.
- 816 Foresti, L., Panziera, L., Mandapaka, P. V., Germann, U., & Seed, A. (2015). Re-  
817 trieval of analogue radar images for ensemble nowcasting of orographic rainfall.  
818 *Meteorol. Appl.*, *22*(2), 141–155. doi: 10.1002/met.1416
- 819 Frei, C., & Schär, C. (1998). A precipitation climatology of the Alps from  
820 high-resolution rain-gauge observations. *International Journal of Clima-*  
821 *tology*, *18*(8), 873–900. doi: 10.1002/(SICI)1097-0088(19980630)18:8<873::  
822 AID-JOC255>3.0.CO;2-9
- 823 Gibergans-Báguena, J., & Llasat, M. (2007, dec). Improvement of the analog fore-  
824 casting method by using local thermodynamic data. Application to autumn  
825 precipitation in Catalonia. *Atmospheric Research*, *86*(3-4), 173–193. Retrieved  
826 from <http://linkinghub.elsevier.com/retrieve/pii/S0169809507000695>  
827 doi: 10.1016/j.atmosres.2007.04.002
- 828 Gobeyn, S., Volk, M., Dominguez-Granda, L., & Goethals, P. L. (2017). Input  
829 variable selection with a simple genetic algorithm for conceptual species dis-  
830 tribution models: A case study of river pollution in Ecuador. *Environmental*  
831 *Modelling and Software*, *92*, 269–316. doi: 10.1016/j.envsoft.2017.02.012
- 832 Guennebaud, G., Jacob, B., & Others. (2010). *Eigen v3*. <http://eigen.tuxfamily.org>.
- 833 Guilbaud, S., & Obled, C. (1998). Prévision quantitative des précipitations  
834 journalières par une technique de recherche de journées antérieures ana-  
835 logues: optimisation du critère d’analogie. *Comptes Rendus l’Académie*  
836 *des Sci. Ser. II, A-Earth Planet. Sci.*, *327*(3), 181–188. Retrieved from  
837 <http://www.sciencedirect.com/science/article/pii/S1251805098800062>  
838 doi: 10.1016/s1251-8050(98)80006-2

- 839 Hamill, T., & Whitaker, J. (2006). Probabilistic quantitative precipitation fore-  
 840 casts based on reforecast analogs: Theory and application. *Monthly Weather*  
 841 *Review*, *134*(11), 3209–3229. doi: 10.1175/mwr3237.1
- 842 Hamill, T. M., Scheuerer, M., & Bates, G. T. (2015). Analog Probabilistic Pre-  
 843 cipitation Forecasts Using GEFs Reforecasts and Climatology-Calibrated  
 844 Precipitation Analyses. *Monthly Weather Review*, *143*(8), 3300–3309. doi:  
 845 10.1175/MWR-D-15-0004.1
- 846 Hersbach, H. (2000). Decomposition of the continuous ranked probability score for  
 847 ensemble prediction systems. *Wea. Forecasting*, *15*(5), 559–570. doi: 10.1175/  
 848 1520-0434(2000)015<0559:dotcrp>2.0.co;2
- 849 Hersbach, H., Bell, B., Berrisford, P., Horányi, A., Sabater, J. M., Nicolas, J., . . .  
 850 Dee, D. (2019). Global reanalysis: goodbye ERA-Interim, hello ERA5.  
 851 *ECMWF Newsletter*(159), 17–24. doi: 10.21957/vf291hehd7
- 852 Holland, J. H. (1992, jul). Genetic Algorithms. *Scientific American*, *267*(1), 66–72.  
 853 doi: 10.1038/scientificamerican0792-66
- 854 Horton, P. (2019a). AtmoSwing: Analog Technique Model for Statistical Weather  
 855 forecastING and downscaling (v2.1.0). *Geoscientific Model Development*,  
 856 *12*(7), 2915–2940. doi: 10.5194/gmd-12-2915-2019
- 857 Horton, P. (2019b, dec). *AtmoSwing v2.1.2 [Software]*. Zenodo. doi: 10.5281/zenodo  
 858 .3559787
- 859 Horton, P. (2021). Analogue methods and ERA5: Benefits and pitfalls. *International*  
 860 *Journal of Climatology*(September 2021), 4078–4096. doi: 10.1002/joc.7484
- 861 Horton, P., & Brönnimann, S. (2019). Impact of global atmospheric reanalyses on  
 862 statistical precipitation downscaling. *Climate Dynamics*, *52*(9-10), 5189–5211.  
 863 doi: 10.1007/s00382-018-4442-6
- 864 Horton, P., Jaboyedoff, M., Metzger, R., Obled, C., & Marty, R. (2012). Spatial re-  
 865 lationship between the atmospheric circulation and the precipitation measured  
 866 in the western Swiss Alps by means of the analogue method. *Nat. Hazards*  
 867 *Earth Syst. Sci.*, *12*, 777–784. doi: 10.5194/nhess-12-777-2012
- 868 Horton, P., Jaboyedoff, M., & Obled, C. (2017, apr). Global Optimization of an  
 869 Analog Method by Means of Genetic Algorithms. *Monthly Weather Review*,  
 870 *145*(4), 1275–1294. doi: 10.1175/MWR-D-16-0093.1
- 871 Horton, P., Jaboyedoff, M., & Obled, C. (2018). Using genetic algorithms to op-  
 872 timize the analogue method for precipitation prediction in the Swiss Alps. *J.*  
 873 *Hydrol.*, *556*, 1220–1231. doi: 10.1016/j.jhydrol.2017.04.017
- 874 Huang, J., Cai, Y., & Xu, X. (2007). A hybrid genetic algorithm for feature selection  
 875 wrapper based on mutual information. *Pattern Recognition Letters*, *28*(13),  
 876 1825–1844. doi: 10.1016/j.patrec.2007.05.011
- 877 Jézéquel, A., Yiou, P., & Radanovics, S. (2017). Role of circulation in European  
 878 heatwaves using flow analogues. *Climate Dynamics*, 1–15. doi: 10.1007/s00382  
 879 -017-3667-0
- 880 Junk, C., Delle Monache, L., & Alessandrini, S. (2015). Analog-based Ensemble  
 881 Model Output Statistics. *Monthly Weather Review*, *143*(7), 2909–2917. doi: 10  
 882 .1175/MWR-D-15-0095.1

- 883 Junk, C., Delle Monache, L., Alessandrini, S., Cervone, G., & von Bremen, L.  
 884 (2015). Predictor-weighting strategies for probabilistic wind power forecasting  
 885 with an analog ensemble. *Meteorologische Zeitschrift*, *24*(4), 361–379. doi:  
 886 10.1127/metz/2015/0659
- 887 Lorenz, E. (1956). *Empirical orthogonal functions and statistical weather prediction*  
 888 (Tech. Rep.). Massachusetts Institute of Technology, Department of Meteorol-  
 889 ogy, Massachusetts Institute of Technology, Dept. of Meteorology.
- 890 Lorenz, E. (1969). Atmospheric predictability as revealed by naturally occurring  
 891 analogues. *J. Atmos. Sci.*, *26*, 636–646. doi: 10.1175/1520-0469(1969)26<636:  
 892 aparbn>2.0.co;2
- 893 Maraun, D., Wetterhall, F., Chandler, R. E., Kendon, E. J., Widmann, M., Brienen,  
 894 S., . . . Thiele-Eich, I. (2010). Precipitation downscaling under climate  
 895 change: Recent developments to bridge the gap between dynamical mod-  
 896 els and the end user. *Reviews of Geophysics*, *48*(RG3003), 1–34. doi:  
 897 10.1029/2009RG000314
- 898 Marty, R. (2010). *Prévision hydrologique d'ensemble adaptée aux bassins à crue*  
 899 *rapide. Elaboration de prévisions probabilistes de précipitations à 12 et 24 h.*  
 900 *Désagrégation horaire conditionnelle pour la modélisation hydrologique. Ap-*  
 901 *plication à des bassins de la région Cév* (Unpublished doctoral dissertation).  
 902 Université de Grenoble.
- 903 Marty, R., Zin, I., Obled, C., Bontron, G., & Djerboua, A. (2012, mar). To-  
 904 ward real-time daily PQPF by an analog sorting approach: Application to  
 905 flash-flood catchments. *J. Appl. Meteorol. Climatol.*, *51*(3), 505–520. doi:  
 906 10.1175/JAMC-D-11-011.1
- 907 Massacand, A. C., Wernli, H., & Davies, H. C. (1998, may). Heavy precipitation on  
 908 the alpine southside: An upper-level precursor. *Geophysical Research Letters*,  
 909 *25*(9), 1435–1438. doi: 10.1029/98GL50869
- 910 Matheson, J., & Winkler, R. (1976). Scoring rules for continuous probability distri-  
 911 butions. *Manage. Sci.*, *22*(10), 1087–1096. doi: 10.1287/mnsc.22.10.1087
- 912 Michalewicz, Z. (1996). *Genetic Algorithms + Data Structures = Evolution Pro-*  
 913 *grams* (3rd editio ed.). Springer-Verlag.
- 914 Obled, C., Bontron, G., & Garçon, R. (2002, aug). Quantitative precipita-  
 915 tion forecasts: a statistical adaptation of model outputs through an ana-  
 916 logues sorting approach. *Atmos. Res.*, *63*(3-4), 303–324. doi: 10.1016/  
 917 S0169-8095(02)00038-8
- 918 Panziera, L., Germann, U., Gabella, M., & Mandapaka, P. V. (2011). NORA-  
 919 Nowcasting of Orographic Rainfall by means of Analogues. *Q. J. R. Meteorol.*  
 920 *Soc.*, *137*(661), 2106–2123. doi: 10.1002/qj.878
- 921 Radanovics, S., Vidal, J.-P., Sauquet, E., Ben Daoud, A., & Bontron, G. (2013).  
 922 Optimising predictor domains for spatially coherent precipitation down-  
 923 scaling. *Hydrology and Earth System Sciences*, *17*(10), 4189–4208. doi:  
 924 10.5194/hess-17-4189-2013
- 925 Raynaud, D., Hingray, B., Zin, I., Anquetin, S., Debionne, S., & Vautard, R.  
 926 (2016). Atmospheric analogues for physically consistent scenarios of surface

- 927 weather in Europe and Maghreb. *International Journal of Climatology*. doi:  
928 10.1002/joc.4844
- 929 Saha, S., Moorthi, S., Pan, H. L., Wu, X., Wang, J., Nadiga, S., . . . Goldberg, M.  
930 (2010). The NCEP climate forecast system reanalysis. *Bull. Amer. Meteor.*  
931 *Soc.*, *91*(8), 1015–1057. doi: 10.1175/2010BAMS3001.1
- 932 Schüepp, M., & Gensler, G. (1980). *Klimaregionen der Schweiz. Die Beobach-*  
933 *tungsnetze der Schweizerischen Meteorologischen Anstalt.*
- 934 Teweles, S., & Wobus, H. B. (1954). Verification of prognostic charts. *Bull. Am. Me-*  
935 *teorol. Soc.*, *35*, 455–463.
- 936 Thompson, J. C., & Carter, G. M. (1972). On some characteristics of the S1  
937 score. *Journal of Applied Meteorology*, *11*(8), 1384–1385. Retrieved from  
938 <http://www.sciencedirect.com/science/article/pii/0032063359900467>  
939 doi: 10.1175/1520-0450(1972)011(1384:OSCOTS)2.0.CO;2
- 940 Vanvyve, E., Delle Monache, L., Monaghan, A. J., & Pinto, J. O. (2015). Wind  
941 resource estimates with an analog ensemble approach. *Renewable Energy*, *74*,  
942 761–773. doi: 10.1016/j.renene.2014.08.060
- 943 Wilson, L. J., & Yacowar, N. (1980). Statistical weather element forecasting in  
944 the Canadian Weather Service. In *Proc. wmo symp. probabilistic stat. methods*  
945 *weather forecast.* (pp. 401–406). Nice, France.
- 946 Woodcock, F. (1980). On the use of analogues to improve regression forecasts. *Mon.*  
947 *Weather Rev.*, *108*(3), 292–297. doi: 10.1175/1520-0493(1980)108(0292:otuoat)  
948 2.0.co;2

# Automated Input Variable Selection for Analog Methods Using Genetic Algorithms

P. Horton<sup>1</sup>, O. Martius<sup>1</sup>, and S. L. Grimm<sup>2</sup>

<sup>1</sup>Institute of Geography, Oeschger Centre for Climate Change Research, University of Bern, Bern,  
Switzerland

<sup>2</sup>Physikalisches Institut, University of Bern, Gesellschaftsstrasse 6, 3012 Bern, Switzerland

## Key Points:

- Genetic algorithms were successful in selecting relevant input variables for the prediction of precipitation by analog methods
- The analogy criteria were automatically selected, resulting in the discovery of a new promising criterion
- The optimization resulted in a structure combining different predictors into a single level of analogy, while outperforming stepwise methods

---

Corresponding author: Pascal Horton, [pascal.horton@giub.unibe.ch](mailto:pascal.horton@giub.unibe.ch)

**Abstract**

Analog methods (AMs) have long been used for precipitation prediction and climate studies. However, they rely on manual selections of parameters, such as the predictor variables and analogy criterion. Previous work showed the potential of genetic algorithms (GAs) to optimize most parameters of AMs. This research goes one step further and investigates the potential of GAs for automating the selection of the input variables and the analogy criteria (distance metric between two data fields) in AMs. Our study focuses on daily precipitation prediction in central Europe, specifically Switzerland, as a representative case. Comparative analysis against established reference methods demonstrates the superiority of the GA-optimized AM in terms of predictive accuracy. The selected input variables exhibit strong associations with key meteorological processes that influence precipitation generation. Further, we identify a new analogy criterion inspired by the Teweles-Wobus criterion, but applied directly to grid values, which consistently performs better than other Euclidean distances. It shows potential for further exploration regarding its unique characteristics. In contrast to conventional stepwise selection approaches, the GA-optimized AM displays a preference for a flatter structure, characterized by a single level of analogy and an increased number of variables. Although the GA optimization process is computationally intensive, we highlight the use of GPU-based computations to significantly reduce computation time. Overall, our study demonstrates the successful application of GAs in automating input variable selection for AMs, with potential implications for application in diverse locations and data exploration for predicting alternative predictands.

**1 Introduction**

Analog methods (AMs) are statistical downscaling techniques (Maraun et al., 2010) that rely on inherent relationships between meteorological predictors, usually at a synoptic scale, and local weather (Lorenz, 1956, 1969). AMs look for similar meteorological situations in the past to that of a target date of interest. They provide a conditional prediction based on the observed predictand values at these analog dates. Daily precipitation has been the predictand of interest, either in the context of operational forecasting (e.g. T. Hamill & Whitaker, 2006; Bliefernicht, 2010; Marty et al., 2012; Horton et al., 2012; T. M. Hamill et al., 2015; Ben Daoud et al., 2016), climate change studies (e.g. Dayon et al., 2015; Raynaud et al., 2016), or past climate reconstruction (Caillouet et al., 2016). AMs are also used for other predictands, such as precipitation radar images (Panziera et al., 2011; Foresti et al., 2015), temperature (Delle Monache et al., 2013; Caillouet et al., 2016; Raynaud et al., 2016; Jézéquel et al., 2017), wind (Delle Monache et al., 2013, 2011; Vanvyve et al., 2015; Alessandrini, Delle Monache, Sperati, & Nissen, 2015; Junk, Delle Monache, Alessandrini, Cervone, & von Bremen, 2015; Junk, Delle Monache, & Alessandrini, 2015), and solar radiation or power production (Alessandrini, Delle Monache, Sperati, & Cervone, 2015; Bessa et al., 2015; Raynaud et al., 2016).

AMs may consist of a stepwise selection of similar meteorological situations based on multiple predictors organized in different consecutive levels of analogy, each of which

55 conditions the subsequent selection. Each predictor consists of a specific meteorologi-  
56 cal variable at a specific time and vertical level (if relevant). The similarity between two  
57 situations is computed using an analogy criterion (distance metric) over a relevant spa-  
58 tial domain. For each level of analogy, a certain number of analogs are selected (Obled  
59 et al., 2002; Bontron, 2004).

60 AMs for predicting precipitation commonly have a first level of analogy based on  
61 the atmospheric circulation. The variable of interest is the geopotential height ( $Z$ ) at var-  
62 ious pressure levels and specific times throughout the day (Table 2; Obled et al., 2002;  
63 Horton et al., 2018). Bontron (2004) introduced a second level of analogy based on a mois-  
64 ture index that is the product of the relative humidity at 850 hPa and the total precip-  
65 itable water (method RM3 in Table 2). Other consecutive studies selected different pres-  
66 sure levels (method RM4 in Table 2) or added a wind component to the moisture index  
67 (Marty, 2010; Horton et al., 2018). Ben Daoud et al. (2016) inserted an additional level  
68 of analogy between the circulation and the moisture analogy based on the vertical ve-  
69 locity at 850 hPa (methods RM6 in Table 2) and named it "SANDHY" for Stepwise Ana-  
70 log Downscaling method for Hydrology (Ben Daoud et al., 2016; Caillouet et al., 2016).

71 To calibrate the method, a semi-automatic sequential procedure (Bontron, 2004;  
72 Radanovics et al., 2013; Ben Daoud et al., 2016) has often been used to optimize the size  
73 of the domain and the number of analogs. However, the predictor variables, vertical lev-  
74 els, temporal windows (time of the day), and analogy criteria were selected manually.  
75 This manual selection requires the comparison of numerous combinations and a compre-  
76 hensive assessment of some parameter ranges. Moreover, the sequential calibration pro-  
77 cedure successively calibrates the different levels of analogy, and thus it does not han-  
78 dle parameters inter-dependencies. Considering these limitations, Horton et al. (2017)  
79 introduced a global optimization of the AM using genetic algorithms (GAs). Using this  
80 approach, an automatic and objective selection of the temporal windows, the vertical lev-  
81 els, the domains, and the number of analogs became possible, improving the method's  
82 prediction skills (Horton et al., 2018). A weighting of the predictor variables has also been  
83 introduced. The only parameters left for a manual selection were the meteorological vari-  
84 ables and the analogy criteria.

85 Selecting predictors for precipitation prediction with AMs in Europe has been the  
86 focus of multiple studies aiming to improve prediction skills (Obled et al., 2002; Bon-  
87 tron, 2004; Gibergans-Báguena & Llasat, 2007; Radanovics et al., 2013; Ben Daoud et  
88 al., 2016). Thus, the relevant predictors are likely to be known nowadays and supported  
89 by expert knowledge. However, transferring AMs to a region with different climatic con-  
90 ditions or to another predictand would involve reconsidering the selected meteorologi-  
91 cal variables. This work aims to test a fully automatic optimization of all AM param-  
92 eters, including the selection of the meteorological variables and even the analogy cri-  
93 teria, using GAs. GAs have already been used for input variable selection (IVS) in other  
94 contexts (D'heygere et al., 2003; Huang et al., 2007; Cateni et al., 2010; Gobeyn et al.,  
95 2017).

96 We here seek to assess the potential of GAs for input variable selection in the con-  
97 text of the analog method. Moreover, we want to test the GAs' ability to jointly select  
98 the distance metric in addition, i.e., the analogy criteria. To compare with well-established  
99 AMs, daily precipitation in central Europe, specifically in Switzerland, has been chosen  
100 as predictand. Also, as is often the case, the AMs were optimized in the perfect prog-  
101 nosis framework, using predictors from reanalyses. This work focuses mainly on the proof  
102 of concept of automatic input variable selection for AMs rather than the details of the  
103 obtained results for the case study.

104 The paper is organized as follows. Section 2 describes the datasets, the fundamen-  
105 tals of AMs, the characteristics of the GAs implementation, the software used, and the  
106 experiment setup details. Section 3 presents the results of different analyses, such as the  
107 selection of the best predictor variable, the relevance of various AM structures, and the  
108 skill of the optimized methods. Section 4 discusses some findings of the work. Finally,  
109 section 5 summarizes the main contributions of the work and open perspectives for ap-  
110 plications of the developed approach.

## 111 2 Material and Methods

### 112 2.1 Data

113 The target variable (predictand) is daily precipitation derived from the RhiresD  
114 gridded dataset from MeteoSwiss. It is a daily aggregation (from 06 UTC of day D to  
115 06 UTC of day D+1) at a 2 km resolution with data from 1961 onward. It is produced  
116 using an interpolation scheme between gauging stations (Frei & Schär, 1998). The grid-  
117 ded data was here spatially aggregated across 25 catchments of about 200 km<sup>2</sup> (Table  
118 1). These catchments were chosen to cover the different climatic regions of Switzerland  
119 (Schüepp & Gensler, 1980), as illustrated in Fig. 1.

120 As often done in the context of the perfect prognosis framework, we used variables  
121 provided by global reanalyses. Even though most reanalyses provide good quality data  
122 over Europe, differences still exist, and the choice of the reanalysis dataset can impact  
123 the skill score of the AM even more significantly than the choice of the predictor vari-  
124 ables (Horton & Brönnimann, 2019). Thus, it was considered advisable to test some of  
125 the following analyses with another reanalysis to assess the robustness of the selected  
126 variables.

127 The main reanalysis used in this work is ERA-Interim (ERA-I, Dee et al., 2011),  
128 which was produced by the European Centre for Medium-Range Weather Forecasts (ECMWF)  
129 and covers the period from 1979 to 2019. The forecast model uses a hybrid sigma-pressure  
130 vertical coordinate on 60 layers and has a T255 horizontal resolution (about 79 km) and  
131 a 30 min time step. The output variables have a grid resolution of 0.75°. The present  
132 work started before the release of ERA5, the successor of ERA-I.

133 The Climate Forecast System Reanalysis (CFSR, Saha et al., 2010), provided by  
134 NCEP, was used for the first experiment to compare the results obtained with ERA-I.  
135 The model used to produce CFSR has a horizontal resolution of T382 (about 38 km) and

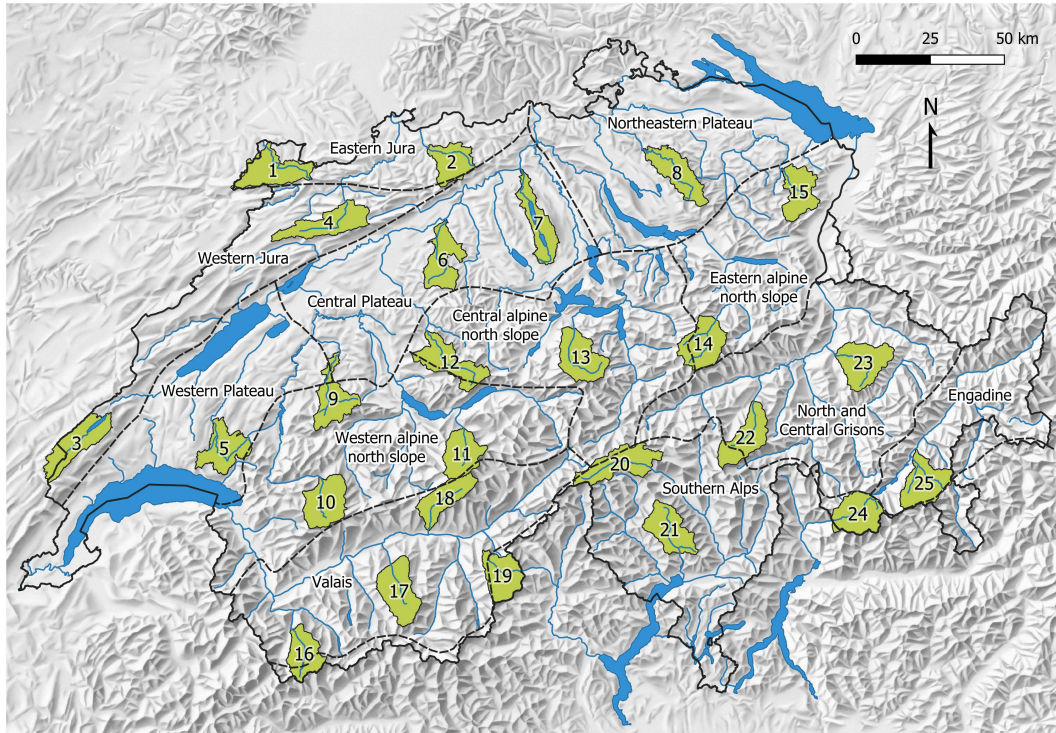


**Figure 1.** Location of the 25 selected catchments in Switzerland along with the climatic regions (dashed lines) and the river network (source: SwissTopo, HADES).

136 64 levels on sigma-pressure hybrid vertical coordinates. The period covered is from 1979  
 137 to August 2019, and the output variables have a spatial resolution of  $0.5^\circ$ .

138 Finally, ERA5 (Hersbach et al., 2019) was used for the last analysis. ERA5 provides  
 139 more variables and a higher spatial grid ( $0.25^\circ$ , but used here at  $0.5^\circ$ ) and tem-  
 140 poral resolution (hourly, but used here at a 3-hourly time step). ERA5 assimilates sig-  
 141 nificantly more data than ERA-I and provides, among others, more consistent sea sur-  
 142 face temperature and sea ice, an improved representation of tropical cyclones, a better  
 143 balance of evaporation and precipitation, and improved soil moisture. ERA5 also relies  
 144 on more appropriate radiative forcing and boundary conditions (e.g., changes in green-  
 145 house gases, aerosols, SST, and sea ice) (Hersbach et al., 2019).

## 146 2.2 Analog Methods

147 AMs are based on the rationale that two similar synoptic situations may produce  
 148 similar local weather (Lorenz, 1956, 1969). It thus consists of extracting past atmospheric  
 149 situations similar to a target date. Selected predictor fields define this similarity. The  
 150 conditional distribution of the predictand of interest (here, daily precipitation) is extracted  
 151 from these analog dates. The analogy is defined by:

- 152 1. The selected meteorological variables (predictors).
- 153 2. The vertical levels at which the predictors are selected.

**Table 1.** Characteristics of the 25 selected catchments in Switzerland

| Id | Name of the river  | Climatic region            | Area<br>(km <sup>2</sup> ) | Mean elevation<br>(m a.s.l.) |
|----|--------------------|----------------------------|----------------------------|------------------------------|
| 1  | L'Allaine          | Eastern Jura               | 209.1                      | 571                          |
| 2  | Ergolz             | Eastern Jura               | 150.3                      | 589                          |
| 3  | L'Orbe             | Western Jura               | 209.3                      | 1229                         |
| 4  | La Birse           | Western Jura               | 203.3                      | 920                          |
| 5  | La Broye           | Western Plateau            | 184.5                      | 791                          |
| 6  | Murg               | Central Plateau            | 184.8                      | 658                          |
| 7  | Aabach             | Central Plateau            | 180.0                      | 562                          |
| 8  | Töss               | Northeastern Plateau       | 189.3                      | 745                          |
| 9  | Sense              | Western alpine north slope | 179.6                      | 1238                         |
| 10 | La Sarine          | Western alpine north slope | 200.8                      | 1779                         |
| 11 | Weisse Lütschine   | Western alpine north slope | 165.0                      | 2149                         |
| 12 | Emme               | Central alpine north slope | 206.9                      | 1151                         |
| 13 | Engelberger Aa     | Central alpine north slope | 204.3                      | 1654                         |
| 14 | Linth              | Eastern alpine north slope | 195.7                      | 1959                         |
| 15 | Sitter             | Eastern alpine north slope | 162.2                      | 1069                         |
| 16 | Dranse d'Entremont | Valais                     | 154.2                      | 2340                         |
| 17 | La Navisence       | Valais                     | 210.5                      | 2541                         |
| 18 | Lonza              | Valais                     | 161.7                      | 2370                         |
| 19 | Doveria            | Southern Alps              | 170.5                      | 2241                         |
| 20 | Ticino             | Southern Alps              | 208.5                      | 2019                         |
| 21 | Verzasca           | Southern Alps              | 187.4                      | 1656                         |
| 22 | Valser Rhein       | North and Central Grisons  | 185.8                      | 2215                         |
| 23 | Plessur            | North and Central Grisons  | 207.7                      | 1928                         |
| 24 | Mera               | Southern Alps              | 190.6                      | 2142                         |
| 25 | Flaz               | Engadine                   | 193.1                      | 2599                         |

- 154 3. The spatial windows (domains) over which the predictors are compared.  
155 4. The hours of the day at which the predictors are considered.  
156 5. The analogy criteria (distance metric to rank candidate situations).  
157 6. Possible weights between the predictors.  
158 7. The number of analog situations  $N_i$  to select for the level of analogy  $i$ .

159 AMs usually start with a seasonal preselection to cope with seasonal effects (Lorenz,  
160 1969). The seasonal preselection is often implemented as a moving window of 120 days  
161 centered around the target date (Bontron, 2004; Marty et al., 2012; Horton et al., 2012;  
162 Ben Daoud et al., 2016). Alternatively, the candidate dates can be preselected based on  
163 similar air temperature at the nearest grid point (Ben Daoud et al., 2016, methods RM5  
164 and RM6 in Table 2). In this work, we used the temporal moving window to reduce the  
165 number of potential candidate dates and, thus, the computing time.

166 The first level of analogy in AMs for precipitation is often based on the atmospheric  
167 circulation using the geopotential height ( $Z$ ) at different pressure levels and hours of the  
168 day (Table 2). The distance (analogy criterion) between two  $Z$  fields is computed on the  
169 vector components of the gradient, i.e., using the difference between adjacent grid cells,  
170 rather than comparing absolute values. The Teweles–Wobus criterion ( $S_1$ , Eq. 1, Tewe-  
171 les & Wobus, 1954; Drosowsky & Zhang, 2003) was identified as the most suited by dif-

**Table 2.** Some analog methods listed by increasing complexity. The analogy criterion is  $S_1$  for Z and RMSE for the other variables.

| Method     | Preselection         | First level                                    | Second level                 | Third level                  | Reference               |
|------------|----------------------|--|------------------------------|------------------------------|-------------------------|
| <b>RM1</b> | $\pm 60$ days        | Z1000@12h<br>Z500@24h                          |                              |                              | Bontron (2004)          |
| <b>RM2</b> | $\pm 60$ days        | Z1000@06h<br>Z1000@30h<br>Z700@24h<br>Z500@12h |                              |                              | Horton et al. (2018)    |
| <b>RM3</b> | $\pm 60$ days        | Z1000@12h<br>Z500@24h                          | MI850@12+24h                 |                              | Bontron (2004)          |
| <b>RM4</b> | $\pm 60$ days        | Z1000@30h<br>Z850@12h<br>Z700@24h<br>Z400@12h  | MI700@24h<br>MI600@12h       |                              | Horton et al. (2018)    |
| <b>RM5</b> | T925@36h<br>T600@12h | Z1000@12h<br>Z500@24h                          | MI925@12+24h<br>MI700@12+24h |                              | Ben Daoud et al. (2016) |
| <b>RM6</b> | T925@36h<br>T600@12h | Z1000@12h<br>Z500@24h                          | W850@06-24h                  | MI925@12+24h<br>MI700@12+24h | Ben Daoud et al. (2016) |

Z, geopotential height; T, air temperature; W, vertical velocity; MI, moisture index.

172 ferent studies (Wilson & Yacowar, 1980; Woodcock, 1980; Guilbaud & Obled, 1998; Bon-  
173 tron, 2004). It is defined as:

$$S_1 = 100 \frac{\sum_i |\Delta \hat{z}_i - \Delta z_i|}{\sum_i \max\{|\Delta \hat{z}_i|, |\Delta z_i|\}} \quad (1)$$

174 where  $\Delta \hat{z}_i$  is the gradient component between the  $i$ th pair of adjacent points from the  
175 geopotential field of the target situation, and  $\Delta z_i$  is the corresponding observed gradi-  
176 ent component in the candidate situation. The gradient components are computed in  
177 both latitude and longitude directions.  $S_1$  ranges from 0 to 200. The smaller the  $S_1$  val-  
178 ues, the more similar the pressure fields. The  $S_1$  criterion characterizes the wind's di-  
179 rection and strength, allowing a comparison of the atmospheric circulation.

180 For other predictors than the geopotential height (e.g., for moisture variables), clas-  
181 sic criteria representing Euclidean distances between grid point values are used: Mean  
182 Absolute Error (MAE) and Root Mean Squared Error (RMSE), the latter being used  
183 most often.

184 The output of the AM is a probabilistic prediction for the target day. It is provided  
185 by the empirical conditional distribution of the  $N_i$  predictand values corresponding to  
186 the  $N_i$  dates selected at the last level of analogy.

187

### 2.3 Genetic Algorithms

188

189

190

191

192

193

194

195

196

GA is a global optimization technique inspired by genetics and natural selection (Holland, 1992). It belongs to the family of evolutionary algorithms and comprises different operators such as natural selection, selection of couples, chromosome crossover, mutation, and elitism. These operators act on parameter sets of the problem to optimize by mixing, combinations, and random modifications. GA aims at combining, over time, the strength of different parameter sets and at exploring the parameters space while converging toward the global optimum. The optimization starts with 2000 random parameter sets (as defined in Sect. 2.2) and is stopped when the best parameter set cannot be improved after 30 iterations.

197

198

199

200

201

202

203

A variant of genetic algorithms (GAs) has been tailored to optimize AMs by Horton et al. (2017). All the method's parameters except the meteorological predictor variables and the analogy criteria have already been successfully optimized using GAs (Horton et al., 2018). The use of GAs provided for the first time an objective and global optimization of AMs, which resulted in gains in prediction skills. To bring the optimization further, the selection of the predictor variables and the analogy criteria were performed here by GAs.

204

205

206

207

208

209

210

211

212

213

214

The reason why the predictor variables and analogy criteria were left out in the previous GA-AM set-up Horton et al. (2017) is the different nature of these variables. The parameters optimized so far by Horton et al. (2017) were quantitative variables, i.e., numerical values (e.g., location and size of the spatial windows or the number of analogs), which have a notion of continuity. The meteorological predictors or analogy criteria, however, are categorical variables that have no relationship among options. They are treated as arrays of independent values by the algorithm. Therefore the mutation operator relying on a search radius in the parameters space (Horton et al., 2017) cannot be applied. Instead, a simple random sampling was used for these parameters when selected for mutation. In addition to the increased difficulty due to the higher number of parameters to optimize, this aspect will likely slow down the optimization.

215

216

217

218

219

220

221

222

223

224

225

226

227

228

In GAs, the mutation operator changes a parameter value (gene) if this parameter was selected to mutate (all parameters have a certain mutation probability). The new value assigned depends on the rules of the mutation operator applied. This operator enables the optimization to explore new areas of the parameters space and was shown to have the most significant impact on the success of the optimization (Horton et al., 2017). Thus, as suggested in Horton et al. (2017), five variants of this operator were used in parallel optimizations (see details in Appendix B): three variants of the non-uniform mutation (Michalewicz, 1996), the multiscale mutation (Horton et al., 2017), and the chromosome of adaptive search radius (Horton et al., 2017). The non-uniform mutation aims to reduce the magnitude of the search in the parameters space with the evolution of the population to transition from the exploration of the whole parameter space to the exploitation of local solutions. This operator has three controlling variables, which makes it difficult to adjust, and thus is used with three different configurations. The multiscale mutation considers both exploration and exploitation in parallel. It has no controlling

229 parameters and no evolution during the optimization. The chromosome of adaptive search  
230 radius was introduced by Horton et al. (2017) and is inspired by the non-uniform mu-  
231 tation. It takes an auto-adaptive approach by adding two chromosomes, one for the mu-  
232 tation rate and one for controlling the search magnitude (see details in Horton et al., 2017).  
233 Therefore, it has no controlling parameters, is thus easier to use, and automatically tran-  
234 sitions from the exploration phase to exploitation.

## 235 2.4 Software

236 The optimization of AMs with GAs is implemented in the open-source AtmoSwing  
237 software<sup>1</sup> (Horton, 2019a) that has been used for this work. AtmoSwing is written in object-  
238 oriented C++ and has been optimized for computational performance. It scales well on  
239 HPC infrastructures as the different members of the GAs populations, i.e., the various  
240 parameter sets, can be assessed in parallel using multiple independent threads. However,  
241 due to the increasingly large number of assessments needed by GAs with the increasing  
242 complexity of the problem, a further reduction in computing time became necessary. In-  
243 deed, while applying AMs to perform a prediction for a single target date is a very fast  
244 and light process, GAs require a substantial amount of parameter assessment over long  
245 calibration periods.

246 A first attempt was based on storing the whole history of the optimization in mem-  
247 ory and looking up for equal – or similar – already-assessed parameters to a newly gen-  
248 erated parameters set. However, this approach turned out to be even more time-consuming  
249 after several generations and led to memory issues for long optimizations.

250 Despite being simple methods, AMs require many comparisons of gridded fields dur-  
251 ing the calibration phase. For example, this work used a 24-year calibration period. For  
252 each target day, a gridded predictor needs to be compared to about 2820 candidate sit-  
253 uations (24\*120-60, using a 120-day temporal window minus 60 days in the target year  
254 that are excluded). Over the entire calibration period, this amounts to about  $24.7 \cdot 10^6$   
255 field comparisons per predictor of the first level of analogy. Here, one optimization re-  
256 quired, on average, about 200 generations made of 2000 individuals, which brings the  
257 average number of grid comparisons to about  $1 \cdot 10^{13}$  per predictor of the first level of  
258 analogy. The comparison of the gridded predictors – i.e., the calculation of the analogy  
259 criteria – was identified by profilers as the most time-consuming task, despite using the  
260 efficient linear algebra library Eigen 3 (Guennebaud et al., 2010).

261 To reduce the processing time, computation using graphics processing units (GPUs)  
262 was implemented for this study in a new release of AtmoSwing, v.2.1.2 (Horton, 2019b).  
263 The calculation of the analogy criteria has been written using NVIDIA’s CUDA. The  
264 implementation details and the results of a benchmark experiment can be found in Ap-  
265 pendix A. When optimizing the methods using ERA5 at a 3-hourly time step and  $0.5^\circ$   
266 resolution, the difference is substantial. One generation (2000 evaluations) took 8 to more

---

<sup>1</sup> <https://atmoswing.org/>

267 than 10 hours using 20 CPU threads, while 50 to 80 minutes were needed using 3 CPU  
 268 threads and 3 GPU devices (NVIDIA GeForce703 RTX 2080).

## 269 2.5 Experiments Setup

270 The experiments were conducted over a 30-year period, from 1981 to 2010, divided  
 271 into a calibration period (CP) and an independent validation period (VP – note that the  
 272 years 2011-2018 were reserved for an additional test period, which was in the end not  
 273 used). To reduce the impact of potential inhomogeneities in the time series, the selec-  
 274 tion of the validation period (VP) was evenly distributed over the entire series (as in Ben  
 275 Daoud, 2010). A total of 6 years was used for the VP by selecting one year out of ev-  
 276 ery five (explicitly: 1985, 1990, 1995, 2000, 2005, 2010). The archive period (AP), where  
 277 the analog dates are being retrieved, is the same as the CP. The VP is also excluded from  
 278 the AP (days from the VP were never used as candidate situations for the selection of  
 279 analogs), as well as a period of  $\pm 30$  days around the target date to exclude potential de-  
 280 pendent meteorological situations. Unless stated otherwise, all results are presented for  
 281 the VP.

282 The GAs optimized all parameters of the method. Only the AM structure (num-  
 283 ber of analogy levels and predictors) was not optimized. Different structures were tested  
 284 in section 3.2. For each level of analogy and each predictor, the following parameters were  
 285 optimized within the corresponding ranges:

- 286 1. Meteorological variable: see section 2.5.1.
- 287 2. Vertical level: see section 2.5.1.
- 288 3. Temporal windows (time of the day): from day D 00 UTC to D+1 06 UTC (c.f.  
 289 precipitation accumulation period, sect 2.1)
- 290 4. Spatial window (domain): latitudes=[35, 55], longitudes=[-10, 20]. The spatial win-  
 291 dows differ between predictors, even in the same level of analogy.
- 292 5. Analogy criterion: see section 2.5.2.
- 293 6. Weight: [0, 1] with a precision of 0.01 (0.05 for experiment 2). The optimizer can  
 294 turn off a variable by setting its weight to zero.
- 295 7. Number of analogs: varies according to the structure, but with an overall range  
 296 of [5, 300] and a step of 5. The optimizer can turn off a level of analogy by set-  
 297 ting its number of analogs to the same value as the previous level of analogy.

298 The CRPS (Continuous Ranked Probability Score; Brown, 1974; Matheson & Win-  
 299 kler, 1976; Hersbach, 2000) was used to assess the skill of the predictions. It evaluates  
 300 the predicted cumulative distribution functions  $F(y)$ , here of the precipitation values  $y$   
 301 associated with the analog situations, compared to the single observed value  $y^0$  for a day  
 302  $i$ :

$$CRPS_i = \int_0^{+\infty} [F_i(y) - H_i(y - y_i^0)]^2 dy, \quad (2)$$

303 where  $H(y - y_i^0)$  is the Heaviside function that is null when  $y - y_i^0 < 0$ , and 1 other-  
 304 wise; the better the prediction, the lower the score.

### 305 **2.5.1 Meteorological Variables**

306 The meteorological variables were considered for different types of vertical levels:  
 307 surface or entire atmosphere (to capture e.g., the moisture content of an entire air col-  
 308 umn), pressure levels (1000, 950, 900, 850, 800, 700, 600, 500, 400, 300, 200 hPa, to cap-  
 309 ture the vertical structure), potential temperature levels (290, 300, 310, 320, 330, 350,  
 310 400 K, necessary to include potential vorticity), and potential vorticity levels. The se-  
 311 lected variables are listed in Table 3. The optimization can pick any variable on any level  
 312 type and value, as long as it is available. Precipitation variables from reanalyses were  
 313 not considered potential predictors. Precipitation is usually not considered as a predic-  
 314 tor in AMs, as a method developed in the perfect prognosis context would then be dif-  
 315 ficult to use in other conditions due to the high uncertainties and the biases associated  
 316 with precipitation predicted by an NWP or a climate model.

317 The variables were standardized (using the overall climatology) on-the-fly by At-  
 318 moSwing when loaded from files. The standardization has no impact on the selection of  
 319 analog situations for a single predictor, but it makes the combination of predictors within  
 320 one level of analogy more balanced, as they might have very different orders of magni-  
 321 tude and units. It allows a more effective optimization of the weights between predic-  
 322 tors.

### 323 **2.5.2 Analogy Criteria**

324 The most common analogy criteria in AMs are the Root Mean Squared Error (RMSE)  
 325 and the Teweles–Wobus criterion ( $S_1$ , see section 2.2). Other criteria were made avail-  
 326 able to the GAs in order to explore potential new characterizations of the analogy met-  
 327 rics. Two of these criteria are new and derived from  $S_1$ . The potential criteria made avail-  
 328 able to the GAs are the following:

- 329 1. RMSE: the Root Mean Squared Error.
- 330 2. MD: the Mean Absolute Difference, or Mean Absolute Error. It differs from the  
 331 RMSE in that the differences are not squared.
- 332 3.  $S_1$ : the Teweles–Wobus index as defined in Eq. 1 from section 2.2. It consists of  
 333 a comparison of the gradients, primarily used for the geopotential height.
- 334 4.  $S_2$ : inspired by the Teweles–Wobus index, we introduced a new criterion based  
 335 on the second derivative of the fields instead of the gradients:

$$S_2 = 100 \frac{\sum_i |\nabla^2 \hat{x}_i - \nabla^2 x_i|}{\sum_i \max\{|\nabla^2 \hat{x}_i|, |\nabla^2 x_i|\}} \quad (3)$$

336 where  $\nabla^2 \hat{x}_i$  is the second derivative between the  $i$ th triplet of adjacent points from  
 337 the predictor field of the target situation, and  $\nabla^2 x_i$  is the corresponding observed

**Table 3.** Selected variables for ERA-I, CFSR, and ERA5 for different types of vertical levels.

| Variable                      | Id    | Unit  | ERA-I |    |    |                | CFSR |    |    |                 | ERA5           |    |
|-------------------------------|-------|---|-------|----|----|----------------|------|----|----|-----------------|----------------|----|
|                               |       |   | PL    | PT | PV | SC             | PL   | PT | PV | SC              | PL             | SC |
| <b>CIRCULATION VARIABLES</b>  |       |   |       |    |    |                |      |    |    |                 |                |    |
| Geopotential height           | Z     | gpm   | •     |    | •  |                | •    |    | •  | •               |                |    |
| Geopotential height anomaly   | ZA    | gpm   |       |    |    |                | •    |    |    |                 |                |    |
| Zonal wind                    | U     | $\text{m s}^{-1}$                           | •     | •  | •  | • <sup>a</sup> | •    | •  | •  | •               | • <sup>a</sup> |    |
| Meridional wind               | V     | $\text{m s}^{-1}$                           | •     | •  | •  | • <sup>a</sup> | •    | •  | •  | •               | • <sup>a</sup> |    |
| Pressure                      | PRES  | Pa  |       | •  | •  | • <sup>c</sup> |      |    | •  | •• <sup>c</sup> | • <sup>c</sup> |    |
| Vertical velocity             | W     | $\text{Pa s}^{-1}$                          | •     | •  |    |                | •    | •  |    |                 | •              |    |
| Divergence                    | D     | $\text{s}^{-1}$                             | •     | •  |    |                |      |    |    |                 | •              |    |
| Vorticity                     | VO    | $\text{s}^{-1}$                             | •     |    |    |                | •    |    |    |                 |                |    |
| Potential vorticity           | PV    | $\text{m}^2 \text{s}^{-1} \text{K kg}^{-1}$ | •     | •  |    |                |      | •  |    |                 | •              |    |
| Stream function               | STRM  | $\text{m}^2 \text{s}^{-1}$                  |       |    |    |                | •    |    |    |                 |                |    |
| Velocity potential            | VPOT  | $\text{m}^2 \text{s}^{-1}$                  |       |    |    |                | •    |    |    |                 |                |    |
| Montgomery potential          | MONT  | $\text{m}^2 \text{s}^{-2}$                  |       | •  |    |                |      |    |    |                 |                |    |
| Montgomery stream function    | MNTSF | $\text{m}^2 \text{s}^{-1}$                  |       |    |    |                |      | •  |    |                 |                |    |
| <b>MOISTURE VARIABLES</b>     |       |   |       |    |    |                |      |    |    |                 |                |    |
| Relative humidity             | RH    | %   | •     |    |    |                | •    | •  |    | •               | •              |    |
| Specific humidity             | SH    | $\text{kg kg}^{-1}$                         | •     | •  |    |                | •    |    |    |                 |                |    |
| Total column water            | TCW   | $\text{kg m}^{-2}$                          |       |    |    | •              |      |    |    |                 | •              |    |
| Total column water vapour     | TCWV  | $\text{kg m}^{-2}$                          |       |    |    | •              |      |    |    | •               |                |    |
| Cloud water                   | CWAT  | $\text{kg m}^{-2}$                          |       |    |    |                |      |    |    | •               |                |    |
| Surface moisture flux         | IE    | $\text{kg m}^{-2} \text{s}^{-1}$            |       |    |    | •              |      |    |    |                 |                |    |
| <b>TEMPERATURE VARIABLES</b>  |       |   |       |    |    |                |      |    |    |                 |                |    |
| Temperature                   | T     | K   | •     |    |    | • <sup>b</sup> | •    | •  | •  | •               | • <sup>b</sup> |    |
| Potential temperature         | PT    | K   |       |    | •  |                |      |    |    |                 |                |    |
| Dewpoint temperature*         | DT    | K   |       |    |    | • <sup>a</sup> |      |    |    |                 |                |    |
| Sea surface temperature       | SST   | K   |       |    |    | •              |      |    |    |                 |                |    |
| 0° C isothermal level         | DEG0L | m   |       |    |    | •              |      |    |    |                 | •              |    |
| <b>RADIATION VARIABLES</b>    |       |   |       |    |    |                |      |    |    |                 |                |    |
| Surf. net solar radiation     | SSR   | $\text{J m}^{-2}$                           |       |    |    | •              |      |    |    |                 | •              |    |
| Surf. solar rad. downwards    | SSRD  | $\text{J m}^{-2}$                           |       |    |    | •              |      |    |    |                 | •              |    |
| Surf. net thermal radiation   | STR   | $\text{J m}^{-2}$                           |       |    |    | •              |      |    |    |                 | •              |    |
| Surf. thermal rad. downwards  | STRD  | $\text{J m}^{-2}$                           |       |    |    | •              |      |    |    |                 | •              |    |
| Surf. latent heat flux        | SLHF  | $\text{J m}^{-2}$                           |       |    |    |                |      |    |    |                 | •              |    |
| Surf. sensible heat flux      | SSHF  | $\text{J m}^{-2}$                           |       |    |    |                |      |    |    |                 | •              |    |
| Top net solar radiation       | TSR   | $\text{J m}^{-2}$                           |       |    |    |                |      |    |    |                 | •              |    |
| Top net thermal radiation     | TTR   | $\text{J m}^{-2}$                           |       |    |    |                |      |    |    |                 | •              |    |
| <b>STABILITY INDICES</b>      |       |   |       |    |    |                |      |    |    |                 |                |    |
| Convective avail. pot. energy | CAPE  | $\text{J kg}^{-1}$                          |       |    |    | •              |      |    |    | •               | •              |    |
| Convective inhibition         | CIN   | $\text{J kg}^{-1}$                          |       |    |    |                |      |    |    | •               | •              |    |
| Best (4 layer) lifted index   | 4LFTX | K   |       |    |    |                |      |    |    | •               |                |    |
| Surface lifted index          | LFTX  | K   |       |    |    |                |      |    |    | •               |                |    |
| Lapse rate                    | LAPR  | $\text{K m}^{-1}$                           |       |    |    |                | •    |    |    |                 |                |    |
| <b>OTHERS</b>                 |       |   |       |    |    |                |      |    |    |                 |                |    |
| Cloud cover                   | CC    | (0 - 1)                                     |       |    |    |                |      |    |    |                 | •              |    |
| Low cloud cover               | LCC   | (0 - 1)                                     |       |    |    |                |      |    |    |                 | •              |    |
| Total cloud cover             | TCC   | (0 - 1)                                     |       |    |    |                |      |    |    |                 | •              |    |
| Snow depth                    | SD    | m of w.e.                                   |       |    |    | •              |      |    |    |                 |                |    |

PL = pressure levels, PT = pot. temp. levels, PV = pot. vorticity levels, SC = single level, surface or total column  
 \*moisture and temperature variable, <sup>a</sup>at 10 m, <sup>b</sup>at 2 m, <sup>c</sup>at mean sea level.

338 second derivative in the candidate situation. Please note that it differs from the  
 339  $S_2$  index from Teweles and Wobus (1954).

340 5.  $S_0$ : as with  $S_2$ , this new criterion derives from  $S_1$  and is processed on the raw grid  
 341 values. It differs from the MD mainly in that it is normalized by the sum of the  
 342 maximum values instead of the number of points:

$$S_0 = 100 \frac{\sum_i |\hat{x}_i - x_i|}{\sum_i \max\{|\hat{x}_i|, |x_i|\}} \quad (4)$$

343 where  $\hat{x}_i$  is the  $i$ th point from the predictor field of the target situation, and  $x_i$   
 344 is the corresponding observed point in the candidate situation. The reason for adding  
 345 such a criterion was accidental, as it was an erroneous implementation of  $S_2$ . How-  
 346 ever, it turned out to be relevant (see sections 3 and 4.2).

347 6. DSD: difference in standard deviation over the spatial window. It is a non-spatial  
 348 criterion, as the location of the features does not matter.

349 7. DMV: absolute difference in mean value. It is also non-spatial, as the means are  
 350 computed over the spatial window before comparison.

### 351 **2.5.3 Design of Experiments**

352 The input variables selection with GAs has been assessed in sequential steps. First,  
 353 GAs were used to identify the single best predictor variables and their associated anal-  
 354 ogy criteria for each catchment (Sect. 3.1). The objective was to assess the consistency  
 355 of the selected variables in the most straightforward configuration. Then, as AMs can  
 356 be made of different levels of analogy with multiple predictors, the second experiment  
 357 assessed the skill associated with different structures and the ability of GAs to deal with  
 358 these, using a limited number of catchments (Sect. 3.2). Based on these results, the third  
 359 experiment performs the input variables selection for each catchment (Sect 3.3).

## 360 **3 Results**

### 361 **3.1 Best Single Variables**

362 The first experiment assesses the use of GAs to select a single predictor variable  
 363 and analogy criterion for each catchment. The selection has been performed on ERA-  
 364 I (Fig. 2) but also on CFSR for comparison (Fig. 3), with six optimizations per catch-  
 365 ment and dataset. The six optimizations were based on different mutation operators (the  
 366 five variants but twice the chromosome of adaptive search radius). The purpose of us-  
 367 ing two reanalyses is to assess the consistency and possible differences in the variables  
 368 selection between two datasets.

369 One of the first elements that can be seen for both datasets is the dominance of  
 370 the  $S_0$  criterion, selected 60% of the time for ERA-I and more than 55% of the time for  
 371 CFSR, along with the other Teweles–Wobus-based criteria (Fig. 4). The other analogy  
 372 criteria were rarely selected, if at all. The same applies to the RMSE, commonly used

373 in analog methods. The GAs could better predict using  $S_0$  as a metric for the Euclid-  
 374 ian distance between the predictor fields. This result is further discussed in Sect. 4.2.

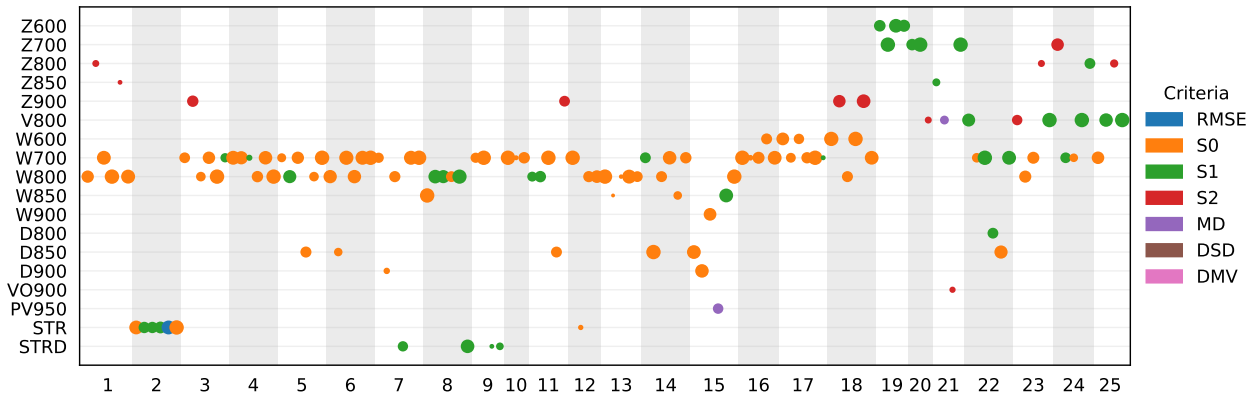


**Figure 2.** Best single variable selected (ordinate; see Table 3 for the variables abbreviations) from ERA-I for the 25 catchments (abscissa). The colors represent the analogy criteria, and the size of the dots is proportional to the skill score of the resulting method (the larger the dots, the better), within a range of 5% of the best result (those with lower skill are hidden).

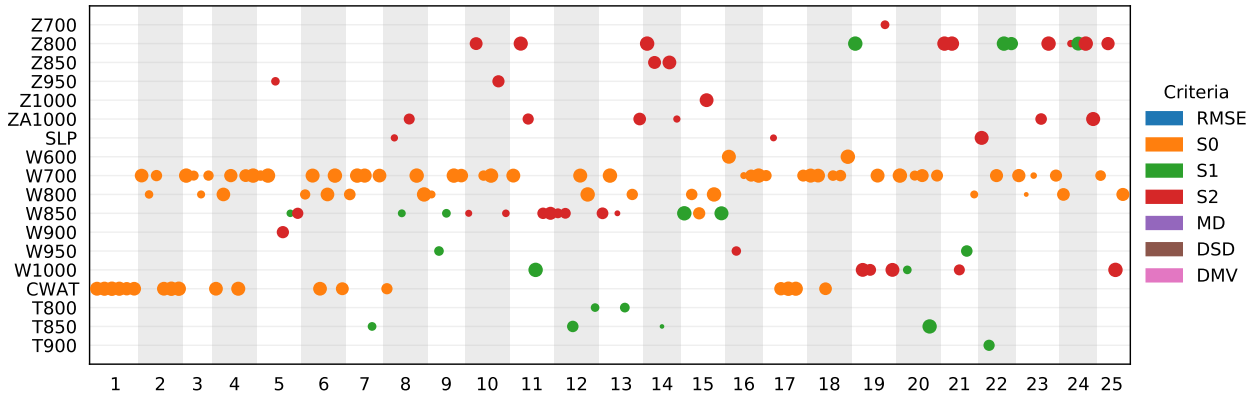


**Figure 3.** Same as Fig. 2 but for CFSR.

375 The variable selection results show some variability per catchment but similar skill  
 376 scores. Although GAs can, in theory, identify the global optimum, this search is highly  
 377 time-consuming for such complex problems, and we have to stop the optimizations at  
 378 a good-enough solution. These factors explain the variability that can be observed in the  
 379 results. Nevertheless, this variability provides information about alternative variables  
 380 with almost the same predictive skills.

381 Figures 2 and 3 demonstrate that optimal variables can vary across different re-  
 382 gions. Figure 5 illustrates this information spatially for ERA-I variables. In terms of sim-  
 383 ilarities, the vertical velocity ( $W$ ) at 700 and 800 hPa is the most frequently selected vari-

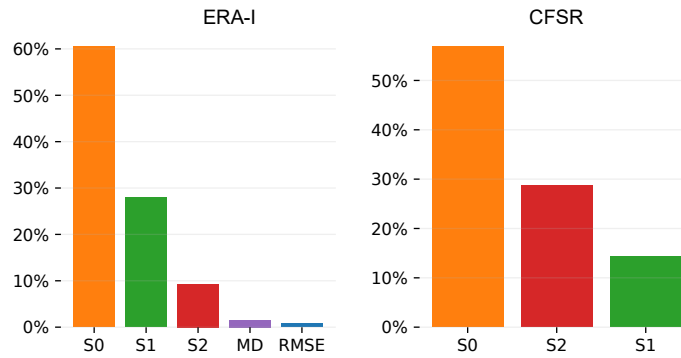


**Figure 4.** Frequency of the criteria selection for both reanalysis datasets.

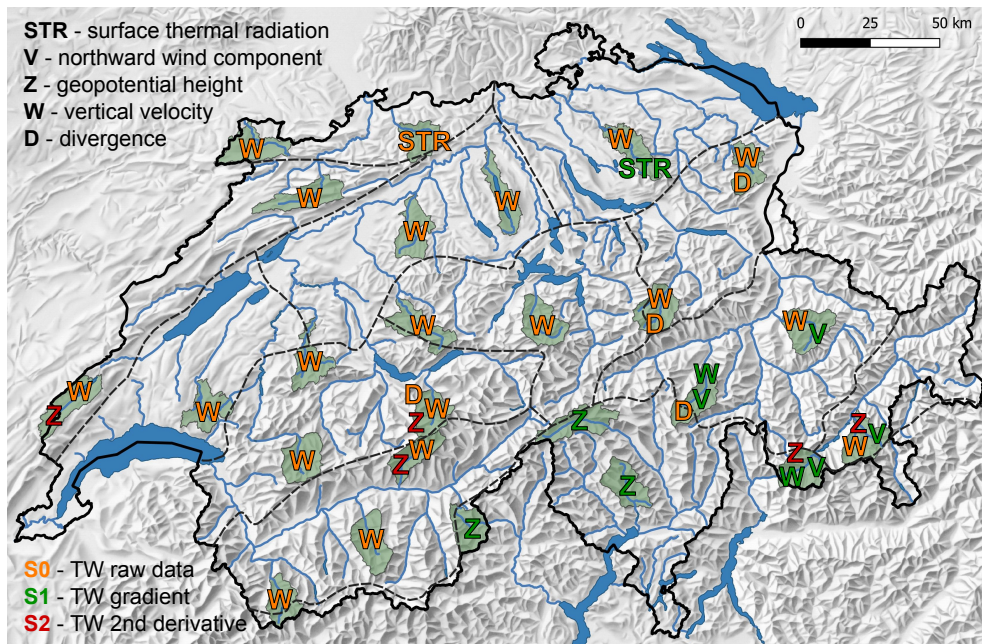


**Figure 5.** Map of the best variables for ERA-I for each catchment.

384 able for both datasets and is quantified using the  $S_0$  criteria. Upward vertical winds at  
 385 these levels are typically associated with precipitation generation. Within the Southern  
 386 Alpine climatic region (catchments 19, 20, 21), Z (based on the  $S_1$  criterion) emerges as  
 387 the best single predictor for ERA-I, which is not so clear with CFSR. Heavy precipita-  
 388 tion events in this region predominantly result from orographic effects related to sustained  
 389 southerly advection of moisture-laden air masses (Massacand et al., 1998). Other regional  
 390 clusters can be observed using ERA-I, such as the meridional wind V (with  $S_1$ ) in the  
 391 eastern part of Switzerland, also likely related to the southerly advection, STR(D) (sur-  
 392 face net thermal radiation and surface thermal radiation downwards) in northern Switzer-  
 393 land, maybe related to cloud cover, and the second derivative of Z (with  $S_2$ ) for several  
 394 catchments at similar latitudes. The second derivative of Z is also frequently selected for  
 395 CFSR. While the variable of cloud water (CWAT) from CFSR is often chosen, it is not  
 396 directly available in ERA-I.

### 3.2 Assessment of AM Structures

The analysis of different AM structures (Sect. 2.5.3) aims to identify the best-performing structures, i.e., the optimal number of analogy levels and predictors. We first considered one to four levels of analogy, with one to four predictors per level. Five optimizations were performed for each of these 16 structures with the different mutation operators. As this assessment requires 80 optimizations, it was performed on only four catchments (L’Allaine (1), Sitter (15), Doveria (19), Flaz (25)). These were selected to maximize the diversity of climatic conditions represented. A complementary analysis was performed on two catchments (L’Allaine (1) and Doveria (19)) to explore the use of up to eight predictors on one and two levels of analogy. These experiments also allowed comparing the performance of the mutation operators for different problem complexities.

Even though the structure is provided to the GAs, it can still evolve to a simpler version by assigning a zero weight to some predictors or by setting the same number of analogs for two successive levels of analogy. This simplification often happened, such as that no solution ended up with the structure 4 x 4 (four levels of analogy with four predictors each). The best-performing methods on the validation period were always made of one or two levels of analogy (Fig. 6 and 7). While some reference methods have up to four levels of analogy (Sect. 2.2), the use of normalized variables and weights might here favor their combination in the same level of analogy. The methods with fewer levels of analogy present less of a hierarchy among the predictors. However, not having a systematic constraint by the atmospheric circulation, as in the reference methods, results in more influence from other variables. Although atmospheric circulation is often of primary importance for heavy precipitation events, there can be situations where it is preferable to relax these constraints. However, we cannot conclude that two levels of analogy are the maximum to be considered, as the optimizer might have failed to optimize complex structures satisfactorily.

The results also depict significant performance differences between the mutation operators (Sect. 2.3). The chromosome of adaptive search radius (option #1) provides the best-performing parameter sets 76.3% of the time for the calibration period and 62.5% of the time for the validation period (Fig. B1). The second best is the non-uniform mutation with a mutation probability ( $p_{mut}$ ) of 0.1 (option #4), being the best option for 11.3% of the optimizations for the calibration period and 21.3% for the validation period. However, the same operator with a mutation probability ( $p_{mut}$ ) of 0.2 (option #5;  $G_{m,r}=100$ ) is the worst-performing option, with a success rate of 1.3% for the calibration period and 2.5% for the validation period. It quite well illustrates the difficulty of tuning such operators and the risk of a badly-configured mutation operator, and thus the benefit of an auto-adaptive option such as the chromosome of adaptive search radius with no controlling parameters. Moreover, it usually performed better for more complex AM structures.

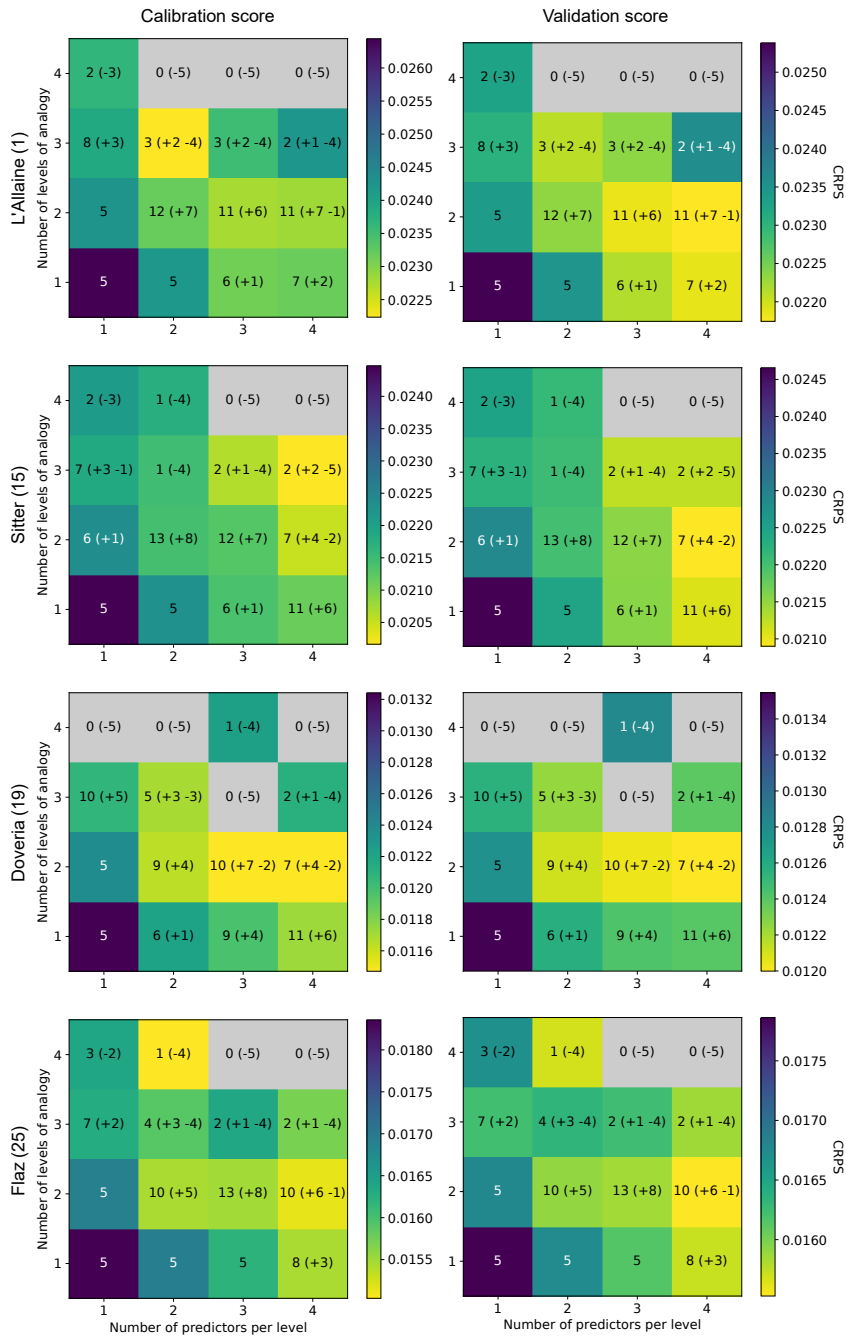


**Figure 6.** CRPS scores obtained for different AM structures with up to four levels of analogy and four variables per level for four catchments in Switzerland. Lower CRPS (yellow) represents a better skill.

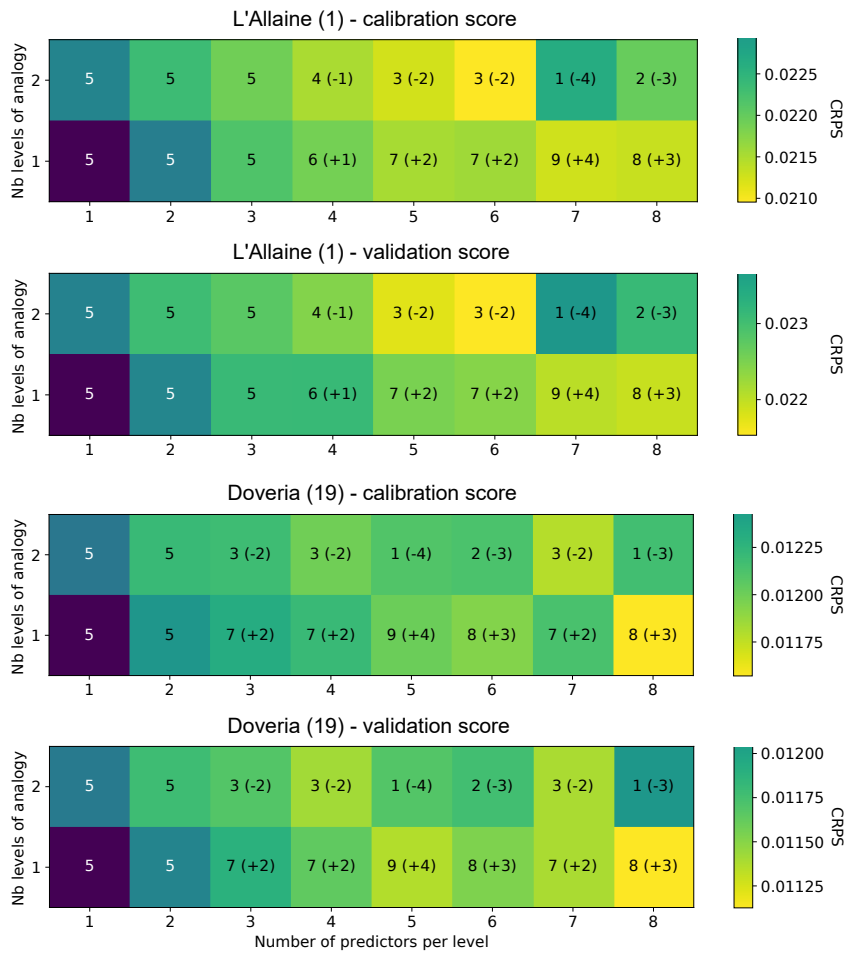


**Figure 7.** CRPS scores obtained for different AM structures with up to two levels of analogy and eight variables per level for two catchments in Switzerland. Lower CRPS (yellow) represents a better skill.

### 436 **3.3 Full Optimization**

437 The third experiment used different AM structures to perform the full input vari-  
438 able selection for each catchment. Only the chromosome of adaptive search radius has  
439 been used because of its higher performance.

#### 440 **3.3.1 Using Variables from ERA-I**

441 Based on the previous results, three AM structures were selected: 1 level of anal-  
442 ogy with 8 (1 x 8) or 12 predictors (1 x 12), and 2 levels with 6 predictors (2 x 6) (Sect.  
443 2.5.3). Two optimizations were performed by structure and catchment. The structure  
444 with two levels of analogy (2 x 6) turned out to be simplified by the GAs to a single level  
445 of analogy (1 x 6) for several catchments. Consequently, this structure resulted in lower  
446 skill scores (Figure 12) as fewer predictors were used. Thus, only structures with a sin-  
447 gle level of analogy (1 x 8 and 1 x 12) are further analyzed here.

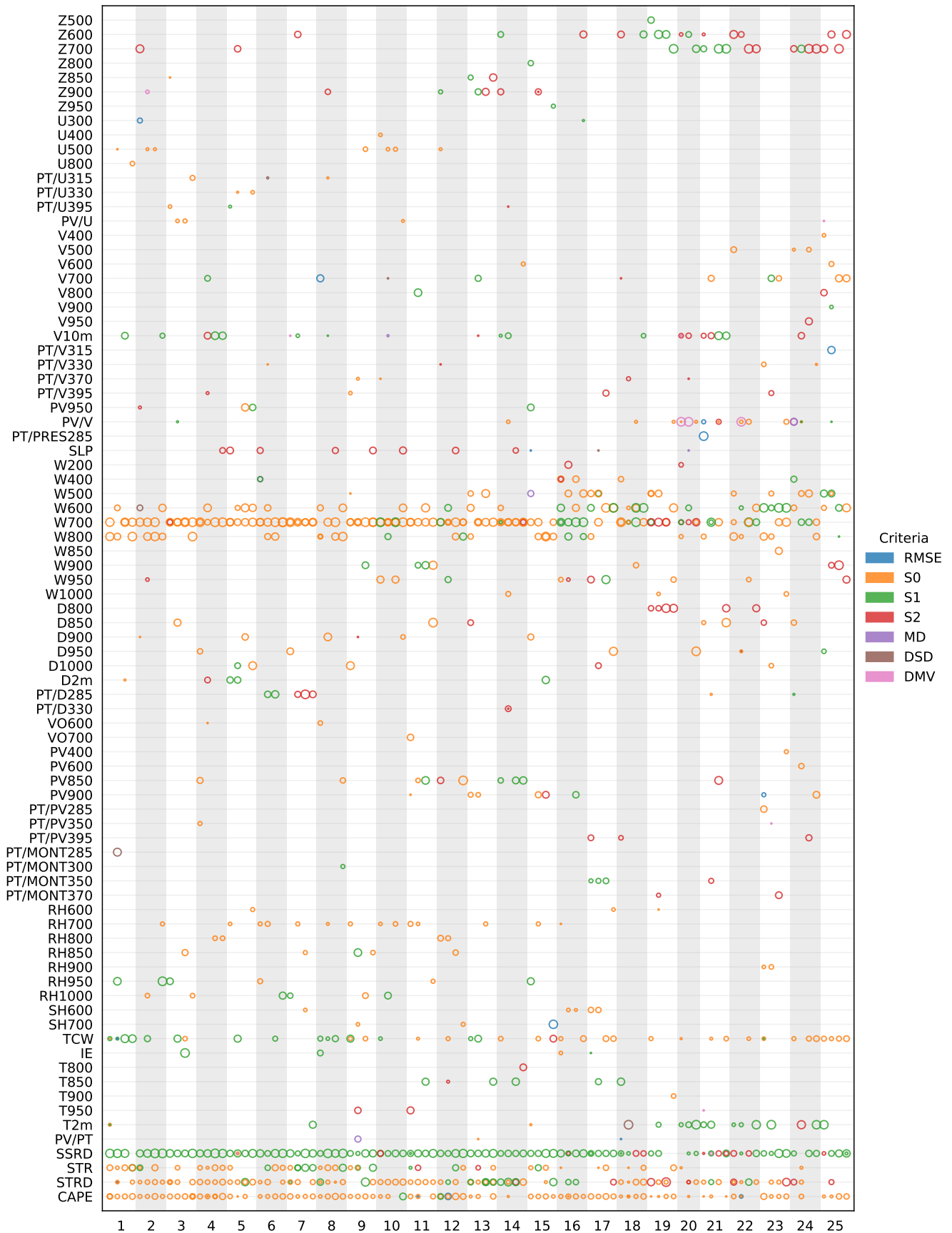


**Figure 8.** Selected variables (see Table 3 for the variables abbreviations) from ERA-I for the 1 x 8 and 1 x 12 structures for the different catchments. The colors represent the analogy criteria, and the size of the dots is proportional to the weight given to the predictor within the range [0.02, 0.2]. Variables that were never selected with a weight equal to or larger than 0.05 are not represented.

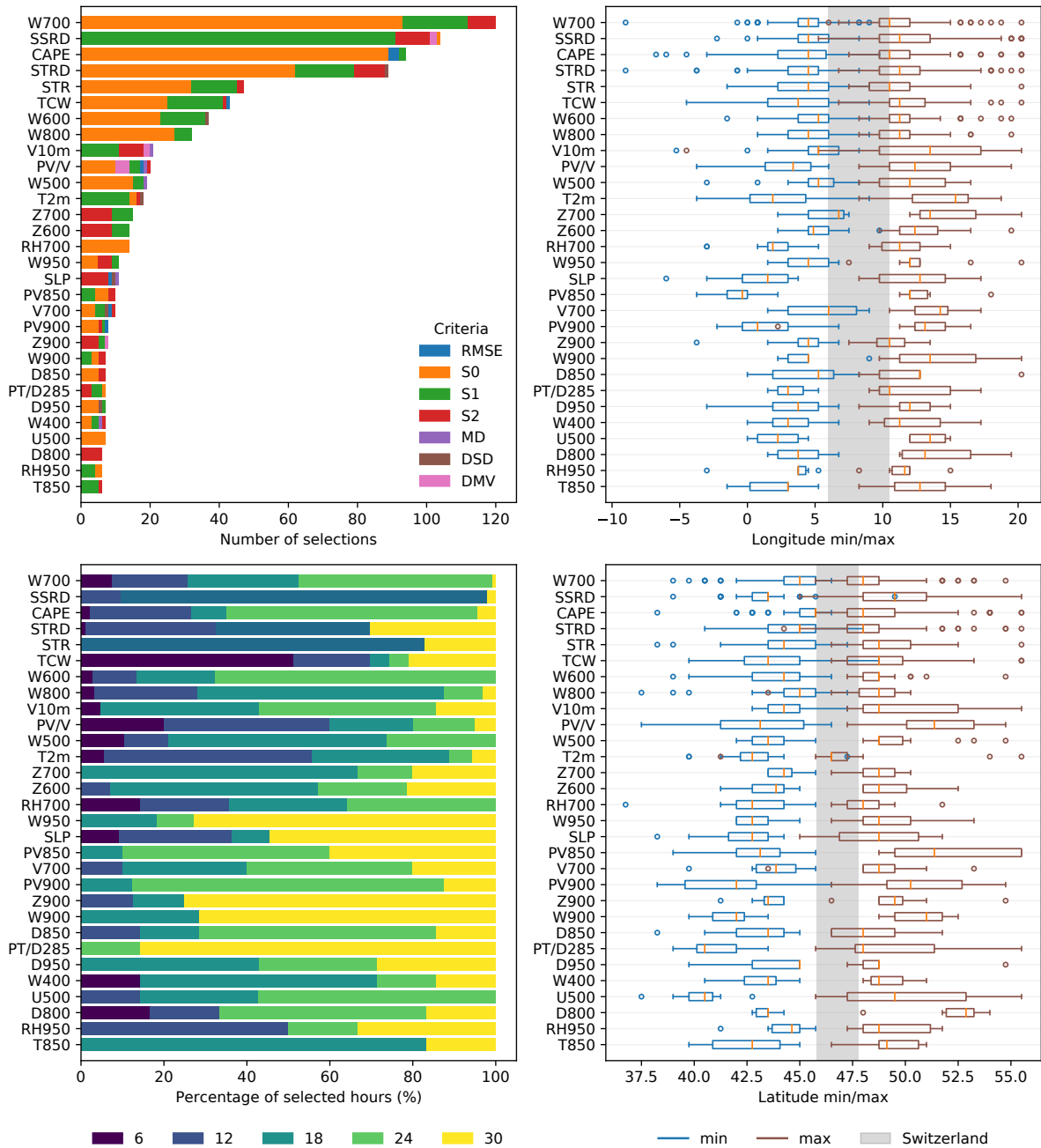


**Figure 9.** Statistics of the 30 most selected variables from ERA-I for the 1 x 8 and 1 x 12 structures for the different catchments (100 optimizations) along with the analogy criteria, the temporal window (30 = next day at 06 UTC; some radiation variables were considered at 15 UTC), and the spatial windows (longitudes and latitudes). The extent of Switzerland is shown in gray on the plots of the spatial windows.

448

449

Figure 8 shows the different variables selected for each catchment along with the analogy criteria (color) and the weights (size). Figure 9 synthesizes the 30 most often

450 selected variables and the associated analogy criteria, temporal windows, and spatial win-  
 451 dows across catchments. These results show again a strong dominance of the  $S_0$ ,  $S_1$ , and  
 452  $S_2$  analogy criteria, with the others being only rarely selected, including RMSE.  $S_0$  is  
 453 most often selected. The properties of  $S_0$  are further investigated in Sect. 4.2.

454 Vertical velocity (W) at 700 hPa (and sometimes at 600 or 800 hPa) is the most  
 455 frequently selected variable, also for catchments that were previously selecting another  
 456 best single variable (Sect. 3.1). Those with higher elevations and located in the south-  
 457 ern part of the country additionally selected W at 500 hPa or even higher.

458 The surface solar radiation downwards (SSRD) is the second most selected vari-  
 459 able and is mainly relevant when compared in terms of gradients ( $S_1$ ) rather than ab-  
 460 solute values. It might thus be used as a proxy for clouds. Other radiation variables oc-  
 461 cupy the fourth and fifth ranks, such as surface thermal radiation downwards (STRD)  
 462 and surface net thermal radiation (STR). These are mainly relevant when compared in  
 463 terms of absolute values ( $S_0$ ), although there is a non-negligible representation of the  $S_1$   
 464 criteria. These can also be used as proxies for cloud cover information.

465 CAPE is the third most selected variable, and the total column water (TCW) is  
 466 the sixth variable. At the ninth position comes the meridional wind at 10 m, but using  
 467  $S_1$  or even  $S_2$ . The derivative of the wind can be informative on the location of frontal  
 468 systems and convergence or divergence zones. Then comes the meridional wind on the  
 469 PV level. The 2 m temperature has the 12th position and is compared in terms of gra-  
 470 dients ( $S_1$ ), which can reflect the position of fronts. Follows the geopotential height (Z)  
 471 at 700 and 600 hPa compared primarily using the second derivatives of the fields ( $S_2$ ).  
 472 The curvature of the geopotential height helps identify and characterize synoptic-scale  
 473 features such as ridges and troughs in the atmosphere. A bit further down on the list,  
 474 SLP is also compared in terms of its second derivative. Other variables such as RH, PV,  
 475 D, and U also populate the 30 best variables.

476 The optimal spatial windows (Figure 9) cover Switzerland most of the time, with  
 477 different extents depending on the variables. For example, while the medians of the op-  
 478 timal domains for W and CAPE are slightly larger than Switzerland, PV is here con-  
 479 sidered on a larger domain. The 2m temperature (T2m) is characterized by unusual, lon-  
 480 gitudinally extended domains, with the main body in southern Switzerland extending  
 481 to the northern Mediterranean. Thus, it likely represents information at a synoptic scale,  
 482 such as the location of fronts, rather than local conditions. Note that SST was also in  
 483 the pool of potential variables but has never been selected as relevant.

484 The optimal temporal windows (time of the day) show substantial variability be-  
 485 tween the predictor variables. At the lower end of the range is TCW, which is consid-  
 486 ered better at the beginning of the precipitation accumulation period (06 UTC). The top  
 487 of the range (06 UTC the next day, corresponding to the end of the accumulation pe-  
 488 riod) was favored by the divergence (D at 285°K) and some low-level W (W900 and W950)  
 489 or Z (Z900). It should be noted here that the radiation variables used were cumulative  
 490 variables that were not decomposed prior to the analysis. Thus, most of the selected tem-  
 491 poral windows correspond to the beginning of the accumulation period, i.e., 15 UTC.

492

### 3.3.2 Using Variables from ERA5

493

494

495

496

497

498

499

500

501

A similar experiment has been conducted using ERA5 and a single method structure (1 x 12). ERA5 has been used at a 3-hourly time step, which might be more relevant than 6-hourly when considering radiation variables, and at a 0.5° spatial resolution. The potential analogy criteria were limited to  $S_0$ ,  $S_1$  and  $S_2$  and the spatial domains were slightly reduced (latitudes=[39, 55], longitudes=[-4, 20]). If previously the weights could be null for a predictor, a minimum of 0.01 was enforced here to force the GAs to select a relevant predictor. Finally, some predictors, often selected in the previous experiment, were fixed: W700 (with  $S_0$  criterion), CAPE (with  $S_0$  criterion), TCW (with  $S_0$  or  $S_1$  criteria); leaving nine predictors unconstrained.

502

503

504

505

506

507

In addition, only the variables found relevant when using ERA-I were selected as potential predictors, thus decreasing the pool of variables. Also, potential temperature levels and PV levels were not considered further. However, cloud cover variables were added to the potential predictors to assess whether SSRD served as a proxy for cloud cover. Thus, this experiment should not be considered a full exploration of ERA5 as it builds on the results obtained for ERA-I.

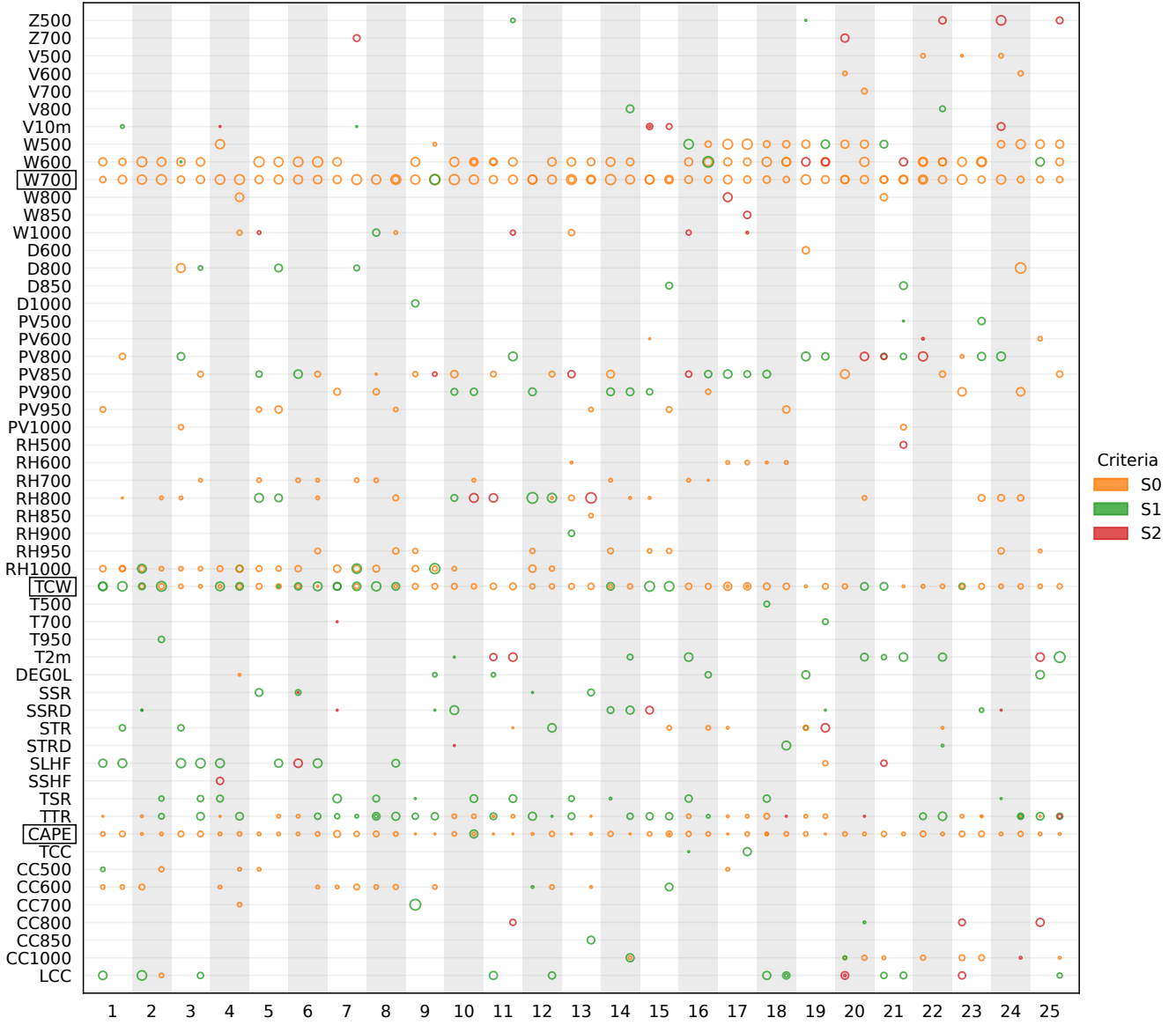


**Figure 10.** Selected variables (see Table 3 for the variables abbreviations) from ERA5 for the 1 x 12 structure for the different catchments. The variables that were forced into the AM are marked with a rectangle. The colors represent the analogy criteria, and the size of the dots is proportional to the weight given to the predictor within the range [0.02, 0.2]. Variables that were never selected with a weight equal to or larger than 0.05 are not represented.

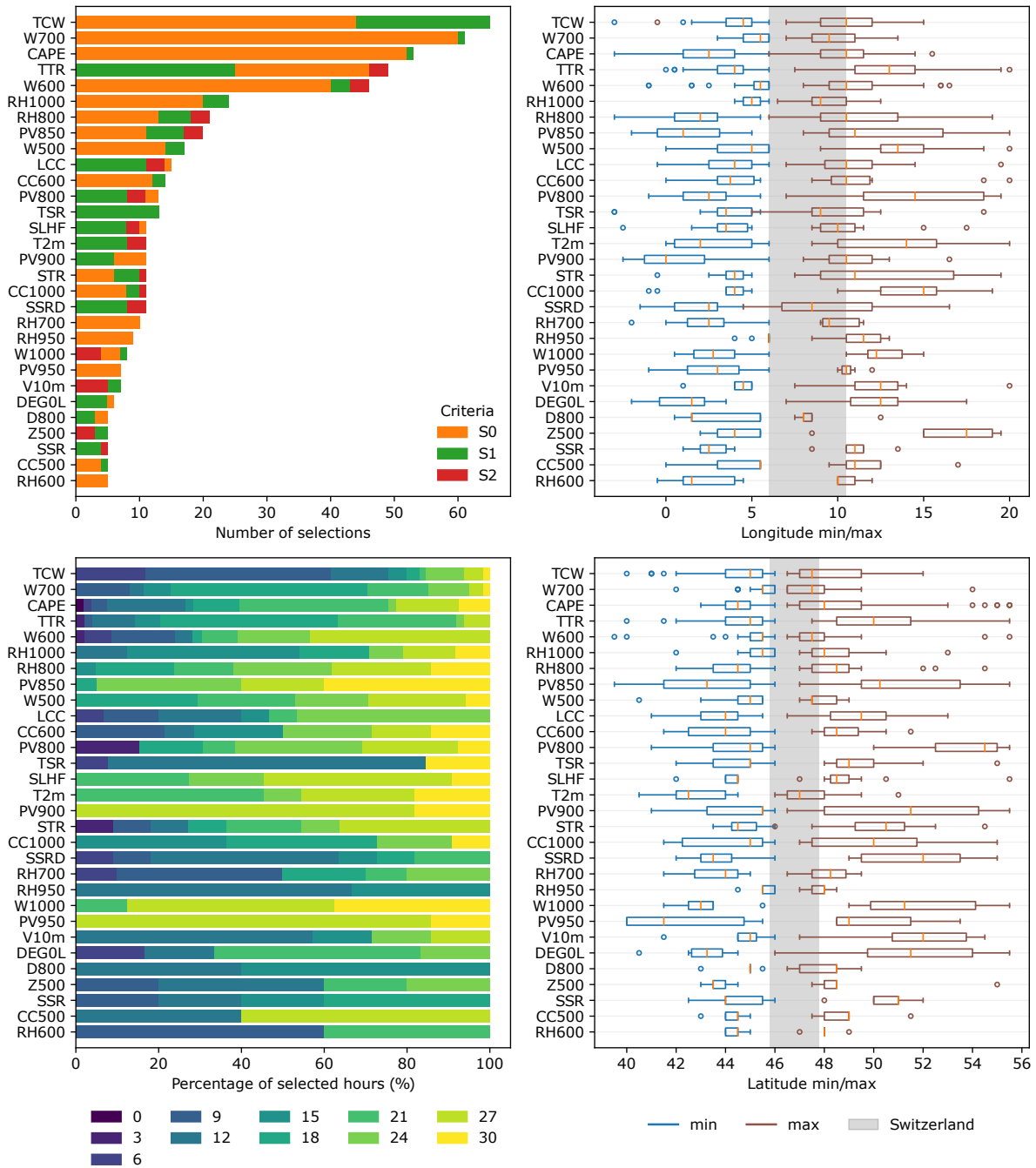


**Figure 11.** Statistics of the 30 most selected variables from ERA5 for the 1 x 12 structure for the different catchments (50 optimizations) along with the analogy criteria, the temporal window (30 = next day at 06 UTC), and the spatial windows (longitudes and latitudes). The extent of Switzerland is shown in gray on the plots of the spatial windows.

508 The selected variables from ERA5 are shown in Figure 10 and 11. When compar-  
 509 ing with ERA-I results, TCW gained importance as it was the most selected variable here.  
 510 Similarly, the relative humidity at 1000 and 850 hPa increased in importance as if its rel-

511 evance improved in ERA5. There were also changes in the radiation variables, with the  
 512 added top (top-of-atmosphere) net thermal radiation (TTR) taking the fourth slot and  
 513 being completed by other ones in the top 30 variables: top net solar radiation (TSR),  
 514 surface latent heat flux (SLHF), surface net thermal radiation (STR), surface solar ra-  
 515 diation downwards (SSRD), and surface net solar radiation (SSR). These variables are  
 516 likely highly correlated, and the selection could be reduced. It can also be noted that  
 517 these variables are still often considered in terms of gradient (using  $S_1$ ), even though cloud  
 518 cover variables were made available. As for cloud cover variables, different ones were se-  
 519 lected in the top 30: the low cloud cover (LCC) and the cloud cover (CC) at 600, 1000,  
 520 and 500 hPa. While LCC was most often considered in terms of gradients, the absolute  
 521 values of the other cloud cover variables were mostly selected. The importance of low  
 522 level PV also increased compared to ERA-I. Conversely, the geopotential height was only  
 523 selected at 500 hPa in the top 30 predictors, SLP is not among the best ones anymore,  
 524 and the presence of the divergence variables also decreased.

525 The optimal spatial domains are comparable with those selected for ERA-I, includ-  
 526 ing the 2-meter temperature extension to the south. As for the temporal windows, TCW  
 527 is again mainly selected between 6 and 12 UTC, and RH at different times of the day.  
 528 PV is often selected at the end of the day, along with W at 1000 hPa, the surface latent  
 529 heat flux (SLHF), and the 2-meter temperature (T2m). The other variables are mainly  
 530 selected during the daytime.

### 531 3.4 Skill Scores

532 To assess the relevance of the methods optimized in this work, they have been com-  
 533 pared to the reference methods (Sect. 2.2). Figure 12 shows the CRPS score improve-  
 534 ment for the different reference and resulting methods compared to the simplest RM1  
 535 method. The CRPS values being heavily influenced by the climatology and thus signif-  
 536 icantly different from one catchment to another, they are best compared relatively to a  
 537 reference catchment-wise.

538 The improvement of the CRPS is shown for the first single variable selection from  
 539 ERA-I (ERA-I GAS 1x1), the full optimizations using ERA-I (ERA-I GAS 1x8, 1x12,  
 540 1/2x6) or ERA5 (ERA5 GAS 1x12). An additional experiment has been attempted by  
 541 pre-selecting the predictor variables (along with their vertical level and their time) and  
 542 the analogy criteria and letting the GAs optimize the weights between these variables,  
 543 along with the spatial domains. To this end, 26 of the most commonly selected ERA5  
 544 variables were provided to the optimizer, organized in a single level of analogy (1x26).  
 545 The results are shown in Appendix C. As shown in Figure 12, this approach does not  
 546 provide the best skill scores. It can be due to non-optimal choices made to homogenize  
 547 the vertical levels or times of the day, for example. In addition, this approach is not com-  
 548 putationally efficient as it requires loading variables that barely play a role in the selec-  
 549 tion of analog situations. Therefore, we do not recommend using such a strategy.

550 One can see in Fig. 12 that the selection of a single best variable (GAS 1x1) al-  
 551 ready achieves better skill than the RM1 method. Obviously, the skill provided by a sin-

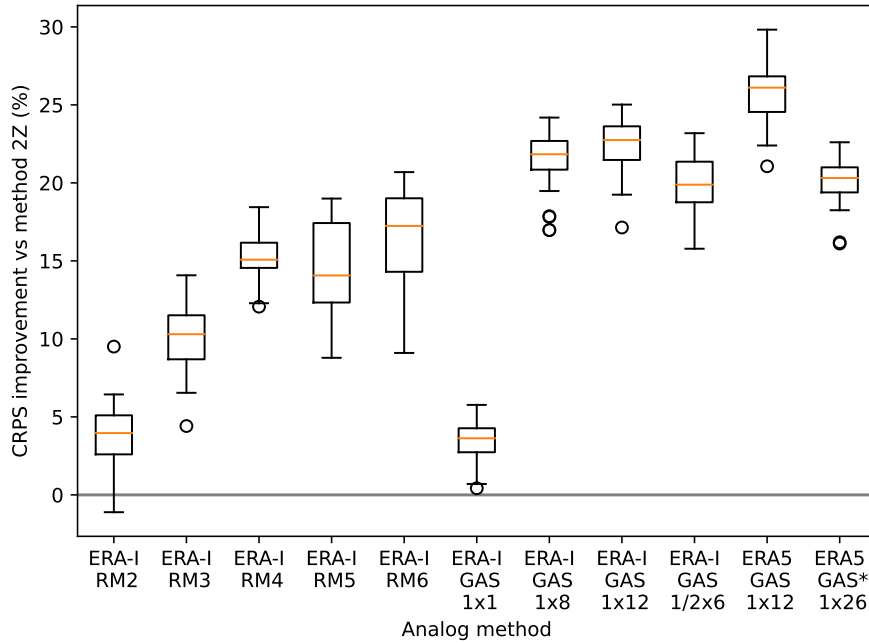


**Figure 12.** Performance scores of the different reference and optimized methods on the validation period for the 25 catchments. The skill score is expressed as a percentage improvement (lower values) in terms of the CRPS when considering RM1 as a benchmark. An LxP code represents the structures, with L being the number of levels of analogy and P being the number of predictors per level.

552 gle variable remains lower than more complex AMs. All other optimized methods per-  
 553 form substantially better than the reference methods. Thus, despite having a single level  
 554 of analogy, they outperform complex stepwise AMs. The gain obtained using ERA5 in-  
 555 stead of ERA-I can be due to higher spatial and temporal resolutions or better variables  
 556 (Horton, 2021). The selection of the predictor variables and the analogy criteria by GAs,  
 557 along with all other parameters, provides AMs that prove relevant, also on the valida-  
 558 tion period.

## 559 4 Discussion

### 560 4.1 Transferability of the Results

561 The main aim of this work was to test the ability of GAs to select input variables  
 562 for analog methods. It was found that GAs could select relevant predictors with the anal-  
 563 ogy criteria to quantify their similarity. However, it may not be optimal to use the se-  
 564 lected predictors in another context blindly. Indeed, the list of potential variables must  
 565 be adapted to the application of the AM.

566 Depending on the application, some specific constraints should be considered for  
 567 optimizing AMs. For example, for use in forecasting, only meteorological variables that  
 568 are considered sufficiently well-predicted should be selected. As for climate impact stud-

569 ies, the availability of meteorological variables is significantly more limited than what  
 570 a reanalysis and standard climate model output can offer. In addition, care should be  
 571 taken to select variables that have a causal effect on the predictand of interest and avoid  
 572 undesirable co-variability.

#### 573 4.2 What About this $S_0$ Criteria?

574 The success of the  $S_0$  criteria over RMSE was unexpected. Overall, the triplet  $S_0$ ,  
 575  $S_1$  and  $S_2$  dominate the selection of analogy criteria.  $S_1$  was developed to verify prog-  
 576 nostic charts (Teweles & Wobus, 1954). It was computed using pressure differences be-  
 577 tween stations arranged in north-south and east-west lines. The "difficulty coefficient"  
 578 (the denominator) reduces the influence of the seasons and weather systems' strength  
 579 on the score. About forty other scores were developed and assessed by Teweles and Wobus  
 580 (1954), but  $S_1$  was the most stable. It was also selected to penalize forecasters who tended  
 581 to be overly conservative by forecasting weak systems too often. Indeed, the denomina-  
 582 tor being the sum of the maximum gradients of the forecast or the observation, the fore-  
 583 cast of a weaker system is more penalized than that of a stronger system. However, this  
 584 could result in the opposite effect as it is safer for the forecaster to predict a stronger  
 585 system with larger gradients and thus make the denominator larger (Thompson & Carter,  
 586 1972).

587 The  $S_0$  and  $S_2$  criteria have the same characteristic as  $S_1$ , i.e., they penalize more  
 588 heavily weaker fields. Let us consider a field F1 with values 50% lower than the target  
 589 field (F), and another one, F2, with values 50% higher. Then,  $S_0(F, F1) = 50$  and  $S_0(F, F2) =$   
 590  $33.3$  while the absolute differences between the target (F) and F1 or F2 are equal. F2  
 591 will then be selected as a better analog. To get the same  $S_0$  value, F2 would need to dou-  
 592 ble the target field values. The consequence is that the selection of analogs based on  $S_0$ ,  
 593  $S_1$  and  $S_2$  is not symmetrical, and these criteria tend to select fields that are close to the  
 594 reference but preferably stronger than weaker.

595 To investigate further the characteristics of  $S_0$ , we considered a variation named  
 596 here  $S_{0obs}$  that uses the observation (here, target situation) values only for the denom-  
 597 inator and not the maximum between observation and forecast (here, candidate analog).  
 598 It is then similar to the MAPE (Mean Absolute Percent Error) and is symmetrical. We  
 599 performed a classic calibration of a simple AM using only W700 with (1) the  $S_0$  crite-  
 600 ria, (2) the RMSE criteria, and (3) the  $S_{0obs}$  criteria. The calibration was performed for  
 601 each setup separately. Using RMSE deteriorates the skill score by 8.7% on average, and  
 602  $S_{0obs}$  also deteriorates the skill score by 9.8%. Thus, the asymmetrical property of  $S_0$   
 603 is beneficial for the prediction.

604 We then considered the reference method RM3 and performed a classic calibration  
 605 for the 25 catchments by replacing one or the other criterion. When using  $S_{1obs}$  ( $S_1$  nor-  
 606 malized by the gradients of the observations only) instead of  $S_1$  for Z, the skill score de-  
 607 teriorates by 4.8% on average. However, when replacing the RMSE of the second level  
 608 of analogy (MI) with  $S_0$ , there is a slight loss in performance of 0.5%. As there is strong  
 609 conditioning by the first level of analogy that provides the sample of candidate analog

610 dates to be subsampled on moisture variables, the criterion of the second level of anal-  
 611 ogy has a lower impact.

612 It seems therefore that the asymmetrical properties of  $S_0$ ,  $S_1$ , and  $S_2$  are benefi-  
 613 cial for the prediction. Analog situations are best considered a bit stronger than weaker  
 614 while being close to the target situation. The CRPS is mainly sensitive to high precip-  
 615 itation values, even more when the precipitation is not transformed (see Bontron, 2004,  
 616 for precipitation transformation). Thus, one hypothesis is that large precipitation events  
 617 being underrepresented in the archive, AMs are better off selecting stronger predictor  
 618 fields, often associated with higher precipitation. It might then play a role of bias com-  
 619 pensation for underrepresented high precipitation events. The reason for such behavior  
 620 should be investigated further.

## 621 5 Conclusions

622 The objective of the work was to assess the ability of GAs to select the input vari-  
 623 ables of the analog method along with the analogy criteria. The experiment was success-  
 624 ful as the selected predictors provided better skills than the reference methods. More-  
 625 over, most of the selected variables can be related to meteorological processes involved  
 626 in precipitation generation. For example, among the most selected variables are: the ver-  
 627 tical velocity (W) at 700 hPa (along with other levels), the total column water (TCW),  
 628 the convective available potential energy (CAPE), radiation variables, the potential vor-  
 629 ticity (PV), the relative humidity (RH), cloud cover variables, wind components, the geopo-  
 630 tential height, air temperature, and the divergence.

631 The selection of analogy criteria also proved fruitful, as there were clear trends to-  
 632 ward a dominant criterion for a given variable. The unexpected result was the success  
 633 of the criterion  $S_0$ , inspired by the Teweles-Wobus criterion. This new  $S_0$  turned out to  
 634 be the most often selected analogy criterion, replacing the RMSE for the characteriza-  
 635 tion of Euclidean distances. Three analogy criteria were most often selected, and all are  
 636 derived from the Teweles-Wobus criterion; one is based on the raw point values, another  
 637 on the gradients, and the third on the second derivative of the fields. All of them are nor-  
 638 malized by the sum of the largest point(pair)-wise values from the target and the can-  
 639 didate fields. This normalization makes the criteria asymmetrical, so that higher values  
 640 are preferred to lower ones. Heavy precipitation, which substantially influences the CRPS,  
 641 is often associated with more dynamic situations, characterized by higher values. The  
 642 GAs may try to compensate for the under-representation of heavy precipitation events  
 643 by favoring situations associated with higher precipitation values. These assumptions  
 644 would need to be further investigated.

645 Another unexpected result is the preferred structure for the analog methods. While  
 646 most reference methods build on a stepwise selection of predictors with successive lev-  
 647 els of analogy subsampling from the previous one by using different predictors, here, the  
 648 GAs preferred a flatter structure, mainly with a single level of analogy, but more vari-  
 649 ables. The reference methods most often start with selecting candidate analogs using the  
 650 geopotential height and then narrowing down the selection using vertical velocity or mois-

651 ture variables. A primary difference with the reference methods is that the variables are  
652 standardized here, and weights are used (and optimized) to combine them in a given level  
653 of analogy. These two elements make the combination of variables with different value  
654 ranges easier. However, it cannot be excluded that deeper structures can provide bet-  
655 ter results, but that GAs did not find these solutions.

656 Such optimization is computationally intensive. The new GPU-based computations  
657 brought significant time improvement, particularly for high-resolution data. Other ap-  
658 proaches could be considered to decrease the computation time, such as a faster explo-  
659 ration of the dataset using a smaller period for data pre-screening, or the division of the  
660 whole period into smaller batches. An alternative could be to reduce the number of days  
661 with small precipitation amounts, as they have a small impact on the CRPS, while weight-  
662 ing their contributions by using a weighted CRPS approach.

663 This work opens new perspectives for input variables selection in the context of the  
664 analog method. While the variables selected in these experiments might not be trans-  
665 ferable to other contexts, the approach was proven successful and can be applied to other  
666 datasets. The potential variables must be chosen wisely regarding the application intended.  
667 Such an approach can, for example, be used to select the relevant variables to predict  
668 precipitation for a new location, or as a data mining technique to explore a dataset to  
669 predict a new predictand of interest.

## 670 **Appendix A GPU Implementation and Benchmark**

671 Several GPU implementations were tested, with the most successful aiming to re-  
672 duce the data copy to the device while increasing the load of parallel processing. It con-  
673 sisted in copying the predictor data to the device and calling the kernel<sup>2</sup> for every tar-  
674 get date, thus assessing all candidates for that target date in one call. The main ben-  
675 efit of this variant is that it allows overlapping – using streams – the calculation of the  
676 analogy criteria on the GPU and other calculations on the CPU, such as the extraction  
677 of the indices corresponding to the candidate dates (using a temporal moving window  
678 of 120 days) and the sorting of the resulting analogy criteria.

679 Threads on the GPU are organized in dynamically defined blocks, with a size from  
680 32 to 1024 threads. Here, every candidate date is assigned to a different block, with in-  
681 ternal loops for cases where the number of grid points is higher than the number of threads  
682 in the block. All analogy criteria need a reduction step to synthesize a two-dimensional  
683 array into a single value. The reduction is part of the analogy criteria calculation and  
684 is thus also done on the GPU. The threads are organized in groups of 32, called warps,  
685 that are synchronous and can access each other’s registers. The reduction on the device  
686 was performed with an efficient warp-based reduction using the CUDA shuffle instruc-  
687 tion. Different block sizes were assessed, and the size of 64 threads was identified as op-  
688 timal as it leaves fewer threads inactive during the reduction. Access to the GPU’s global  
689 memory has also been kept to a minimum due to its higher latency.

---

<sup>2</sup> A kernel is a numerical function executed in parallel on the GPU.

690 The Google benchmark library was used to assess the computing time of different  
 691 AM structures – single or two levels of analogy and up to four predictors per level – along  
 692 with various grid sizes. Figure A1 shows the results for the analogy criterion  $S_1$ , with  
 693 gradients being pre-processed using CPUs only (counted in the total time). The other  
 694 analogy criteria showed similar results. The task consisted of extracting analogs for 32  
 695 years using the other 31 years as archives for candidate situations within a 120-days tem-  
 696 poral window. It makes a total of  $43.5 \cdot 10^6$  field comparisons per predictor of the first  
 697 level of analogy.

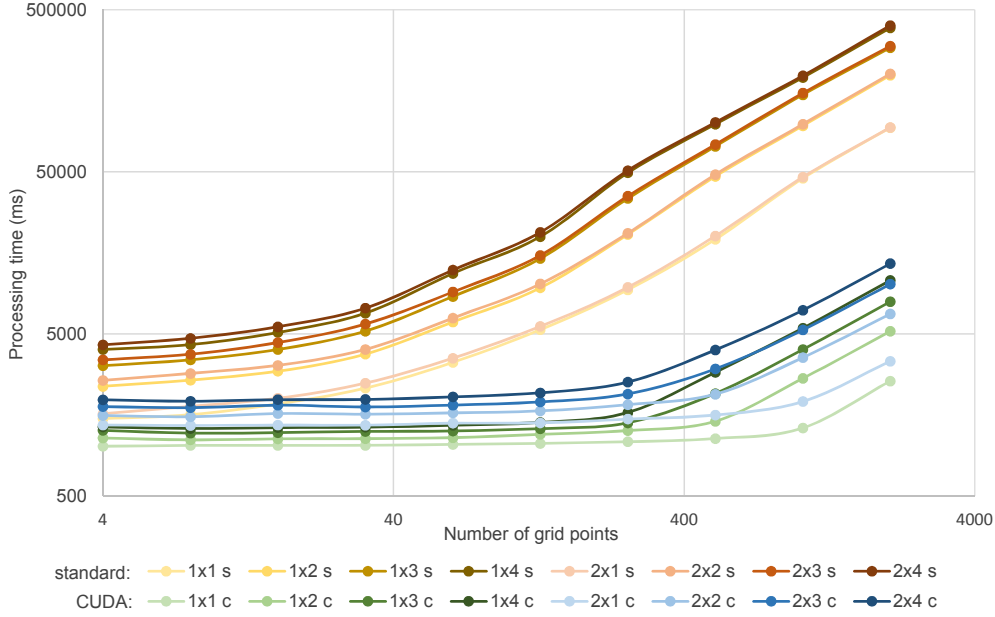


**Figure A1.** Computing time for the extraction of analogs over 32 years using the  $S_1$  criteria for different grid sizes and various structures of AMs. An LxP code represents the structures, with L being the number of levels of analogy and P being the number of predictors per level. Time is given for using (s) standard CPUs and (c) CUDA on GPUs (NVIDIA GeForce RTX 2080). Note the logarithmic axes.

698 The experiment was conducted on the UBELIX cluster of the University of Bern,  
 699 using the same node for the whole benchmark and processing on a single NVIDIA GeForce  
 700 RTX 2080 graphics card. The CPU processing – using the linear algebra library Eigen  
 701 3 (Guennebaud et al., 2010) – was done on a single thread. Although AtmoSwing can  
 702 parallelize the calculation of the analogy criteria on multiple CPU threads, it uses a sin-  
 703 gular thread for this task when optimizing with GAs because it parallelizes the evaluation  
 704 of the different individuals on multiple threads. With GPUs, it still assesses the individ-  
 705 uals on multiple CPU threads, each of them being able to use a different GPU device  
 706 to calculate the analogy criteria. It is thus parallelizing both on CPUs and GPUs.

707 The benchmark (Fig. A1) shows that the GPU computations are systematically  
 708 faster than those on the CPU, and this difference increases with the number of grid points.  
 709 The GPU computations were 13 times faster on average and up to 38 times faster (5.2 sec

710 instead of 3.3 min) when using 2048 points. Model outputs and reanalyses show an in-  
 711 crease in spatial resolution; thus, the impact on the computation time will become in-  
 712 creasingly important. When using CPU only, adding a predictor in the first level of anal-  
 713 ogy has a much higher impact on time than adding a second level of analogy. It is ex-  
 714 plained by the fact that it needs to process the analogy criteria for the whole archive for  
 715 each predictor of the first level of analogy, while the second level has only a few candi-  
 716 date situations to assess.

## 717 **Appendix B Performance of the Mutation Operators**

718 As suggested in Horton et al. (2017), five variants of the mutation operator were  
 719 used in parallel optimizations:

- 720 1. Chromosome of adaptive search radius (Horton et al., 2017)
- 721 2. Multiscale mutation (Horton et al., 2017)
- 722 3. Non-uniform mutation ( $p_{mut}=0.1$ ,  $G_{m,r}=50$ ,  $w=0.1$ )
- 723 4. Non-uniform mutation ( $p_{mut}=0.1$ ,  $G_{m,r}=100$ ,  $w=0.1$ )
- 724 5. Non-uniform mutation ( $p_{mut}=0.2$ ,  $G_{m,r}=100$ ,  $w=0.1$ )

725 where  $p_{mut}$  is the mutation probability,  $G_{m,r}$  is the maximum number of gener-  
 726 ations (G) during which the magnitude of the research varies, and  $w$  is a chosen thresh-  
 727 old to maintain a minimum search magnitude when  $G > G_{m,r}$ .

728 Figure B1 shows the performance of these five mutation operators for different AM  
 729 structures and the different catchments considered in Sect. 3.2. Overall, the chromosome  
 730 of adaptive search radius has a success rate of 76.25% in calibration and 62.5% in val-  
 731 idation, the multiscale mutation 7.5%, and 8.75% respectively, and the non-uniform mu-  
 732 tation with its different options: (3) 11.25% and 10%, (4) 11.25% and 21.25%, and (5)  
 733 1.25% and 2.5% respectively.

734 Thus, it is quite clear that the chromosome of adaptive search radius obtains the  
 735 best results, all the more so with more complex structures, i.e., more predictor variables.  
 736 Although its success rate decreases slightly in validation, it remains much larger than  
 737 the other options. The non-uniform mutation shows significant variability of performance  
 738 depending on its options.

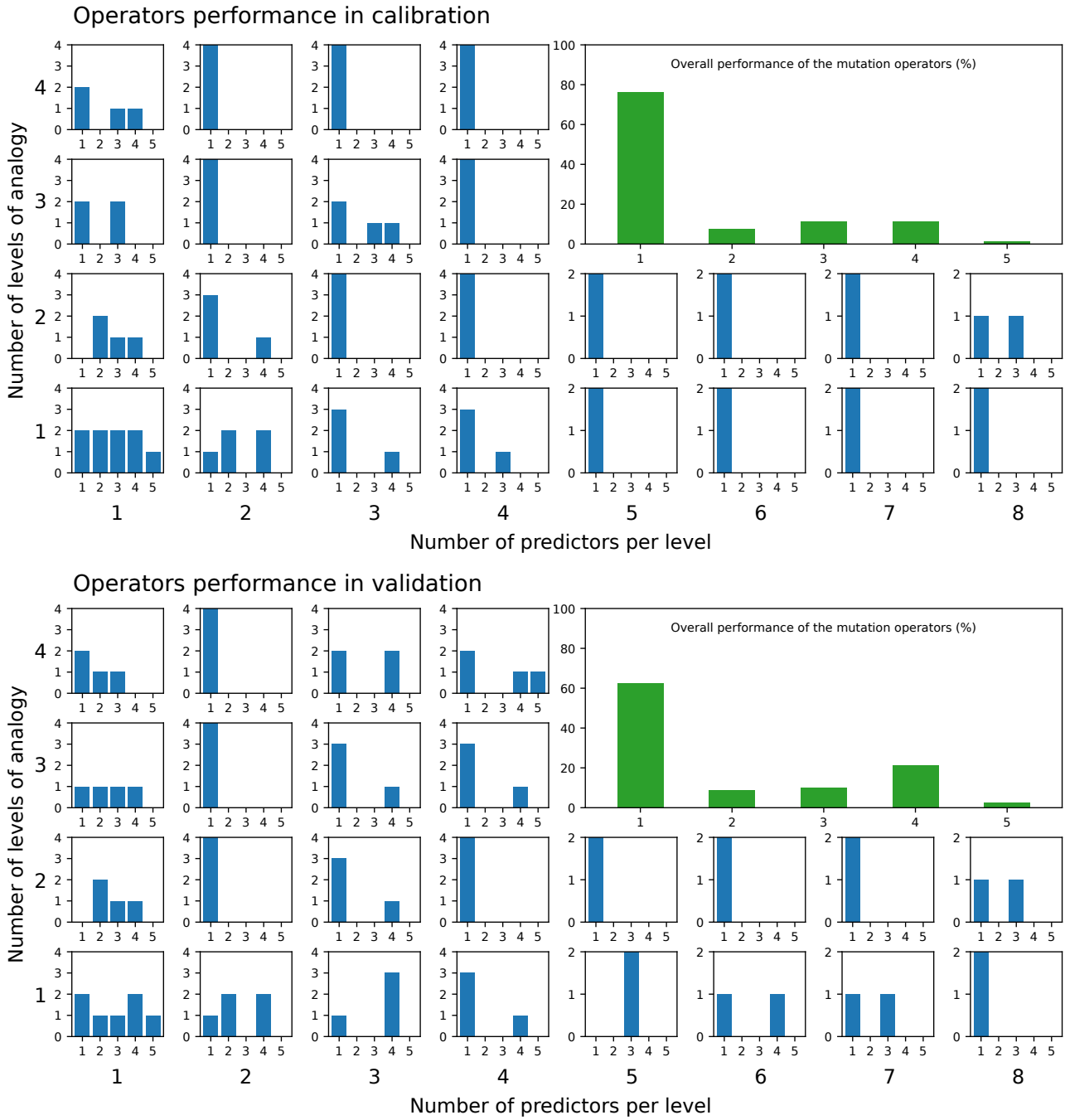


**Figure B1.** Performance of the five mutation operators (Sect. 2.3) for different AM structures and the different catchments considered in Sect. 3.2. The values represent the number of optimizations for one mutation operator that resulted in the best performing AM. Results are shown for both calibration and validation. When multiple operators obtain the same skill score, they all get a point.

**739 Appendix C An Attempt to Constrain the Algorithms**

740 An additional experiment has been attempted by pre-selecting the predictor vari-  
741 ables (along with their vertical level and their time) and the analogy criteria and letting  
742 the GAs optimize the weights between these variables, along with the spatial domains.  
743 To this end, 26 of the most commonly selected ERA5 variables were provided to the op-  
744 timizer, organized in a single level of analogy. The results are shown in Figure C1 and  
745 depict high weight values for  $W$  at 600 and 700 hPa. Surprisingly,  $Z_{700}$  based on  $S_2$  also  
746 gets relatively high weight values.

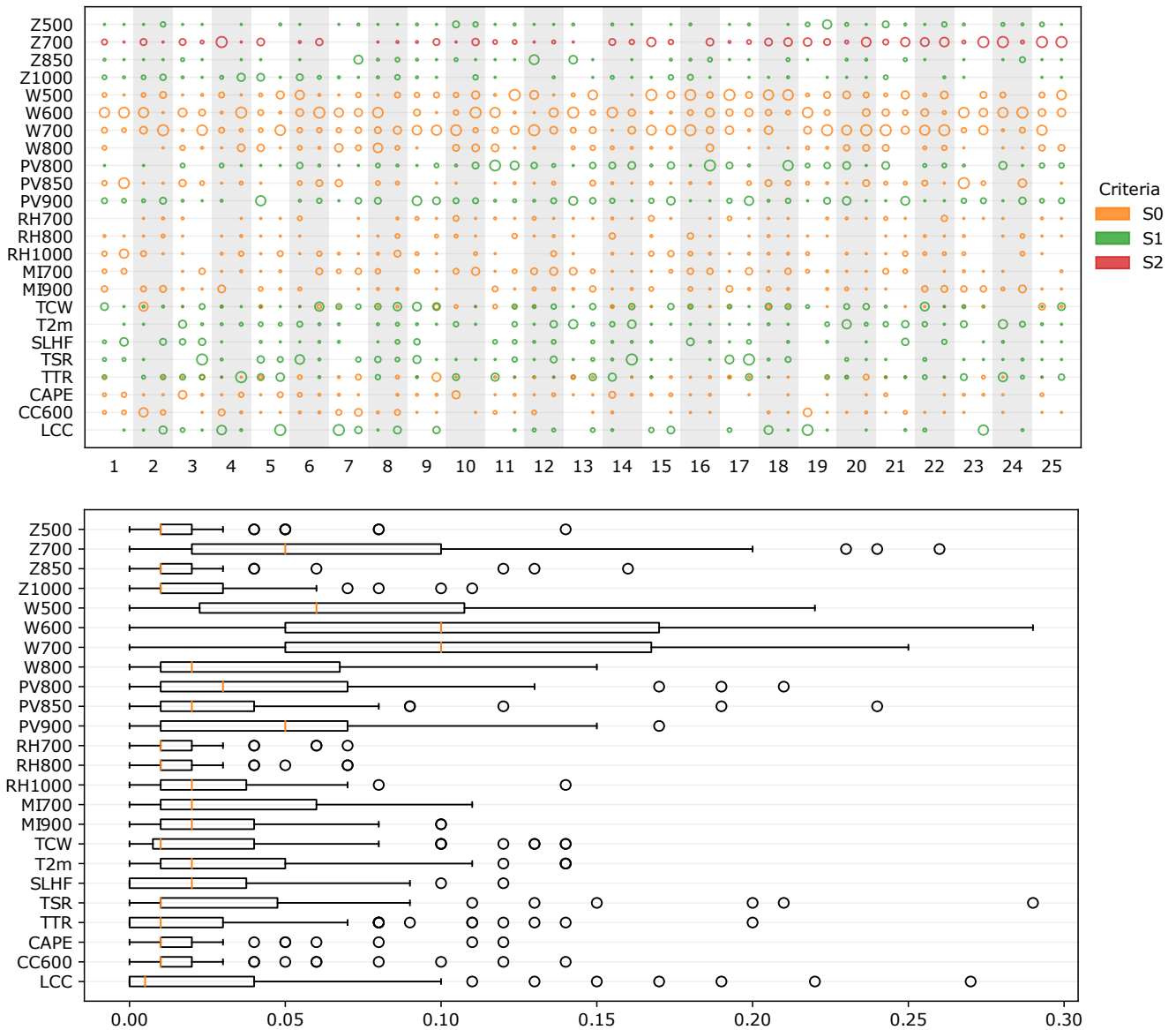


**Figure C1.** Results of the optimization with preselected 26 variables for the different catchments. (top) The colors represent the analogy criteria, and the size of the dots is proportional to the weight given to the predictor within the range [0.01, 0.2]. (bottom) Boxplot of the weight values for the different variables.

## Open Research

Reanalysis datasets can be obtained from the respective providers (see Acknowledgements). Precipitation data can be obtained from MeteoSwiss (for research purpose only). The software used, AtmoSwing (<https://atmoswing.org>, Horton, 2019a), is open-source and can be used without restrictions.

## Acknowledgments

Precipitation time series were provided by MeteoSwiss. The catchment extents were provided by the Hydrological Atlas of Switzerland (hydrologicalatlas.ch). The ERA-Interim reanalysis was obtained from the ECMWF Data Server at <http://apps.ecmwf.int/datasets>. The Climate Forecast System Reanalysis (CFSR) was obtained from the Computational & Information Systems Lab (CISL) Research Data Archive (<http://rda.ucar.edu/>). The CFSR project is carried out by the Environmental Modeling Center (EMC), National Centers for Environmental Prediction (NCEP). ERA5 (Complete ERA5 global atmospheric reanalysis) was obtained from the C3S climate data store (CDS) at <https://cds.climate.copernicus.eu>. Calculations were performed on UBELIX (<http://www.id.unibe.ch/hpc>), the HPC cluster at the University of Bern.

## References

- Alessandrini, S., Delle Monache, L., Sperati, S., & Cervone, G. (2015). An analog ensemble for short-term probabilistic solar power forecast. *Applied Energy*, *157*, 95–110. doi: 10.1016/j.apenergy.2015.08.011
- Alessandrini, S., Delle Monache, L., Sperati, S., & Nissen, J. N. (2015). A novel application of an analog ensemble for short-term wind power forecasting. *Renewable Energy*, *76*, 768–781. doi: 10.1016/j.renene.2014.11.061
- Ben Daoud, A. (2010). *Améliorations et développements d’une méthode de prévision probabiliste des pluies par analogie*. (Unpublished doctoral dissertation). Université de Grenoble.
- Ben Daoud, A., Sauquet, E., Bontron, G., Obled, C., & Lang, M. (2016). Daily quantitative precipitation forecasts based on the analogue method: improvements and application to a French large river basin. *Atmos. Res.*, *169*, 147–159. doi: 10.1016/j.atmosres.2015.09.015
- Bessa, R., Trindade, A., Silva, C. S., & Miranda, V. (2015). Probabilistic solar power forecasting in smart grids using distributed information. *International Journal of Electrical Power & Energy Systems*, *72*, 16–23. doi: 10.1016/j.ijepes.2015.02.006
- Bliefernicht, J. (2010). *Probability forecasts of daily areal precipitation for small river basins* (Unpublished doctoral dissertation). Universität Stuttgart.
- Bontron, G. (2004). *Prévision quantitative des précipitations: Adaptation probabiliste par recherche d’analogues. Utilisation des Réanalyses NCEP/NCAR et application aux précipitations du Sud-Est de la France*. (Unpublished doctoral dissertation). Institut National Polytechnique de Grenoble.
- Brown, T. (1974). *Admissible Scoring Systems for Continuous Distributions*. (Tech. Rep.). Retrieved from <http://eric.ed.gov/?id=ED135799>
- Caillouet, L., Vidal, J.-P., Sauquet, E., & Graff, B. (2016). Probabilistic precipitation and temperature downscaling of the Twentieth Century Reanalysis over France. *Clim. Past*, *12*(3), 635–662. doi: 10.5194/cp-12-635-2016
- Cateni, S., Colla, V., & Vannucci, M. (2010). Variable selection through genetic algorithms for classification purposes. *Proceedings of the 10th IASTED International Conference on Artificial Intelligence and Applications, AIA 2010*,

- 795 6–11. doi: 10.2316/p.2010.674-080
- 796 Dayon, G., Boé, J., & Martin, E. (2015, feb). Transferability in the future climate of  
797 a statistical downscaling method for precipitation in France. *J. Geophys. Res.*  
798 *Atmos.*, *120*(3), 1023–1043. doi: 10.1002/2014JD022236
- 799 Dee, D. P., Uppala, S. M., Simmons, A. J., Berrisford, P., Poli, P., Kobayashi, S.,  
800 ... Vitart, F. (2011). The ERA-Interim reanalysis: Configuration and perfor-  
801 mance of the data assimilation system. *Quart. J. Roy. Meteor. Soc.*, *137*(656),  
802 553–597. doi: 10.1002/qj.828
- 803 Delle Monache, L., Eckel, F. A., Rife, D. L., Nagarajan, B., & Searight, K. (2013).  
804 Probabilistic Weather Prediction with an Analog Ensemble. *Mon. Weather*  
805 *Rev.*, *141*, 3498–3516. doi: 10.1175/MWR-D-12-00281.1
- 806 Delle Monache, L., Nipen, T., Liu, Y., Roux, G., & Stull, R. (2011). Kalman Fil-  
807 ter and Analog Schemes to Postprocess Numerical Weather Predictions. *Mon.*  
808 *Weather Rev.*, *139*(11), 3554–3570. doi: 10.1175/2011MWR3653.1
- 809 D’heygere, T., Goethals, P. L., & De Pauw, N. (2003). Use of genetic algo-  
810 rithms to select input variables in decision tree models for the prediction of  
811 benthic macroinvertebrates. *Ecological Modelling*, *160*(3), 291–300. doi:  
812 10.1016/S0304-3800(02)00260-0
- 813 Drosowsky, W., & Zhang, H. (2003). Verification of Spatial Fields. In I. T. Jol-  
814 liffe & D. B. Stephenson (Eds.), *Forecast verif. a pract. guid. atmos. sci.* (pp.  
815 121–136). Wiley.
- 816 Foresti, L., Panziera, L., Mandapaka, P. V., Germann, U., & Seed, A. (2015). Re-  
817 trieval of analogue radar images for ensemble nowcasting of orographic rainfall.  
818 *Meteorol. Appl.*, *22*(2), 141–155. doi: 10.1002/met.1416
- 819 Frei, C., & Schär, C. (1998). A precipitation climatology of the Alps from  
820 high-resolution rain-gauge observations. *International Journal of Clima-*  
821 *tology*, *18*(8), 873–900. doi: 10.1002/(SICI)1097-0088(19980630)18:8<873::  
822 AID-JOC255>3.0.CO;2-9
- 823 Gibergans-Báguena, J., & Llasat, M. (2007, dec). Improvement of the analog fore-  
824 casting method by using local thermodynamic data. Application to autumn  
825 precipitation in Catalonia. *Atmospheric Research*, *86*(3-4), 173–193. Retrieved  
826 from <http://linkinghub.elsevier.com/retrieve/pii/S0169809507000695>  
827 doi: 10.1016/j.atmosres.2007.04.002
- 828 Gobeyn, S., Volk, M., Dominguez-Granda, L., & Goethals, P. L. (2017). Input  
829 variable selection with a simple genetic algorithm for conceptual species dis-  
830 tribution models: A case study of river pollution in Ecuador. *Environmental*  
831 *Modelling and Software*, *92*, 269–316. doi: 10.1016/j.envsoft.2017.02.012
- 832 Guennebaud, G., Jacob, B., & Others. (2010). *Eigen v3*. <http://eigen.tuxfamily.org>.
- 833 Guilbaud, S., & Obled, C. (1998). Prévision quantitative des précipitations  
834 journalières par une technique de recherche de journées antérieures ana-  
835 logues: optimisation du critère d’analogie. *Comptes Rendus l’Académie*  
836 *des Sci. Ser. II, A-Earth Planet. Sci.*, *327*(3), 181–188. Retrieved from  
837 <http://www.sciencedirect.com/science/article/pii/S1251805098800062>  
838 doi: 10.1016/s1251-8050(98)80006-2

- 839 Hamill, T., & Whitaker, J. (2006). Probabilistic quantitative precipitation fore-  
 840 casts based on reforecast analogs: Theory and application. *Monthly Weather*  
 841 *Review*, *134*(11), 3209–3229. doi: 10.1175/mwr3237.1
- 842 Hamill, T. M., Scheuerer, M., & Bates, G. T. (2015). Analog Probabilistic Pre-  
 843 cipitation Forecasts Using GEFs Reforecasts and Climatology-Calibrated  
 844 Precipitation Analyses. *Monthly Weather Review*, *143*(8), 3300–3309. doi:  
 845 10.1175/MWR-D-15-0004.1
- 846 Hersbach, H. (2000). Decomposition of the continuous ranked probability score for  
 847 ensemble prediction systems. *Wea. Forecasting*, *15*(5), 559–570. doi: 10.1175/  
 848 1520-0434(2000)015<0559:dotcrp>2.0.co;2
- 849 Hersbach, H., Bell, B., Berrisford, P., Horányi, A., Sabater, J. M., Nicolas, J., . . .  
 850 Dee, D. (2019). Global reanalysis: goodbye ERA-Interim, hello ERA5.  
 851 *ECMWF Newsletter*(159), 17–24. doi: 10.21957/vf291hehd7
- 852 Holland, J. H. (1992, jul). Genetic Algorithms. *Scientific American*, *267*(1), 66–72.  
 853 doi: 10.1038/scientificamerican0792-66
- 854 Horton, P. (2019a). AtmoSwing: Analog Technique Model for Statistical Weather  
 855 forecastING and downscaling (v2.1.0). *Geoscientific Model Development*,  
 856 *12*(7), 2915–2940. doi: 10.5194/gmd-12-2915-2019
- 857 Horton, P. (2019b, dec). *AtmoSwing v2.1.2 [Software]*. Zenodo. doi: 10.5281/zenodo  
 858 .3559787
- 859 Horton, P. (2021). Analogue methods and ERA5: Benefits and pitfalls. *International*  
 860 *Journal of Climatology*(September 2021), 4078–4096. doi: 10.1002/joc.7484
- 861 Horton, P., & Brönnimann, S. (2019). Impact of global atmospheric reanalyses on  
 862 statistical precipitation downscaling. *Climate Dynamics*, *52*(9-10), 5189–5211.  
 863 doi: 10.1007/s00382-018-4442-6
- 864 Horton, P., Jaboyedoff, M., Metzger, R., Obled, C., & Marty, R. (2012). Spatial re-  
 865 lationship between the atmospheric circulation and the precipitation measured  
 866 in the western Swiss Alps by means of the analogue method. *Nat. Hazards*  
 867 *Earth Syst. Sci.*, *12*, 777–784. doi: 10.5194/nhess-12-777-2012
- 868 Horton, P., Jaboyedoff, M., & Obled, C. (2017, apr). Global Optimization of an  
 869 Analog Method by Means of Genetic Algorithms. *Monthly Weather Review*,  
 870 *145*(4), 1275–1294. doi: 10.1175/MWR-D-16-0093.1
- 871 Horton, P., Jaboyedoff, M., & Obled, C. (2018). Using genetic algorithms to op-  
 872 timize the analogue method for precipitation prediction in the Swiss Alps. *J.*  
 873 *Hydrol.*, *556*, 1220–1231. doi: 10.1016/j.jhydrol.2017.04.017
- 874 Huang, J., Cai, Y., & Xu, X. (2007). A hybrid genetic algorithm for feature selection  
 875 wrapper based on mutual information. *Pattern Recognition Letters*, *28*(13),  
 876 1825–1844. doi: 10.1016/j.patrec.2007.05.011
- 877 Jézéquel, A., Yiou, P., & Radanovics, S. (2017). Role of circulation in European  
 878 heatwaves using flow analogues. *Climate Dynamics*, 1–15. doi: 10.1007/s00382  
 879 -017-3667-0
- 880 Junk, C., Delle Monache, L., & Alessandrini, S. (2015). Analog-based Ensemble  
 881 Model Output Statistics. *Monthly Weather Review*, *143*(7), 2909–2917. doi: 10  
 882 .1175/MWR-D-15-0095.1

- 883 Junk, C., Delle Monache, L., Alessandrini, S., Cervone, G., & von Bremen, L.  
 884 (2015). Predictor-weighting strategies for probabilistic wind power forecasting  
 885 with an analog ensemble. *Meteorologische Zeitschrift*, *24*(4), 361–379. doi:  
 886 10.1127/metz/2015/0659
- 887 Lorenz, E. (1956). *Empirical orthogonal functions and statistical weather prediction*  
 888 (Tech. Rep.). Massachusetts Institute of Technology, Department of Meteorol-  
 889 ogy, Massachusetts Institute of Technology, Dept. of Meteorology.
- 890 Lorenz, E. (1969). Atmospheric predictability as revealed by naturally occurring  
 891 analogues. *J. Atmos. Sci.*, *26*, 636–646. doi: 10.1175/1520-0469(1969)26<636:  
 892 aparbn>2.0.co;2
- 893 Maraun, D., Wetterhall, F., Chandler, R. E., Kendon, E. J., Widmann, M., Brienen,  
 894 S., . . . Thiele-Eich, I. (2010). Precipitation downscaling under climate  
 895 change: Recent developments to bridge the gap between dynamical mod-  
 896 els and the end user. *Reviews of Geophysics*, *48*(RG3003), 1–34. doi:  
 897 10.1029/2009RG000314
- 898 Marty, R. (2010). *Prévision hydrologique d'ensemble adaptée aux bassins à crue*  
 899 *rapide. Elaboration de prévisions probabilistes de précipitations à 12 et 24 h.*  
 900 *Désagrégation horaire conditionnelle pour la modélisation hydrologique. Ap-*  
 901 *plication à des bassins de la région Cév* (Unpublished doctoral dissertation).  
 902 Université de Grenoble.
- 903 Marty, R., Zin, I., Obled, C., Bontron, G., & Djerboua, A. (2012, mar). To-  
 904 ward real-time daily PQPF by an analog sorting approach: Application to  
 905 flash-flood catchments. *J. Appl. Meteorol. Climatol.*, *51*(3), 505–520. doi:  
 906 10.1175/JAMC-D-11-011.1
- 907 Massacand, A. C., Wernli, H., & Davies, H. C. (1998, may). Heavy precipitation on  
 908 the alpine southside: An upper-level precursor. *Geophysical Research Letters*,  
 909 *25*(9), 1435–1438. doi: 10.1029/98GL50869
- 910 Matheson, J., & Winkler, R. (1976). Scoring rules for continuous probability distri-  
 911 butions. *Manage. Sci.*, *22*(10), 1087–1096. doi: 10.1287/mnsc.22.10.1087
- 912 Michalewicz, Z. (1996). *Genetic Algorithms + Data Structures = Evolution Pro-*  
 913 *grams* (3rd editio ed.). Springer-Verlag.
- 914 Obled, C., Bontron, G., & Garçon, R. (2002, aug). Quantitative precipita-  
 915 tion forecasts: a statistical adaptation of model outputs through an ana-  
 916 logues sorting approach. *Atmos. Res.*, *63*(3-4), 303–324. doi: 10.1016/  
 917 S0169-8095(02)00038-8
- 918 Panziera, L., Germann, U., Gabella, M., & Mandapaka, P. V. (2011). NORA-  
 919 Nowcasting of Orographic Rainfall by means of Analogues. *Q. J. R. Meteorol.*  
 920 *Soc.*, *137*(661), 2106–2123. doi: 10.1002/qj.878
- 921 Radanovics, S., Vidal, J.-P., Sauquet, E., Ben Daoud, A., & Bontron, G. (2013).  
 922 Optimising predictor domains for spatially coherent precipitation down-  
 923 scaling. *Hydrology and Earth System Sciences*, *17*(10), 4189–4208. doi:  
 924 10.5194/hess-17-4189-2013
- 925 Raynaud, D., Hingray, B., Zin, I., Anquetin, S., Debionne, S., & Vautard, R.  
 926 (2016). Atmospheric analogues for physically consistent scenarios of surface

- 927 weather in Europe and Maghreb. *International Journal of Climatology*. doi:  
928 10.1002/joc.4844
- 929 Saha, S., Moorthi, S., Pan, H. L., Wu, X., Wang, J., Nadiga, S., . . . Goldberg, M.  
930 (2010). The NCEP climate forecast system reanalysis. *Bull. Amer. Meteor.*  
931 *Soc.*, *91*(8), 1015–1057. doi: 10.1175/2010BAMS3001.1
- 932 Schüepp, M., & Gensler, G. (1980). *Klimaregionen der Schweiz. Die Beobach-*  
933 *tungsnetze der Schweizerischen Meteorologischen Anstalt.*
- 934 Teweles, S., & Wobus, H. B. (1954). Verification of prognostic charts. *Bull. Am. Me-*  
935 *teorol. Soc.*, *35*, 455–463.
- 936 Thompson, J. C., & Carter, G. M. (1972). On some characteristics of the S1  
937 score. *Journal of Applied Meteorology*, *11*(8), 1384–1385. Retrieved from  
938 <http://www.sciencedirect.com/science/article/pii/0032063359900467>  
939 doi: 10.1175/1520-0450(1972)011(1384:OSCOTS)2.0.CO;2
- 940 Vanvyve, E., Delle Monache, L., Monaghan, A. J., & Pinto, J. O. (2015). Wind  
941 resource estimates with an analog ensemble approach. *Renewable Energy*, *74*,  
942 761–773. doi: 10.1016/j.renene.2014.08.060
- 943 Wilson, L. J., & Yacowar, N. (1980). Statistical weather element forecasting in  
944 the Canadian Weather Service. In *Proc. wmo symp. probabilistic stat. methods*  
945 *weather forecast.* (pp. 401–406). Nice, France.
- 946 Woodcock, F. (1980). On the use of analogues to improve regression forecasts. *Mon.*  
947 *Weather Rev.*, *108*(3), 292–297. doi: 10.1175/1520-0493(1980)108(0292:otuoat)  
948 2.0.co;2